

**Novel methods and therapeutic  
approaches for diagnosis and treatment of  
Huntington's Disease**

**Inauguraldissertation**

zur

Erlangung der Würde eines Doktors der Philosophie  
vorgelegt der  
Philosophisch-Naturwissenschaftlichen Fakultät  
der Universität Basel

von

Andreas Weiss  
aus Deutschland

Basel, 2008



Genehmigt von der Philosophisch-Naturwissenschaftlichen Fakultät auf Antrag von

Fakultätsverantwortlicher: Prof. Dr. Markus A. Rüegg

Dissertationsleiter: Dr. Paolo Paganetti

Korreferent: Prof. Dr. Martin Spiess

Basel, den 16. 09. 2008

Prof. Dr. Eberhard Parlow

Dekan

# CONTENTS

<b>TABLE OF ABBREVIATIONS</b>	<b>1</b>
<b>1 SUMMARY</b>	<b>3</b>
<b>2 INTRODUCTION</b>	<b>5</b>
<b>2.1 Huntington's Disease</b>	<b>5</b>
2.1.1 History	5
2.1.2 Clinical manifestations of Huntington's Disease	6
2.1.3 Neuropathology of Huntington's Disease	7
2.1.4 Metabolic defects in Huntington's Disease	9
2.1.5 Current treatment possibilities of Huntington's Disease	9
2.1.6 The genetics of Huntington's Disease	11
2.1.6.1 Genetic anticipation in Huntington's Disease	13
2.1.7 Huntingtin Protein	14
2.1.7.1 Wild-type huntingtin	14
2.1.7.2 Gain-of-function or loss-of-function?	16
2.1.7.3 Structural changes of the mutated huntingtin protein	16
2.1.8 Potential pathogenic molecular mechanisms Huntington's Disease	18
<b>2.2 Time resolved fluorescence resonance energy transfer</b>	<b>20</b>
2.2.1 Fluorescence resonance energy transfer (FRET)	20
2.2.2 Time resolved FRET	21
<b>3 AIMS OF THE THESIS</b>	<b>23</b>
<b>4 RESULTS</b>	<b>24</b>
<b>4.1 Inducible mutant huntingtin expression in a neuronal cell model leads to transcriptional dysregulation and cell death</b>	<b>24</b>
4.1.1 SUMMARY	25
4.1.2 INTRODUCTION	26
4.1.3 MATERIAL AND METHODS	28
4.1.4 RESULTS	31
4.1.5 DISCUSSION	37
<b>4.2 Sensitive biochemical aggregate detection reveals aggregation onset before symptom development in cellular and murine models of Huntington's Disease</b>	<b>39</b>
4.2.1 SUMMARY	40
4.2.2 INTRODUCTION	41
4.2.3 MATERIALS AND METHODS	43
4.2.4 RESULTS	47
4.2.5 DISCUSSION	60
<b>4.3 Development of a method for the high-throughput-quantification of cellular protein levels</b>	<b>63</b>
4.3.1 SUMMARY	64
4.3.2 INTRODUCTION	65
4.3.3 MATERIALS AND METHODS	67
4.3.4 RESULTS	70
4.3.5 DISCUSSION	
<b>4.4 Single-step detection of soluble mutant huntingtin in cellular, animal and human tissue samples: a bioassay for Huntington's Disease</b>	<b>82</b>
4.4.1 SUMMARY	83

4.4.2	INTRODUCTION	84
4.4.3	MATERIALS AND METHODS	86
4.4.4	RESULTS	89
4.4.5	DISCUSSION	96
<b>5</b>	<b>GENERAL DISCUSSION AND OUTLOOK</b>	<b>99</b>
<b>6</b>	<b>REFERENCES</b>	<b>102</b>
	<b>ACKNOWLEDGMENTS</b>	<b>123</b>
	<b>CURRICULUM VITAE</b>	<b>124</b>

## TABLE OF ABBREVIATIONS

aa857-25Q	857 amino acids of human huntingtin protein with 25 polyglutamine repeats
aa857-72Q	857 amino acids of human huntingtin protein with 72 polyglutamine repeats
AGERA	Agarose Gel Electrophoresis for Resolving Aggregates
BDNF	brain-derived neurotrophic factor
BSI	Rheoswitch ligand
DMEM	Dublecco's Modified Eagle Medium
DMSO	dimethylsulfoxide
DTT	dithiothreitol
EDTA	ethylenediaminetetraacetic acid
Ex1-25Q	human exon 1 of huntingtin protein with 25 polyglutamine repeats
Ex1-72Q	human exon 1 of huntingtin protein with 72 polyglutamine repeats
FBS	foetal bovine serum
FRET	fluorescence resonance energy transfer or Förster resonance energy transfer
HD	Huntington's Disease
Hdh150	knock-in full-length mutant huntingtin mouse model
HN10	mouse hippocampal neuroblastoma cell line
Htt	huntingtin protein
G418	geneticin
GFP	green fluorescent protein
mHtt	mutated polyQ huntingtin protein
NMDA	N-methyl D-aspartate
PBS	phosphate buffered saline
PCR	polymerase chain reaction
PFA	paraformaldehyde
PolyQ	polyglutamine
PMSF	phenylmethanesulphonylfluoride
Q	glutamine
Q25Htt1-857	see aa857-25Q
R6/2 mice	transgenic exon1 mutant huntingtin mouse model
Rf	retardation factor
RSL	Rheoswitch ligand
SCA	spino-cerebellar ataxia
SDS-PAGE	sodium dodecyl sulfate polyacrylamide gel electrophoresis

TBS	tris buffered saline
Tris	tris(hydroxymethyl)-aminomethan
Wk	week
Wt	wild-type

## **1 SUMMARY**

Huntington's Disease is a neurodegenerative disorder characterized by motor dysfunction, emotional disturbance, dementia and weight loss. The disorder is caused by an autosomal dominant expansion of a CAG repeat encoding for a polyglutamine stretch in exon 1 of the huntingtin gene. Mutated huntingtin gains a neurotoxic function, leading to the onset of clinical symptoms mostly in mid-life. The progression of Huntington's Disease is characterized by a marked degeneration of gray and white brain matter. A loss of vulnerable neurons, most notably striatal medium-sized spiny neurons, is observed, while resistant populations are spared. No cure for Huntington's Disease exists and the disorder progresses relentlessly with a lethal outcome about two decades after diagnosis.

In my thesis I explored four main projects. As the reported cellular dysfunctions in Huntington's Disease are numerous, I generated an inducible, neuronal model to investigate the effects of mutant huntingtin expression at the cellular level (Chapter 4.1). This inducible model allowed for adjustable expression levels of different wild-type and mutant huntingtin fragments in proliferating or differentiated HN10 neuroblastoma cells, thus providing the ability to examine huntingtin protein effects under different cellular conditions. I was able to show that this model displays key major characteristics found in Huntington's Disease patients like transcriptional dysregulation, mutant huntingtin aggregation and decrease in cell viability. Subsequently, I made use of this newly designed cellular model to develop huntingtin detection methods to further investigate the biological role of soluble or aggregated mutant huntingtin for Huntington's Disease development and progression.

Since the role of huntingtin aggregate formation in Huntington's Disease is still under debate, I designed a simple method based on agarose gel electrophoresis for qualitative and quantitative characterization of huntingtin aggregates in my second project. Using this method, I proceeded to analyze samples of cellular and animal Huntington's Disease models and was able to show that in the brain of transgenic R6/2 mice aggregates became larger as a function of age and disease progression. Importantly, I showed that in primary striatal neurons and in brains of two Huntington's Disease mouse models (transgenic R6/2 and HdhQ150 knock-in mice), aggregate formation preceded detection of any functional deficits, supporting the theory that aggregates play an important pathogenic role in Huntington's Disease (Chapter 4.2).

In the third project, I developed a method for the detection of intracellular mutant huntingtin, the causative agent of Huntington's Disease. I generated a small recombinant protein tag which is recognized by a pair of readily available, high affinity monoclonal antibodies, thus

making this method generally applicable for detection of other recombinant proteins. Using this tag I was able to establish a time resolved fluorescence resonance energy transfer (time resolved FRET) based assay which allows for rapid, sensitive and robust detection of cellular mutant huntingtin levels. I miniaturized this assay to a homogeneous 1536 well microplate format and demonstrated that the assay system is suitable for the identification of compounds that increase or decrease the levels of huntingtin protein (Chapter 4.3).

In the fourth project, by using antibodies specific against endogenous huntingtin epitopes, I expanded this time resolved FRET detection method to monitor the levels of endogenous soluble mutant huntingtin in cellular, animal and human samples. I showed that the soluble mutant huntingtin levels inversely correlate with the amount of mutant huntingtin aggregates in the brains of aging R6/2 mice. Importantly, I was able to quantify mutant huntingtin concentrations in blood fractions from Huntington's Disease patients, providing for the first time a bioassay to assess the relevance of mutant huntingtin levels as a marker for disease progression. This biomarker could help to monitor the efficacy of drug treatments aimed at lowering mutant huntingtin levels in preclinical and clinical trials (Chapter 4.4).

## 2 INTRODUCTION

### 2.1 Huntington's Disease

Huntington's Disease, also sometimes referred to as Huntington's Chorea, is the most common autosomal-dominant neurodegenerative disorder with a prevalence of 5 to 8 cases per 100'000. Disease symptoms include severe motor dysfunctions (chorea), psychiatric alterations and progressive dementia with onset normally in middle-age. The solitary cause for Huntington's Disease is an elongation of a polyglutamine repeat at the amino terminus of the ubiquitously expressed huntingtin protein. The underlying pathophysiological mechanisms of mutant huntingtin are yet to be elucidated. Currently, aside from limited symptomatic treatments against emotional disturbances or chorea, no effective treatment for Huntington's Disease which can prolong the life expectancy of patients or stop their cognitive decline exist.

#### 2.1.1 History

The term "chorea" for the classification of movement disorders has been first used by Paracelsus, professor of medicine at the university of Basel in the 16<sup>th</sup> century (Paracelsus, 1527). First records with reports of chronic choreas, today accepted to describe Huntington's Disease patients, were published in the middle of the 19<sup>th</sup> century (Dunlison, 1848; Lund, 1860; Waters, 1842). The eponymous publication which described in detail not only the choreic movements but also the progressive dementia as well as the clear hereditary nature of the disease was published by George Huntington in 1872 (Huntington, 1872), (Figure 1). Huntington's Disease rose to public attention in 1952 when the American folk singer Woody Guthrie was diagnosed with the disease. His death in 1967 prompted the foundation of the Committee to Combat Huntington's Disease, one of the first patient support groups that greatly increased fund-raising for research and public awareness of the disease.

The improved conditions for Huntington's Disease research were reflected in the research milestones over the next decades. In 1983, the chromosomal localization of the disease was discovered (Gusella et al., 1983) and in 1993 the gene responsible for Huntington's Disease was isolated and characterized (Group, 1993a). Since then, research progress has included the design of the first animal model (Mangiarini et al., 1996), the discovery of intracellular huntingtin aggregates (Davies et al., 1997) and several hypothesis for toxic mechanisms of

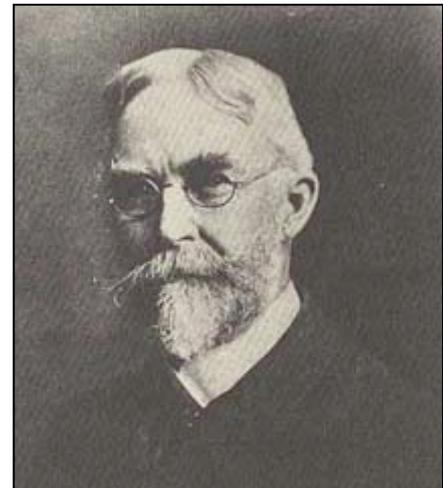


**Figure 1: George Huntington.** Reproduced from the "Huntington number" of Neurographs (1908).

action were put forward (Bates, 2003). However, despite of this remarkable progress, no treatment tackling the underlying mechanisms of action causing Huntington's Disease is available today.

### **2.1.2 Clinical manifestations of Huntington's Disease**

Even though the sole cause of Huntington's Disease in every patient is a single mutational event causing a CAG trinucleotide expansion in the huntingtin gene, the clinical manifestations are found to be diverse and can be mistaken for other neurodegenerative diseases like Huntington's Disease-like 2 (Greenstein et al., 2007; Margolis et al., 2004; Rudnicki et al., 2008; Walker et al., 2003) or dentatorubropallidoluyisian atrophy (Nakano et al., 1985). In addition, even though symptom onset mostly occurs between 30 to 50 years of age, juvenile and late-onset cases are frequent, widening the possible range of symptom onset to 2-85 years of age (Hayden et al., 1987; Osborne et al., 1982). Approximately 44-72% of these variations in age of onset can be explained by the length of the CAG repeat, making the trinucleotide and the resulting polyglutamine repeat length in the huntingtin protein the most important determinant for the age of onset (Myers, 2004; Wexler et al., 2004). Because of the wide variety in symptoms and ages of onset, misdiagnoses based on clinical symptoms used to occur regularly (Bateman et al., 1992; Folstein et al., 1986) and molecular testing for CAG repeat length became key for precise diagnosis of Huntington's Disease (Kremer et al., 1994). Since molecular testing will be performed only in patients suspected to show clinical symptoms of Huntington's Disease or patients known to be at risk because of their family history, it is important to note that no singular symptomatic finding is sufficient for a clinical diagnosis. In the early disease stages, minor alterations in intellectual capacity, increased anxiety and personality changes are observed (Kirkwood et al., 2000; Kirkwood et al., 2001; Penney et al., 1990) although these changes are often attributed retrospectively after a more certain diagnosis based on more profound symptoms or molecular testing.

The classical phenotype in the mid-course of Huntington's Disease progression is characterized by motor abnormalities. The motor impairments include chorea (rapid, random and uncontrollable movements (Dunghison, 1848; Huntington, 1872; Lang, 1989; Lund, 1860; Penney et al., 1990; Waters, 1842; Young et al., 1986)), bradykinesia (decrease of movement speed (Thompson et al., 1988)) and dystonia (abnormal movements with increased muscle tone (Andrich et al., 2007; Bittenbender and Quadfasel, 1962)). Even though chorea is by far the most prominent clinical manifestation found in over 90% of all Huntington's Disease patients, it is a poor marker for disease progression as chorea intensity tends to change in a

non-predictable manner from patient to patient and is often replaced in later stages of the disease by other motor impairments such as dystonia (Mahant et al., 2003; Young et al., 1986). In advanced stages of Huntington's Disease, independent living becomes impossible for the patients due to severe motor impairment and increased cognitive decline (Nance and Sanders, 1996). These later disease stages are often accompanied by increased sleep disturbances (Hansotia et al., 1985; Silvestri et al., 1995) and weight loss (Morales et al., 1989; Sanberg et al., 1981). Patients die prematurely of complications associated with the disease such as pneumonia or dysphagia (Lanska et al., 1988a; Lanska et al., 1988b) with the median duration between onset of symptoms and time of death being 15 to 20 years (Foroud et al., 1999).

### 2.1.3 Neuropathology of Huntington's Disease

In the past, asymptomatic and early symptomatic disease stages were thought not to be accompanied by distinct neuropathological changes. However, more recent studies were able to show alterations in cytoskeletal proteins in cortical neurons even at these early presymptomatic timepoints (DiProspero et al., 2004; Modregger et al., 2002). Furthermore,

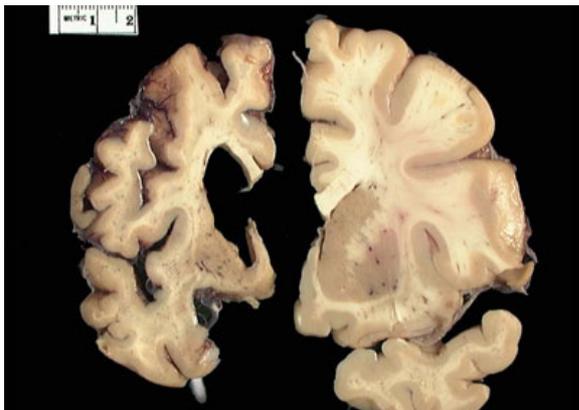


**Figure 2: Comparison of normal brain (right) to a brain of a late stage Huntington's Disease patients (left).** General atrophy of the Huntington brain is visible in all brain areas with most severe atrophy apparent in the striatum. Photo courtesy of the Harvard Brain Tissue Resource Center.

advances in MRI imaging allowed to visualize cortical thinning and atrophy in presymptomatic mutation carriers, providing a possible neurological explanation for the very early psychiatric alterations (Kassubek et al., 2004; Peinemann et al., 2005; Rosas et al., 2001; Rosas et al., 2006).

Brains from patients with advanced stages of Huntington's Disease show a general atrophy with weight reduction of about 10 to 20% (Figure 2). Affected brain areas with distinctive neuronal loss include the hippocampus, cortical layers 3, 5 and 6, Purkinje cells of the cerebellum, tuberal nuclei of the hypothalamus as well as the centromedial-parafascicular complex of the thalamus (Bates et al., 2002; Jeste et al., 1984; Kremer et al., 1991; Spargo et al., 1993). Despite this widespread neuronal loss, neurodegeneration in Huntington's Disease is still considered to be remarkably selective because of the strikingly severe and distinct atrophy in the most affected brain region, the striatum (Bruyn, 1979; Roos et al., 1985; Vonsattel et al., 1985). In this area almost all of the medium-sized spiny striatal neurons are lost in the later stages of the disease, while large

striatal neurons, aspiny interneurons and striatal astrocytes are relatively resistant to Huntington's Disease related degeneration (Cicchetti et al., 2000; Ferrante et al., 1987a; Ferrante et al., 1987b). The striatum itself comprises the caudate nucleus and putamen and interconnects to subcortical nuclei (such as globus pallidus, subthalamic nucleus and substantia nigra) which influence movement, motivation and reward behavior through modulation of higher brain areas (Alexander, 1994; Alexander and Crutcher, 1990; Hoover and Strick, 1999). In healthy individuals, the medium-sized striatal neurons send inhibitory signals to the external and internal segments of the globus pallidus as well as to the substantia nigra pars reticulata, (Figure 3, left side).

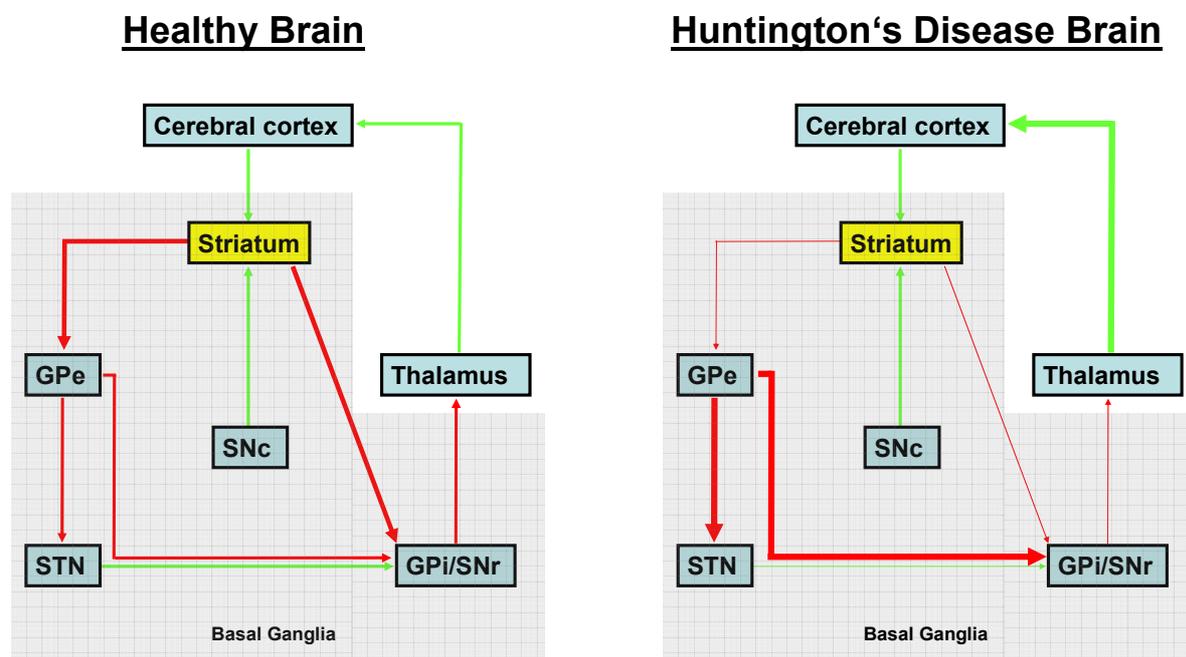


**Figure 3: Basal Ganglia pathways in healthy and Huntington's Disease brain, simplified schematic view, modified from Bates et al., 2002.** Brain regions of the basal ganglia encircled in grey. The striatum, the most severely affected brain region in Huntington's Disease is depicted in yellow. Widespread neurodegeneration in the striatum causes a decrease of its inhibitory function in the basal ganglia pathway. This results in decreased activation of the basal ganglia output regions (GPi/SNr) which have an inhibitory effect on thalamic nuclei. Therefore, subsequent increased excitation of the thalamus due to lacking inhibitory input from the basal ganglia occurs and are thought to be the cause for the uncontrolled movement and psychiatric alterations seen in Huntington's Disease patients. GPe: Globus pallidus external segment; GPi: Globus pallidus internal segment; STN: Subthalamic nucleus; SNr: Substantia nigra pars reticulata; SNc: Substantia nigra pars compacta.

These nuclei project inhibitory axons to the thalamus, a brain region of the diencephalon which in turn projects to higher cortical regions and is thought to have a "selective mediator" role for prethalamic signals to be interpreted by the cortex (Alexander et al., 2006; Jones, 2002; Percheron et al., 1996). In patients affected by Huntington's Disease, this circuitry appears to be severely disturbed due to the almost complete loss of medium-sized spiny

neurons in the striatum (Figure 3, right side). The decreased inhibitory signaling from the striatum to other subcortical nuclei of the basal ganglia leads to overexcitation of the thalamus and is thought to be responsible for the various psychiatric and motor symptoms seen in Huntington's Disease.

#### **2.1.4 Metabolic defects in Huntington's Disease**

Because of the severe brain atrophy and the resulting clinical symptoms, Huntington's Disease is primarily considered to be a neurodegenerative disorder. However, over the past four decades it has become more and more apparent that this is a too restrictive disease definition and that patients display various symptoms which are most likely connected to widespread, systemic metabolic defects. Early studies in the 1960s and 70s reported a dysfunction in amino acid, glucose and fatty acid metabolism (Perry et al., 1969; Phillipson and Bird, 1977; Podolsky and Leopold, 1977) as well as weight loss in Huntington's Disease patients (Bruyn and von Wolferen, 1973). Further studies found that this massive weight loss occurs despite sufficient calorie intake and that weight loss cannot be simply explained by the increased and uncontrollable muscle movements associated with Huntington's Disease (Farrer and Meaney, 1985; Kremer and Roos, 1992; Morales et al., 1989; Sanberg et al., 1981). These findings as well as reports of increased prevalence of diabetes mellitus in Huntington's Disease patients (Farrer, 1985), support the hypothesis of a general, systemic metabolic defect caused by Huntington's Disease.

Over the last decade, detailed metabolomic studies became feasible due to the emergence and improvement of sensitive detection methods like nuclear magnetic resonance (NMR) or gas chromatography-time-of-flight-mass spectrometry (GC-TOF-MS). Metabolic profiling of 30 Huntington's Disease and 20 healthy patients reported dysregulation of amino acid metabolism in Huntington's Disease, verifying the earlier studies (Underwood et al., 2006). The study identified several metabolites such as leucine, ethylene glycol and hydroxybutyric acid with serum levels differing significantly between asymptomatic gene carriers and patients with first disease symptoms, thus providing a possible biomarker profile for disease onset and early disease progression. However, additional, larger scaled metabolomic studies are needed to verify these results.

#### **2.1.5 Current treatment possibilities of Huntington's Disease**

Even though over 110 clinical phase I to III trials for Huntington's Disease have been reported (Bonelli et al., 2004), no treatment recommendation of clinical relevance has emerged. In fact,

only very limited symptomatic treatment possibilities for Huntington's Disease exist which can be subdivided into three classes: treatment of motor disturbances, treatment of psychiatric alterations and neuroprotective treatments (Bonelli and Hofmann, 2007; Bonelli et al., 2004; Walker, 2007).

Treatment of motor impairments mostly focus on using antipsychotic drugs to decrease chorea such as haloperidol (Barr et al., 1988; Girotti et al., 1984; Leonard et al., 1975) or tetrabenazine (Jankovic and Beach, 1997; Ondo et al., 2002). While showing significant improvements on the Unified Huntington's Disease Rating Scale in some of the studies, regular side-effects limit their use for clinical treatment. An alternative treatment strategy is based on the "excitotoxin theory" which proposes an excess of excitatory neurotransmitters such as glutamate as reason for the motor impairments and neurodegeneration (DiFiglia, 1990). In an attempt to counter this overexcitatory stimuli, NMDA-receptor antagonists such as ketamine or riluzole have been tested in clinical trials. While ketamine failed to show any beneficial effects and to the contrary caused a decline in memory performance (Murman et al., 1997), riluzole improved chorea symptoms in a number of earlier studies (Group, 2003; Bodner et al., 2001; Rosas et al., 1999; Seppi et al., 2001). However, a recent larger European level I trial with 537 patients did not report any neuroprotective or beneficial symptomatic effects (Landwehrmeyer et al., 2007).

Attempts to ameliorate the psychiatric symptoms associated with Huntington's Disease are mostly aimed at treating the frequent cases of depression and dementia. Common antidepressants like fluoxetine (Como et al., 1997; De Marchi et al., 2001) or clozapine (Bonuccelli et al., 1994; Colosimo et al., 1995; Sajatovic et al., 1991) showed positive results in case studies but larger controlled trials against depression in Huntington's Disease are necessary for verification. Mild beneficial effects against dementia have been reported for riluzole (Seppi et al., 2001) and minocycline (Bonelli et al., 2003) in open-label trials, but generally no approved dementia treatment exists for Huntington's Disease patients.

The efficacy of neuroprotective treatments is more difficult to access because of the lack of reliable markers. Nevertheless, several clinical trials with potentially neuroprotective compounds have been reported for Huntington's Disease. Treatment with unsaturated fatty acids as plasma membrane components which can alter the probability of a cell to undergo apoptosis showed beneficial effects in smaller studies (Puri et al., 2002; Vaddadi et al., 2002) but positive results could not be reproduced in a more recent and larger scaled level I trial (Puri et al., 2005). Similarly, treatment with the caspase inhibitor minocycline (Chen et al., 2000; Scarabelli et al., 2004) was found to be safe, free of adverse effects at lower doses

(HuntingtonStudyGroup, 2004) and significantly improved motor and neuropsychological functions after 6 and 24 months of treatment in an open-label pilot study (Bonelli, 2004). However, another level III study with minocycline did not report any beneficial effects (Thomas et al., 2004). Critically, a recent minocycline trial with 412 ALS patients showed that minocycline treated patients performed significantly worse in functional capacity than placebo treated patients, prompting the authors of the ALS study to raise serious concerns about minocycline treatment in other neurodegenerative diseases, including Huntington's Disease (Reynolds, 2007). Another treatment strategy has been aimed at enhancing mitochondrial oxidative functions known to be affected in Huntington's Disease. Use of coenzyme Q10, an essential component of the mitochondrial electron transport chain (Crane et al., 1957), showed no beneficial effects (HuntingtonStudyGroup, 2001), whereas treatment with creatine resulted in an improvement of brain metabolites (Tabrizi et al., 2003; Tabrizi et al., 2005) as well as a decrease of serum 8-hydroxy-2'-deoxyguanosine, a marker for oxidative DNA injury, in Huntington's Disease patients (Hersch et al., 2006). However, a double-blind placebo-controlled study showed no beneficial effect on motor symptoms or cognitive performance after creatine treatment for 1 year (Verbessem et al., 2003).

Taken together, the efficacy of various potentially therapeutic compounds for Huntington's Disease remains to be proven. Importantly, all clinical studies so far have been symptomatic treatment attempts and no potential treatment aimed at curing Huntington's Disease or prolonging the life expectancy of patients exists, resulting in a very high unmet medical need for this disease.

### **2.1.6 The genetics of Huntington's Disease**

The huntingtin gene, localized on chromosome 4p16.3 (Gusella et al., 1983), was identified in 1993 through a joint effort of six international research groups (Group, 1993a). It comprises 67 exons and encodes for a large protein of 348 kDa whose exact function(s) remain to be elucidated. The mutation underlying Huntington's Disease is an expansion of a CAG repeat above a pathogenic length in the coding region of exon 1 of the huntingtin gene. In healthy individuals, CAG length normally varies between 10 to 35 repeats while patients carrying one allele with 40 or more CAG repeats will develop Huntington's Disease with 100% certainty. Repeat sizes of 36 to 39 are associated with a reduced disease penetrance (Andrew et al., 1993; Brinkman et al., 1997; Duyao et al., 1993) (Figure 4).

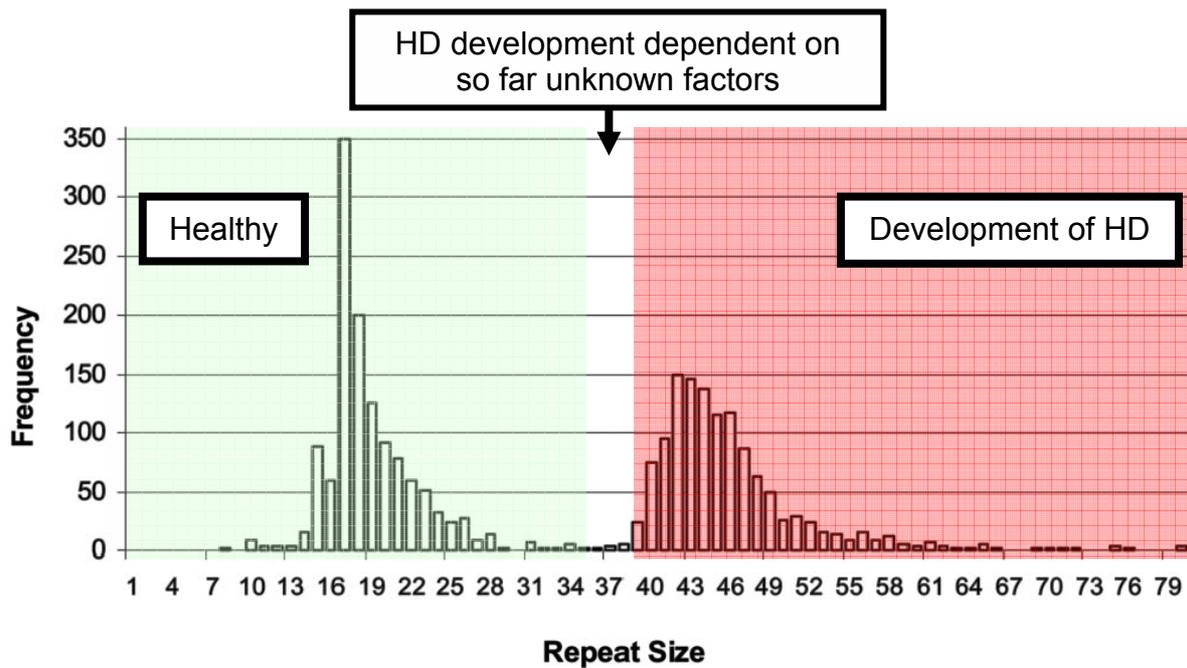


**Figure 4: Distribution of CAG repeat sizes in healthy and Huntington’s Disease patients, taken and modified from Myers, 2004.** Healthy patients (green area) carry repeats between 10 and 35 with the most common repeat lengths being 17 to 20 CAG triplets. Individuals with a CAG repeat size of 40 or more will develop Huntington’s Disease. Repeat sizes from 36 to 39 can result in development of Huntington’s Disease but penetrance is reduced and so far unknown factors seem contribute to the development of disease symptoms.

It should be noted that even though the length of the CAG repeat generally correlates statistically well with the age of onset, the strength of this correlation is mostly due to a small number of early-onset Huntington’s Disease cases with a CAG repeat length of 60 or more. However, the vast majority of Huntington’s Disease patients (~95%, (Myers, 2004)) carry a repeat length between 40 to 55 CAGs. When plotting the CAG repeat size against the age of onset it becomes apparent that for the majority of Huntington’s Disease patients, CAG repeat length is an insufficient predictor for age of onset as e.g. patients with a CAG repeat length between 40 and 44 can display first Huntington’s Disease symptoms as early as ~30 years of age and as late as ~70 years of age (Figure 5).

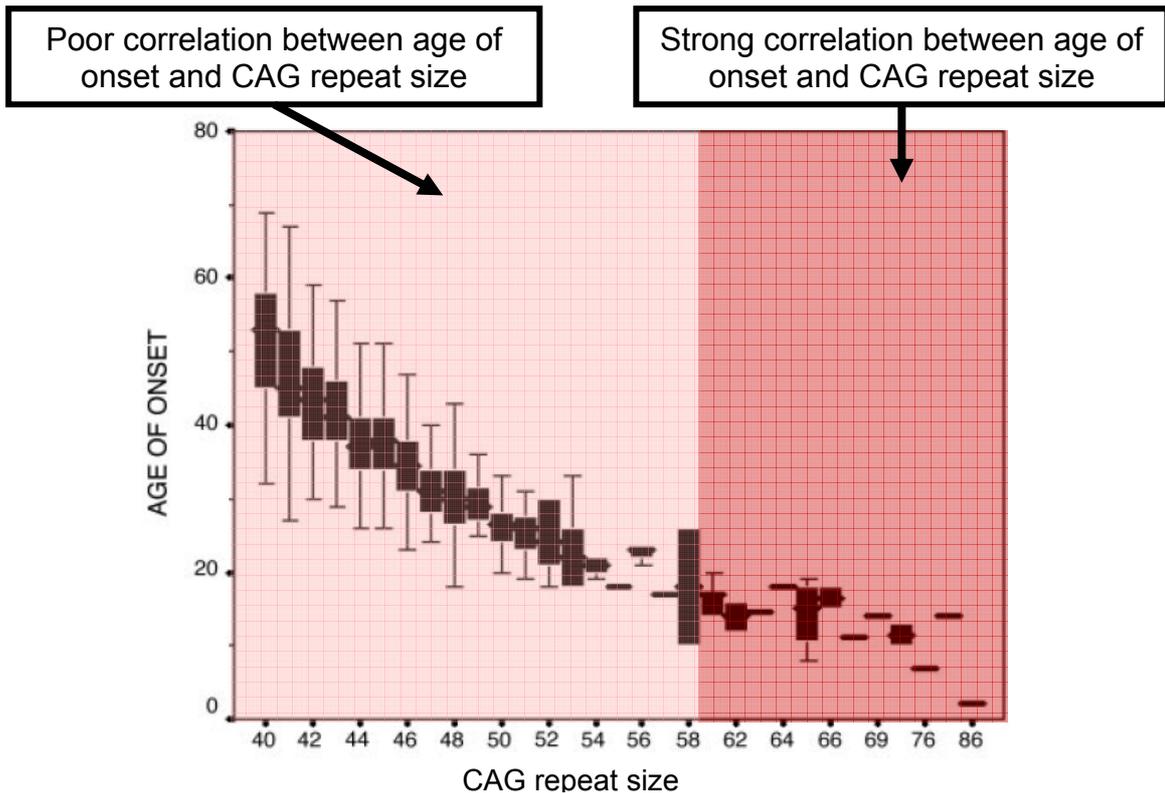


**Figure 5: CAG repeat length and age of onset in Huntington’s Disease, taken and modified from Wexler et al., 2004.** For CAG repeat sizes between 40 and 58, repeat size accounts for 44% of the variance in age of onset with a correlation coefficient of  $r = -0.66$  (light red area). Longer repeat sizes result in early onset forms of Huntington’s Disease (dark red area). In these juvenile forms of Huntington’s Disease, age of onset correlates stronger with repeat length ( $r = -0.81$ ) and CAG repeat length accounts for 72% of variance in age of onset.

The search for genetic modifiers for age of onset besides the CAG repeat length in the huntingtin gene yielded several candidates which seem to modulate age of onset independent of CAG repeat length such as glutamate receptor GRIK2 (GluR6) (Chattopadhyay et al., 2003), human caspase activated DNase (hCAD) (Chattopadhyay et al., 2005), ubiquitin carboxy-terminal hydrolase L1 (UCHL1) (Metzger et al., 2006b), drosophila homeobox homologue 1 (MSX1) (Djousse et al., 2004), NMDA receptor subunits (Arning et al., 2005), apolipoprotein E  $\epsilon 2\epsilon 3$  (Kehoe et al., 1999), huntingtin interacting proteins HIP1 and HIP14 (Metzger et al., 2006a). While these multiple genetic findings are encouraging, verified functional connections in terms of disease modifying mechanisms of action for these candidate genes are still lacking.

### 2.1.6.1 Genetic anticipation in Huntington’s Disease

A striking feature of Huntington’s Disease genetics is the instability of the CAG repeat length from one generation to the next. In approximately 75% of all Huntington’s Disease cases, the CAG length changes, with expansion of the repeat length being more common than repeat contraction (Wheeler et al., 2007). Since repeat length correlates with age of onset, an earlier

disease phenotype is often observed in successive generations (Ridley et al., 1988; Ridley et al., 1991). This phenomenon termed “genetic anticipation” was first reported for myotonic dystrophy, another trinucleotide repeat disorder (Fleischer, 1918; Fu et al., 1992; Howeler et al., 1989; Penrose, 1948) and has since been observed in several trinucleotide repeat disorders (Gouw et al., 1994; Ikeuchi et al., 1995; Koide et al., 1994; Ranum et al., 1994; Takiyama et al., 1999; Vaisanen et al., 1996).

The molecular mechanisms responsible for the trinucleotide instabilities are not yet fully understood. In Huntington’s Disease, epidemiologic reports showed that decreased age of onset is often associated with paternal inheritance (Barbeau, 1970; Bird et al., 1974; Conneally, 1984; Ridley et al., 1991; Wheeler et al., 2007), indicating a possibly increased gametic CAG repeat instability in sperm cells, a finding that was later confirmed in molecular studies (Leeflang et al., 1995; MacDonald et al., 1993). Because of these reports, erroneous DNA replication was long speculated to be solely responsible for the repeat length instability. However, more recent studies showed increased CAG repeat length mosaicism not only in gametic cells but also in somatic brain tissue where the CAG repeat length elongations in different brain regions correlated well with Huntington’s Disease neuropathology, with the striatum and the cerebral cortex displaying the largest repeat elongations (Kennedy et al., 2003; Shelbourne et al., 2007; Telenius et al., 1994). While the observed somatic instability in different brain regions in human tissue might still be due to instability in replicating non-neuronal cells rather than postmitotic neurons, a recent publication proved specific CAG instability even in non-replicating, terminally differentiated neurons in mouse models of Huntington’s Disease. Furthermore, this study showed an increased CAG repeat instability in neuronal cells dissected from human striata when compared to non-neuronal cell types (Gonitel et al., 2008).

## **2.1.7 Huntingtin Protein**

### **2.1.7.1 Wild-type huntingtin**

Wild-type huntingtin is a 3144 amino acids large, soluble protein which is ubiquitously expressed, with highest expression levels in testes and the central nervous system (Figure 6). It has no relevant sequence homology with other proteins and its potentially complex cellular functions are poorly understood. Subcellular localization showed huntingtin association with the nucleus (Kegel et al., 2002), the Golgi complex, the endoplasmic reticulum (Hilditch-Maguire et al., 2000), synaptic vesicles (DiFiglia et al., 1995; Velier et al., 1998), the microtubule network (Hoffner et al., 2002) as well as mitochondria (Orr et al., 2008; Petrasch-

Parwez et al., 2007; Rockabrand et al., 2007). Huntingtin contains 36 HEAT domains which are supposed to be involved in protein-protein-interactions (Andrade and Bork, 1995) and consist of a series of three amino acids which are repeated ~10 times along a 37-47 amino acid stretch. Huntingtin also contains a carboxyterminal nuclear export signal (Xia et al., 2003), indicating a possible role as a cytosol-nucleus transporter protein or as a transcription modulating protein. The aminoterminal part of huntingtin contains various protease cleavage sites (Gafni and Ellerby, 2002; Gafni et al., 2004; Goldberg et al., 1996; Wellington et al., 2002; Wellington et al., 1998; Wellington et al., 2000b) and the polyglutamine repeat which is expanded in Huntington's Disease (Group, 1993a). Importantly, polyglutamine rich regions are also found in transcription factors like TBP or CREB (Everett and Wood, 2004; Friedman et al., 2008; Kim et al., 2002; McCampbell et al., 2000; Perez et al., 1998; van Roon-Mom et al., 2005). The cleavage and subsequent release of the aminoterminal segment containing the polyglutamine sequence facilitates fragment localization to the nucleus (Davies et al., 1997; DiFiglia et al., 1997; Kim et al., 2001; Lunkes et al., 2002).

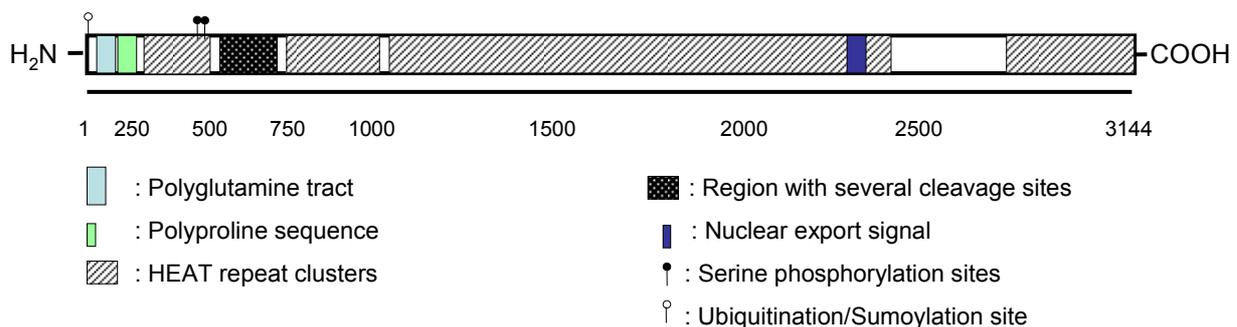


**Figure 6: The huntingtin protein.** Huntingtin is a 348 kDa large protein whose wild-type functions are still to be elucidated. The protein consists of numerous HEAT repeats which are hypothesized to be involved in protein-protein interactions, a polyglutamine region mutated at the aminoterminal part in Huntington's Disease, a polyproline region supposed to enhance protein solubility and a region containing several caspase and calpain cleavage sites. Several posttranslational modifications such as aminoterminal SUMOylation/ubiquitination or serine phosphorylations have been reported which are hypothesized to influence mutant huntingtin toxicity.

Wild-type huntingtin is reported to have numerous cellular functions. Studies showed that it is anti-apoptotic through inhibition of pro-caspase9 cleavage and caspase 3 activation (Leavitt et al., 2006; Rigamonti et al., 2000; Rigamonti et al., 2001), it controls the cortical production of BDNF, a neurotrophin known to regulate striatal survival (Alcantara et al., 1997; Fusco et al., 2003; Nakao et al., 1995; Zuccato et al., 2001; Zuccato et al., 2005; Zuccato et al., 2003), it is involved in vesicular transport (Gauthier et al., 2004; Gunawardena et al., 2003; Trushina et al., 2004) and it is reported to be involved in regulating gene transcription (Dunah et al., 2002; Holbert et al., 2001; Zuccato et al., 2001).

### **2.1.7.2 Gain-of-function or loss-of-function?**

Despite these numerous reported functions of wild-type huntingtin for normal cellular mechanisms and survival, Huntington's Disease is widely considered a gain-of-function disease which is caused by newly adopted toxic properties of the mutated protein rather than a loss-of-function disease. This is supported by several observations. First, heterozygote knock out mouse models with loss of one wild-type huntingtin allele do not show any disease phenotype (Duyao et al., 1995; Zeitlin et al., 1995) while heterozygote mutant huntingtin knock-in mouse models display Huntington's Disease like symptoms (Lin et al., 2001; Shelbourne et al., 1999). Second, transgenic mouse models which express mutant huntingtin or mutant huntingtin fragments in addition to the normal levels of endogenous wild-type huntingtin, suffer from strikingly severe neurodegeneration and Huntington's Disease symptoms (Hodgson et al., 1999; Hurlbert et al., 1999; Mangiarini et al., 1996; Reddy et al., 1998; Schilling et al., 1999; Shehadeh et al., 2006). Similarly, rat models with artificial expression of mutant huntingtin through lentiviral delivery exhibit Huntington's Disease symptoms despite the presence of two endogenous wild-type huntingtin alleles (de Almeida et al., 2002; Regulier et al., 2004). Finally, unspecific knockdown of both wild-type and mutant huntingtin mRNA through RNA interference in mouse models improves disease symptoms (DiFiglia et al., 2007; Harper et al., 2005; Machida et al., 2006; Rodriguez-Lebron et al., 2005; Wang et al., 2005), supporting the theory that it is not the decrease of wild-type but the gain of mutant huntingtin expression which causes Huntington's Disease. However, it cannot be excluded that loss of wild-type function contributes to a smaller extent to disease development and progression.

### **2.1.7.3 Structural changes of the mutated huntingtin protein**

As mentioned above, 100% penetrance in Huntington's Disease is associated with a mutated huntingtin protein in which the aminoterminal polyglutamine sequence is expanded over a critical threshold of 39 glutamines. Long polyglutamine repeats can undergo a transient conformational change in which the random-coil adopts a polar zipper conformation that is stabilized by hydrogen bonds between the amides (Figure 7) (Perutz et al., 1994). The newly formed polar zipper conformation results in a cylindrical, parallel  $\beta$ -sheet structure with one helical turn requiring 20 glutamines (Perutz et al., 2002a). However, this singular helical turn itself is unstable as the ends of the helix cannot form hydrogen bonds needed for helix stability. Importantly, a helix containing 40 or more glutamines displays two successive turns, enabling hydrogen bond formation between the two turns, thereby greatly enhancing overall

stability. A similar  $\beta$ -sheet formation has been observed in amyloid fibrils formed by yeast prion protein Sup35 as well as amyloid  $\beta$  peptide found in Alzheimer's Disease (Balbirnie et al., 2001; Benzinger et al., 2000; Perutz et al., 2002b). In all these disorders the  $\beta$ -sheet helices are proposed to act as a nuclearization seed for other monomers leading to fibril- and ultimately aggregate formation.

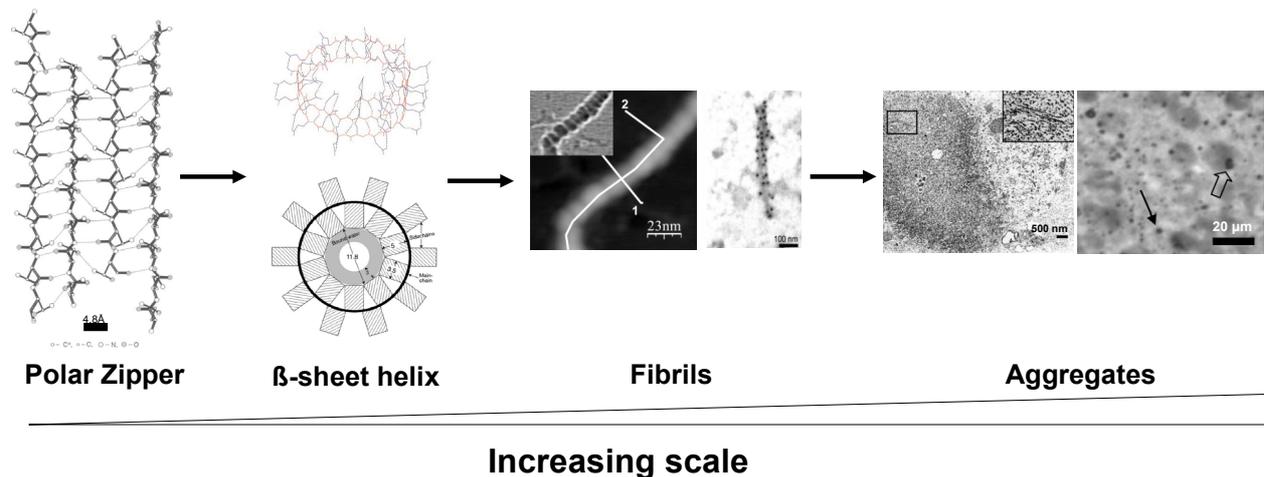


**Figure 7: Polymerisation events leading to aggregation of mutant huntingtin fragments, modified composite picture: Polar Zipper and  $\beta$ -sheet helices pictures taken from Perutz et al., 2002a and Perutz et al., 1994, fibrils and aggregates pictures taken from Diaz-Hernandez et al., 2004.** Hydrogen bonds between polyglutamines result in a polar zipper conformational arrangement between polyglutamine repeat stretches. These polar zipper strands in turn form water-filled helical  $\beta$ -sheet structures whose stability increases with increasing polyglutamine repeat length. Assembly of several of these  $\beta$ -sheet helices into fibrils leads in the end to the formation of large intracellular aggregates.

Studies in *in vitro* and *in vivo* Huntington's Disease models showed that full length mutant huntingtin has to be cleaved in order to undergo the described sequential aggregation steps (Cooper et al., 1998; Graham et al., 2006; Lunkes et al., 2002; Scherzinger et al., 1997; Scherzinger et al., 1999). It is hypothesized that uncleaved mutant huntingtin is prevented from fibrillar polymerization because of steric hindrance resulting from the size of the full length protein. The small, soluble aminoterminal mutated huntingtin fragments are then prone for stable conformational changes and thus have the ability to form fibrils and aggregates. Therefore, cleavage of mutant huntingtin and release of critical intracellular levels of mutant huntingtin fragments appears to be the rate limiting step in aggregate formation.

While the conformational changes of mutant huntingtin and the subsequent formation of large aggregates are its most striking characteristics, the role of these mutant huntingtin aggregates for Huntington's Disease are under debate and contradicting reports about aggregate toxicity have been published. Studies supporting a toxic role of huntingtin aggregates demonstrated that formation of nuclear but not cytosolic aggregates result in cell death (Bates, 2003; Chen et al., 2001; Chen et al., 2002; Saudou et al., 1998; Yang et al., 2002). *In vivo* experiments

using a mouse model conditionally expressing mutant huntingtin showed that development of symptoms depended on the continuous expression of the transgene. Interestingly, switching off mutant huntingtin production not only stopped disease progression but also reversed the aggregate load in the mouse brain (Martin-Aparicio et al., 2001; Yamamoto et al., 2000). However, these findings have to be interpreted with care as they merely show correlation between aggregate formation and Huntington’s Disease progression and not necessarily causation. Reports using time-lapse single cell microscopy question the toxic role of huntingtin aggregates by showing that neuronal death is dependent on the amount of diffuse mutant huntingtin inside the cell and not the number of aggregates. Interestingly, neurons displaying aggregate formation seem to survive even longer than those without visible aggregates suggesting a neuroprotective role for aggregates as a molecular sink for soluble pathogenic mutant huntingtin forms (Arrasate et al., 2004; Saudou et al., 1998).

### 2.1.8 Potential pathogenic molecular mechanisms Huntington’s Disease

The exact cause for cell death resulting from expression of either soluble mutant huntingtin species or formation of insoluble huntingtin aggregates remains unclear and various toxic mechanisms have been suggested including impairment of vesicle transport, transcriptional dysregulation, mitochondrial dysfunction and proteasome blockage (Figure 8).

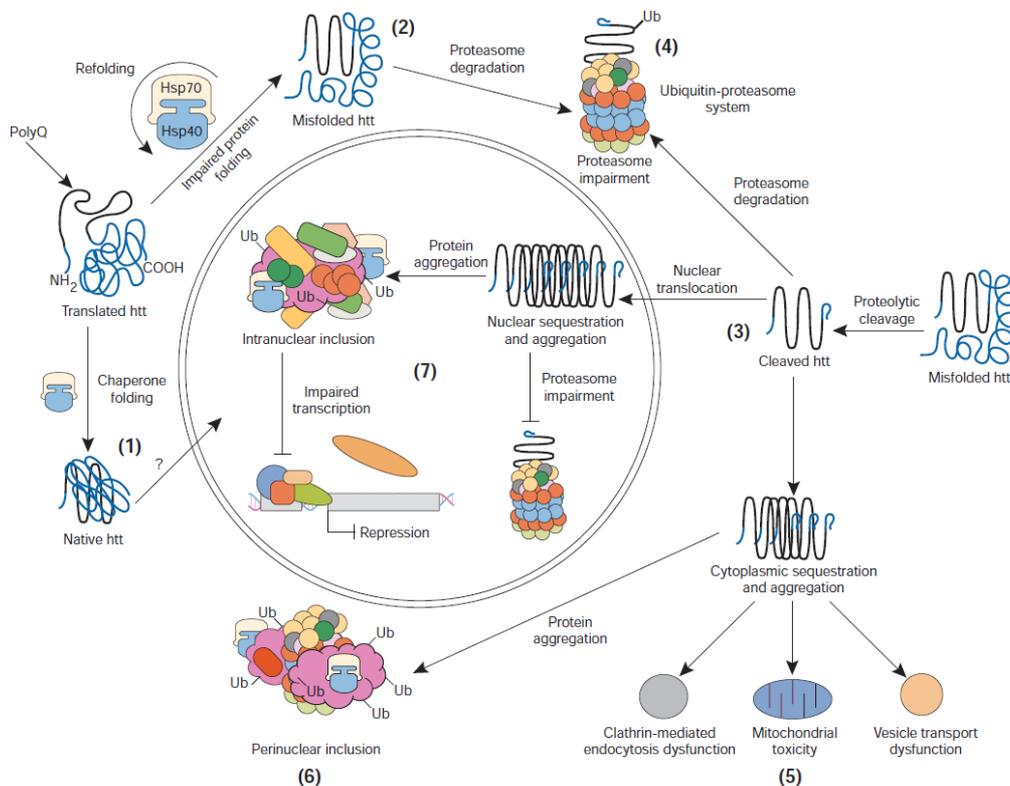


**Figure 8: Possible pathogenic mechanisms of mutated huntingtin protein, taken from Landles and Bates, 2004.**

Numerous groups have reported transcriptional dysregulation in Huntington's Disease caused by association of different transcription factors like specificity protein 1 (SP1) (Dunah et al., 2002; Hodges et al., 2006; Luthi-Carter et al., 2002a; Luthi-Carter et al., 2002b), cyclic AMP (cAMP) response element binding (CREB) protein (Glass et al., 2000; Jiang et al., 2006; Nucifora et al., 2001; Wyttenbach et al., 2001) or TATA-box binding protein (TBP) (Schaffar et al., 2004) with mutant huntingtin. As a result, these transcription factors are sequestered into intranuclear aggregates thereby leading to a general decrease in expression levels of their target genes (Figure 8, #7).

Possibly related to the reported transcriptional dysregulations is the finding of mitochondrial impairment in Huntington's Disease. Expression of the transcriptional coactivator peroxisome proliferator-activated receptor-gamma coactivator 1 (PGC-1alpha) is regulated by CREB (Herzig et al., 2001). PGC-1-alpha is a key regulator of cellular metabolism and mitochondriogenesis (Puigserver and Spiegelman, 2003). Interestingly, PGC-1alpha is consistently downregulated in Huntington's Disease animal models as well as in patients resulting in mitochondrial dysfunctions (Cui et al., 2006; Weydt et al., 2006). In addition, PGC1-alpha knock-out mice display a specific striatal degeneration phenotype similar to the one observed in Huntington's Disease (Leone et al., 2005; Lin et al., 2004). Besides these indirect links between mitochondrial impairment in Huntington's Disease through transcriptional dysregulation, direct association of mutant huntingtin with mitochondria has been reported which results in specific dysfunctions of complexes II and III of the mitochondrial respiratory chain and oxidative damage (Orr et al., 2008; Solans et al., 2006) (Figure 8, #5).

Another possible reason for mutant huntingtin toxicity could be the direct impairment of the ubiquitin-proteasome system. Various studies reported an inability of the proteasome machinery to degrade peptides containing long polyQ-repeats, resulting in a blockage of the proteasome degradation pathway and subsequent cellular changes of the ubiquitin system in Huntington's Disease patients (Bence et al., 2001; Bennett et al., 2007; Jana et al., 2001) (Figure 8, #4).

Because of the great variety of the affected cellular mechanisms in Huntington's Disease, the exact reasons for mutant huntingtin toxicity are still not fully understood. Interestingly, recent findings suggest that efforts to pinpoint a specific pathogenic mechanism of action in Huntington's Disease might be impossible as the numerous reported dysfunctions might be secondary due to a general, unspecific impairment in cellular protein homeostasis. This could be caused by the flux of misfolded proteins acting as additional stressors to the chaperone

system, which is responsible to keep the balance between folding, translocation and protein clearance (Morimoto, 2008; Prahlad et al., 2008).

Therefore, treatments aiming to restore specifically only one impaired cellular mechanism in Huntington's Disease might be condemned to fail. Thus, recent discovery work for therapeutics have been expanded to include potential therapies which influence the misfolding or the clearance of mutant huntingtin thereby tackling the most upstream event leading to Huntington's Disease. This includes e.g. the upregulation of the chaperone system (Perrin et al., 2007; Zourlidou et al., 2007), inhibition of mutant huntingtin cleavage (Kim et al., 2006) or induction of the autophagy degradation pathway (King et al., 2008; Yamamoto et al., 2006).

## 2.2 Time resolved fluorescence resonance energy transfer

### 2.2.1 Fluorescence resonance energy transfer (FRET)

The eponymous report with the first description of resonance energy transfer was published six decades ago by Förster (Förster, 1948). Fluorescence resonance energy transfer (FRET) is a quantum-mechanical phenomena based on energy coupling through the dipoles of two fluorescent molecules which occurs when two fluorophores are in close proximity to each other. Under such conditions, excitation of the donor fluorophore results in emission from the acceptor fluorophore at expense of donor-emission, presumed that the emission spectrum of the donor overlaps with the excitation spectrum of the acceptor (Stryer, 1978). Förster showed that efficiency of FRET ( $E_{\text{FRET}}$ ) is largely dependent on the distance "r" between the two fluorophores (Figure 9):

$$E_{\text{FRET}} = 1 / [1 + (r / R_0)^6]$$

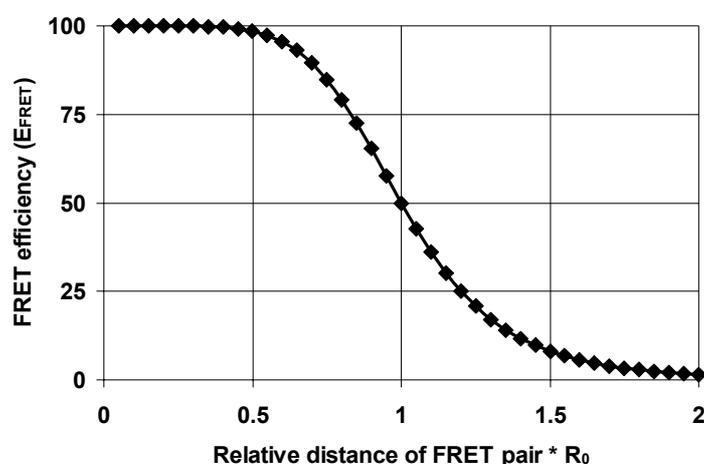


Figure 9: FRET efficiency in dependence to the distance of the two fluorophores.

The Förster radius  $R_0$  is the distance for a defined fluorophore pair where  $E_{\text{FRET}}$  equals 50%. It is a non-empirical value and can be calculated through:

$$R_0 = [2.8 * 10^{17} * \kappa^2 * Q_D * \epsilon_A * J(\lambda)]^{1/6} \text{ nm}$$

with  $\kappa^2$  being the dipole orientation factor,  $Q_D$  the fluorescence quantum yield of the donor when acceptor is absent,  $\epsilon_A$  the maximum acceptor extinction coefficient and  $J(\lambda)$  being the overlap integral between donor and acceptor spectra. Since all the variables determining  $R_0$  only influence its value by the sixth power, the normal  $R_0$  limit for FRET pairs using fluorophores with a strong maximum acceptor extinction coefficient as well as a high quantum yield of the donor is around 4 to 6 nm (Patterson et al., 2000; Wu and Brand, 1994). While FRET is routinely used for imaging experiments investigating e.g. protein-protein-interactions it has some technological limitations like photobleaching or bleed-through between the two fluorophores (light which is supposed to excite only the donor also excites directly the acceptor fluorophore because of overlap in the excitation spectra). More importantly for drug discovery purposes, a further limitation inherent to the nature of FRET exists which complicates its application in high-throughput compound screens. In large automated primary screens designed to test 100'000 to over 1 millions compounds with a sample size of  $n=1$ , readout reliability and assay robustness is a prerequisite for any successful screen. Since FRET is severely affected by numerous possible screening artifacts such as autofluorescence of compounds or cellular components as well as light scattering resulting from precipitating compounds, FRET based readouts become highly unreliable under most high-throughput screening conditions. However, a related technology termed time resolved FRET can overcome most of these limitations.

### 2.2.2 Time resolved FRET

The disadvantages of normal FRET for high-throughput screening can be overcome by the use of rare earth complexes. These complexes are characterized by an organic trisbipyridine cryptate which engulfs a lanthanide ion such as europium<sup>3+</sup> (Alpha et al., 1987). Light excitation of the complex results in a controlled energy transfer from the organic cage to the europium<sup>3+</sup> ion. The lanthanide ion subsequently emits a very long-lived fluorescence which is not affected by photobleaching.

For several reasons, these properties make the europium cryptate an excellent donor fluorophore for a time resolved FRET when used in combination with an acceptor fluorophore

(Mathis, 1993). First, rare earth ion cryptates display very large Förster radii of up to 9 nm as opposed to the 4 to 6 nm found in common fluorophores, enabling acceptor-donor interactions over much larger distances, thus simplifying their use for immunodetection methods (Bazin et al., 2001). Second, the unique long-lived emission from the cryptate-ion complex allows for time-dependent separation of the fluorescence artifacts which limit normal FRET assays from the specific time delayed excitation of the FRET acceptor fluorophore (Figure 10). Third, the possibility of time resolved measurements for wavelengths specific for the donor as well as the acceptor fluorophore results in a ratiometric readout which automatically corrects for assay volume errors as well as signal quenching or scattering, thereby increasing assay robustness and reliability (Imbert et al., 2007).

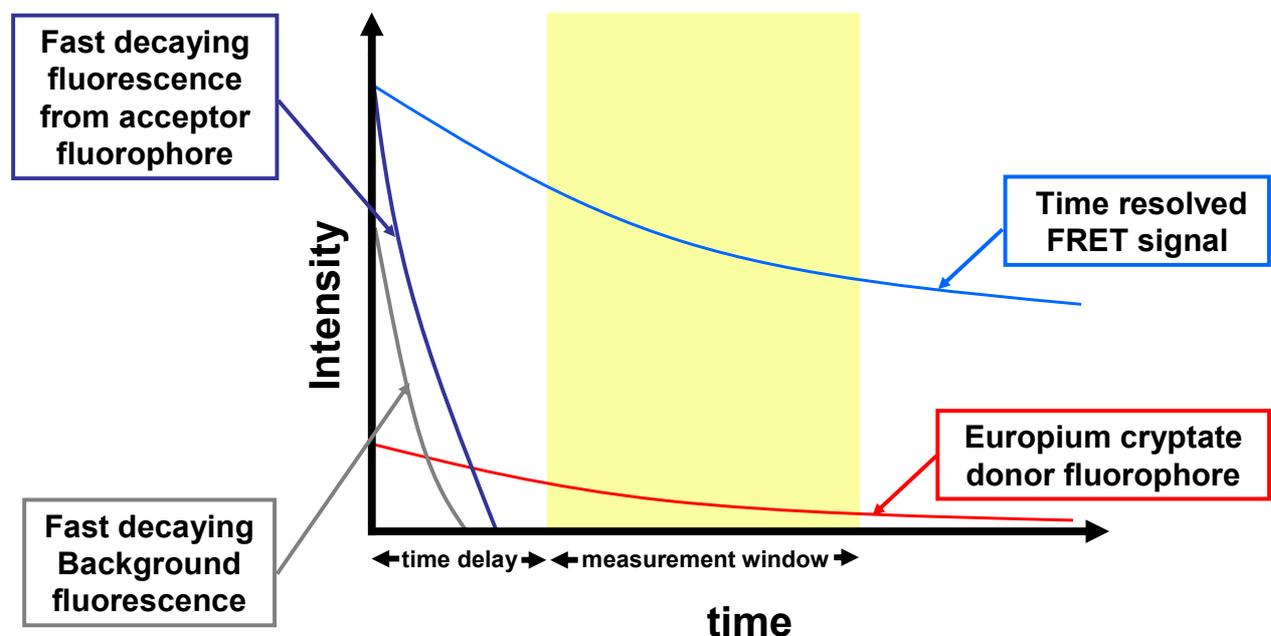


**Figure 10: Schematic presentation of time resolved FRET.** The time dependent intensity decay for four different fluorescence signals in a homogenous sample system where fluorophore-labeled antibodies are present in excess over their antigen is shown. After excitation of the sample, the matrix background fluorescence (grey) of the sample and the fluorescence resulting from the direct flash excitation of the acceptor fluorophore-labeled antibody (dark blue) decrease rapidly. Introducing a time delay of  $\sim 100 \mu\text{s}$  between sample excitation and fluorescence measurement therefore allows for separation of this nonspecific fluorescence from the specific time resolved FRET signal. In contrast to this short lived matrix fluorescence, the europium cryptate donor fluorophore-labeled antibody displays a very long lived (up to 1 ms) emission after flash excitation (red). When the donor fluorophore-labeled antibody and the acceptor fluorophore-labeled are in close proximity to each other as a result of binding to the same antigen, a fluorescence resonance energy transfer occurs between the two fluorophores thus resulting in a time resolved FRET signal (light blue) whose intensity is directly proportional to the amount of antigen present in the sample.

### **3 AIMS OF THE THESIS**

At present, the pathogenesis of mutant huntingtin remains enigmatic, also due to insufficient characterization and quantification of the interplay between soluble and aggregated mutant huntingtin species. Therefore, my goal was to monitor huntingtin protein levels in its soluble and aggregated form and to find new methods and treatments to characterize or influence the balance between these conformational species.

In order to study mutant huntingtin levels under controlled conditions, my first goal was to establish a cellular model system recapitulating major aspects found in Huntington's Disease patients such as aggregation of mutant huntingtin and transcriptional dysregulation. As the precise pathogenic mechanisms of mutant huntingtin protein in neurons are yet not fully understood, the cellular model should display greatest possible flexibility to study the effect of wild-type and mutant huntingtin expression under a variety of cellular conditions. Using my cellular model, I aimed to establish a biochemical method for the precise and sensitive quantification and characterization of huntingtin aggregates.

In parallel, since only symptomatic treatments for Huntington's Disease exist, another goal of this thesis was to develop a highly sensitive, rapid, automated and robust quantification assay based on time resolved fluorescence resonance energy transfer. This assay enabled me to examine new therapeutic approaches by identifying compounds which directly modify the level of mutated huntingtin protein. In addition, if the search for compounds lowering mutant huntingtin in the cellular model is successful, I needed to establish a method enabling me to monitor the amount of mutant huntingtin during disease progression also in living human patients. I therefore aimed at creating a novel bioassay with reliable and easy quantification of human mutant huntingtin in readily accessible tissue samples.

## **4 RESULTS**

### **4.1 Inducible mutant huntingtin expression in a neuronal cell model leads to transcriptional dysregulation and cell death**

**Andreas Weiss, Dorothee Bleckmann, Stephan Grueninger, Muriel Stefani, Natacha Stoehr, Emmanuel Lacroix, Miriam Bibel, Etienne Régulier and Paolo Paganetti**

Neuroscience Discovery, Novartis Institutes for BioMedical Research, Basel, Switzerland

#### **4.1.1 SUMMARY**

Expansion of a polyglutamine repeat at the aminoterminal part of huntingtin protein leads to Huntington's Disease, an autosomal-dominant neurodegenerative disorder characterized by impaired motor performance and severe brain atrophy. The proposed pathogenic cellular mechanisms of mutant huntingtin protein are numerous and include formation of intracellular huntingtin protein aggregates, transcriptional dysregulation, neurite dystrophy and mitochondrial dysfunction. Here, we describe a novel neuronal model with inducible expression of wild-type and mutant huntingtin fragments under proliferating and differentiating conditions. We further demonstrate that the induced expression of aminoterminal fragments of mutant huntingtin causes transcriptional dysregulation and cellular dysfunction. Recapitulation of the pathogenic findings from human patients in these cells recommends this neuronal model for further investigations of the biological mechanism of mutant huntingtin, allowing us to characterize the development and the pathology of Huntington's Disease on a cellular level.

### 4.1.2 INTRODUCTION

Huntington's Disease (HD) is an inherited, autosomal-dominant neurodegenerative disorder whose main clinical symptoms include chorea, cognitive decline and weight loss (Nance and Sanders, 1996; Young et al., 1986). Patients normally display first disease symptoms in mid-age with a relentless disease progression and premature death 15 to 20 years after appearance of clinical symptoms (Foroud et al., 1999). The disorder is caused by a mutated and expanded polyglutamine (polyQ) stretch in the huntingtin protein (Htt), a 348 kDa large, ubiquitously expressed protein with yet unclear cellular function (Group, 1993a; Gusella et al., 1983). Cleavage of full-length mutated Htt leads to the release of aggregation prone aminoterminal Htt fragments carrying the expanded polyQ repeat (Cooper et al., 1998; Lunkes et al., 2002; Scherzinger et al., 1999). The cause for cell death as a result of mutant Htt expression is yet not fully understood and different pathogenic mechanisms have been proposed, including impaired axonal trafficking and microtubule destabilization (Gunawardena et al., 2003; Trushina et al., 2003), transcriptional dysregulation (Hodges et al., 2006; Jiang et al., 2006; Schaffar et al., 2004; Wyttenbach et al., 2001) and mitochondrial dysfunction (Solans et al., 2006).

Various cellular models for HD have been developed to study the effect of mutant huntingtin expression on cellular mechanisms. Non-neuronal primary cells from HD patients have been used to study CAG repeat variability (Manley et al., 1999a) or calcium homeostasis (Sawa et al., 1999). Expression of mutant Htt in murine primary neuronal cultures results in neuritic degeneration and induction of apoptotic pathways (Li et al., 2000; Saudou et al., 1998). Immortalized striatal neurons showed increased vulnerability to mitochondrial toxins and impaired mitochondrial complex II function in presence of stable mutant Htt expression (Ruan et al., 2004; Trettel et al., 2000).

While the use of primary neuronal cultures or stable expressing cell lines vastly increased the understanding of HD pathology, such cellular models display several drawbacks for their use in drug discovery purposes such as the limited availability of primary cultures and the possible adaptation to the toxic insult in cell lines stably expressing mutant Htt. To overcome these disadvantages, we developed a neuronal model which recapitulates cellular dysfunctions seen in HD patients but is available in unlimited cell numbers and provides flexibility for future experiments. We chose the neuroblastoma line HN10, a readily transfectable neuronal line which can be cultured under mitotic and post-mitotic conditions (Lee et al., 1990; Sommerfeld et al., 2000). To eliminate adaptational clonal effects, we created HN10 cell lines with inducible expression of different wild-type and mutant Htt constructs. In this study, we

show that this inducible neuronal model reproduces key pathogenic mechanisms found in HD patients and provides a valuable in vitro system for drug discovery research in HD.

### **4.1.3 MATERIAL AND METHODS**

#### **Cell culture**

For keeping the HN10 cells in a mitotically active state, cultures were grown in proliferating media (high-glucose DMEM (Gibco), 10% FCS, penicillin + streptomycin) at 37°C and 5 % CO<sub>2</sub>. Exchange of the medium and splitting of the cells occurred every 2-3 days. In order to keep the cells under differentiating, post-mitotic conditions, proliferating cells were collected and resuspended in proliferating media and plated in 20% confluency on dishes precoated with 20 µg/µl laminin (SIGMA). After 1 day, proliferating media was removed and cells were cultured in differentiating media (serum-free media, supplements (Brewer et al., 1993), 45 µM retinoic acid (SIGMA)) until time of the readout. For immunohistochemistry, cells were fixed with 4% paraformaldehyde and stained with the anti-huntingtin antibody 2B7 (custom designed by GENOVAC, Freiburg, Germany), the anti-huntingtin mEM48 antibody (Millipore, MAB 5374) or the anti-polyglutamine antibody m1C2 (Millipore, MAB 1574) and Hoechst nuclei stain (Invitrogen) according to standard immunohistochemistry protocol.

#### **Creation of stable inducible clones**

Parental HN10 cells were transfected with the receptor pNEBR-R1 plasmid part of the inducible rheoswitch mammalian system (New England Biolabs). Transfected cells were seeded in a dilution series on 96-well plates to statistically achieve singular clones in the higher diluted wells and cultured under selection with 1 mg/ml geneticin (Invitrogen). After 2 weeks of selection, >30 identifiable clone colonies from the highest diluted wells were picked and reseeded on a 24-well plate. Selected clones were compared to the parental HN10 cell line in terms of morphology, speed of growth and their ability to differentiate. After this preselection 21 remaining clones were transiently transfected with a luciferase reporter plasmid and cultured for 2 days with or without inducer. Clone with best induction ratio was selected to develop four stable HN10 cell lines with inducible expression of the aminoterminal huntingtin fragments exon1-25Q, exon1-72Q, aa857-25Q and aa857-72Q.

#### **Western blot and AGERA**

Monomeric and aggregated huntingtin fragments were detected by western blot or AGERA as described in Weiss et al., 2008.

### **Real time PCR**

Exon1-72Q clone was cultured under proliferating or differentiating conditions with or without inducer. RNA was isolated with RNeasy Mini kit (Qiagen). Real time PCR was performed with customized TaqMan® microfluidic card arrays (Applied Biosystems) according to manufacturers protocol. Eight different samples were analyzed simultaneously for 15 probes + 18S control. 100 to 150 ng of total RNA were used in the First-Strand cDNA synthesis according to manufacturers protocol (Invitrogen, SuperScript III Platinum). The cDNA was added to the microfluidic card using 30 µl cDNA, 50 µl 2x Platinum qPCR SuperMix-UDG with ROX and 100 µl DEPC water. After two centrifugations at 1000 g for 1 min, the micro fluidic card was sealed and analyzed. After an incubation at 50°C for 2 min, samples were denatured at 94.5°C for 2 min. The following parameters were then set for optimal amplification of selected probes during 45 cycles: 97°C for 30 sec and 59.7°C for 1 min. Data were extracted and Ct values normalized by 18S calibration.

### **Protein and aconitase measurements**

For protein and aconitase measurements, proliferating or differentiating HN10-exon1-72Q clone was cultured on 24-well plates under noninduced or induced conditions. After 1, 2 and 3 days of cell culture, wells were washed 3x with PBS and protein content of each well was measured with BCA™ Protein Assay Kit (Perbio). The aconitase activity assay was adapted from previously described methods (Gardner et al., 1994; Hausladen and Fridovich, 1996). Briefly, wells were washed with 100 µl of PBS followed by addition of 30 mM sodium citrate, 0.5 mM MnCl<sub>2</sub>, 50 mM Tris, 0.2 mM NADP, 2 U/ml isocitrate dehydrogenase, 1 % Triton, pH 7.5. After mixing, kinetic measurements were done at 37°C in Fluoroskan microplate fluorometer with 355/460 nm over 30 min.

### **Neurite quantification**

Analysis of neurite outgrowth was performed with LI-COR Biosciences In-Cell Western™ assay. Exon1-25Q and exon1-72Q clone were cultured under differentiating conditions with or without inducer for up to 6 days on clear 96-well plates. HN10 neurites can be visualized with anti-tubulin immunohistochemistry. For this, cells were fixed with 4% paraformaldehyde and stained with anti-tubulin (Abcam). After washing, cells were incubated with IRDye 800CW anti-mouse secondary antibody (LI-COR Biosciences) and DRAQ5™ nuclei stain (Biostatus Limited). Quantification of tubulin and nuclei was performed with Odyssey®

imager & software (LI-COR Biosciences). The ratio of tubulin stain and cell number (nuclei stain) reflected the amount of neurites per cell formed under the different conditions.

### **Caspase 3/7 activity**

Exon1-25Q and exon1-72Q clone were cultured under differentiating conditions with or without inducer for up to 5 days on an opaque 96-well plates. Caspase 3/7 activity was determined using the Caspase-Glo 3/7 Assay (Promega) as recommended by the manufacturer using a RUBYstar reader (BMG Labtech).

#### 4.1.4 RESULTS

##### Inducible expression of wild-type and mutant huntingtin fragments in a neuronal cell line

Aminoterminal mutant huntingtin fragments carrying an expanded polyQ stretch are toxic *in vitro* and *in vivo* through a gain-of-function mechanism but the precise pathogenic cellular mechanism are yet not fully understood (Arrasate et al., 2004; Hurlbert et al., 1999; Mangiarini et al., 1996; Schilling et al., 1999; Varma et al., 2007). To examine in detail toxic mechanism(s) of action of mutant huntingtin fragments, *in vitro* models are needed which recapitulate the cellular defects found in patients. We thus generated four stable neuronal HN10 clone lines with inducible expression of short (exon1) or long (aa857) amino-terminal Htt fragments carrying either a wild-type (25Q) or a mutant (72Q) polyQ length (Figure 11A). All cell lines displayed no basal expression, whereas the expression levels of Htt fragments were readily detectable upon induction (Figure 11B). Expression of Htt was confirmed by immunohistochemistry. Notably, only the expression of the exon1-72Q fragment resulted in visible aggregate formation in a subset of cells (Figure 11C).

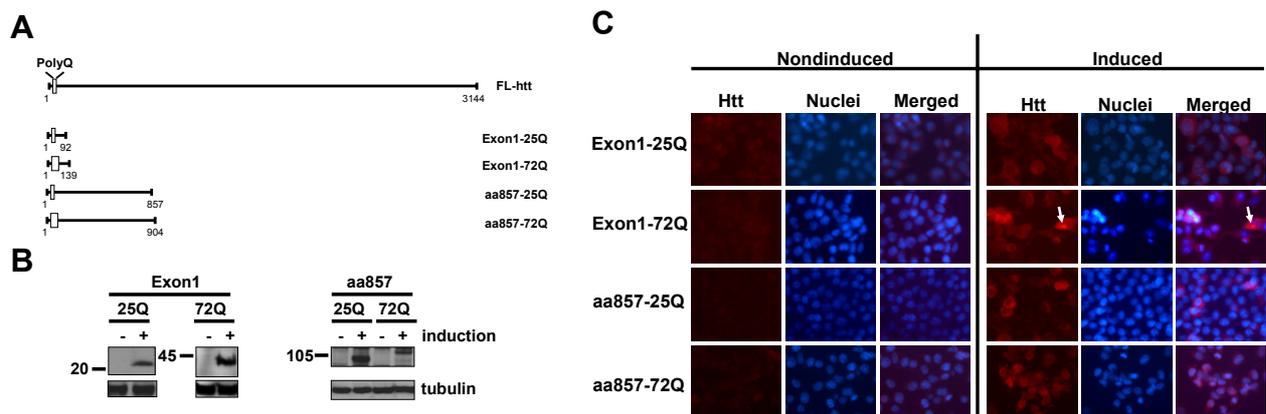


**Figure 11: Inducible expression of wild-type and mutant huntingtin fragments in clonal HN10 cell lines.** **A:** Wild-type (25Q) and mutant (72Q) huntingtin fragments used for creation of stable and inducible HN10 clones in comparison to the endogenous full length huntingtin. **B:** Western blots of huntingtin expressing HN10 clones cultured with or without inducer. No basal expression is detectable in absence of inducing ligand. **C:** Immunohistochemistry of huntingtin expressing HN10 clones cultured with or without inducer. After 5 days of induction, expression of exon1-72Q fragment leads to aggregate formation in a subset of cells (arrow) whereas clones expressing exon-25Q, aa857-25Q and aa857-72Q do not show any detectable aggregate formation.

After the addition of inducer, an increase in Htt fragment levels was observed over 24 hours, whereas the subsequent removal of the inducer from the culture medium caused a time dependent decrease of the Htt fragments (Figure 12A and Figure 12B). Further quantification of fragment expression levels revealed a dose dependency correlating with the concentration of the inducer in the culture medium (Figure 12C). Supporting the immunohistochemical observation, aggregate formation after induction of exon1-Q72 expression was confirmed

with AGERA (Weiss et al., 2008) (Figure 12D) while expression of the two wild-type constructs or of the larger aa857-72Q construct did not lead to any detectable aggregate levels even when using this sensitive biochemical aggregate detection method (data not shown).

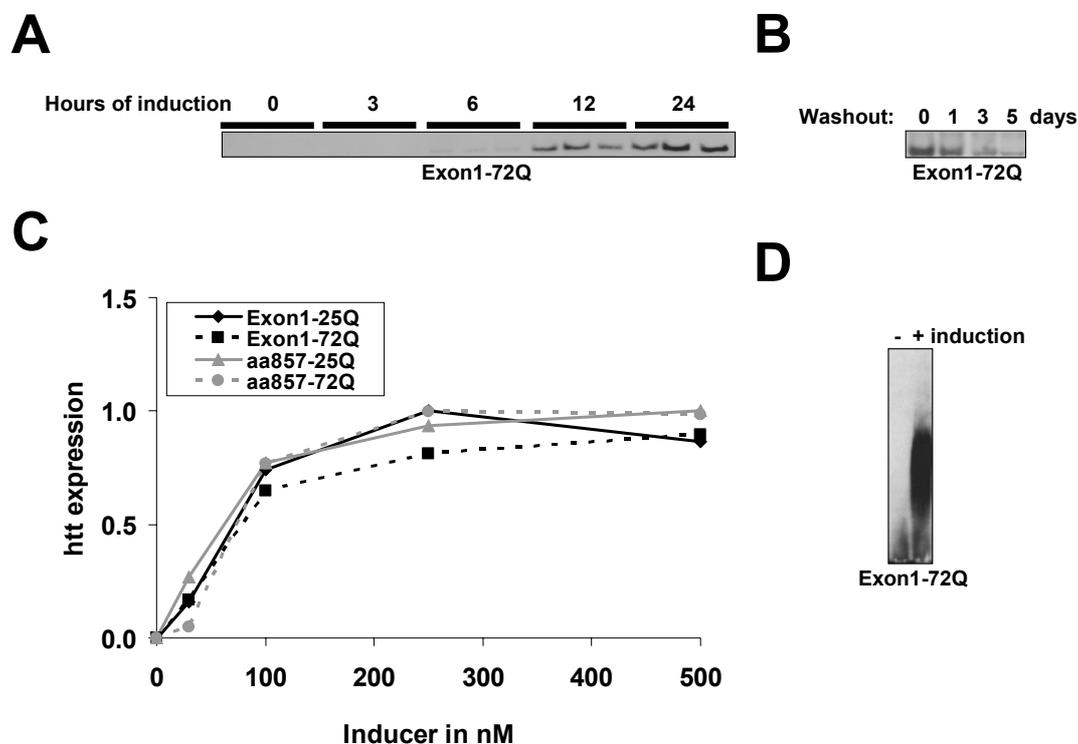


**Figure 12: Time dependent induction of exon1-Q72 monomer expression and aggregation formation.** **A:** Addition of inducer to the culture medium leads to a time dependent increase of exon1-72Q expression with first detectable protein levels after 6 h (biological triplicates). **B:** Removal of the inducer from the culture medium leads to decreasing exon1-72Q levels over time. **C:** Increasing inducer concentrations to the culture medium of exon1-25Q, exon1-72Q, aa857-25Q and aa857-72Q clones reveal dose dependent huntingtin fragment expression response for all 4 clones (western blot quantification). **D:** AGERA blot of noninduced or induced exon1-72Q cells reveals detectable aggregate levels after induction.

A common finding in HD models is that the length of the huntingtin construct carrying the polyQ repeat influences aggregate formation and severity of disease symptoms. Full length mutant huntingtin is cleaved into smaller fragments (Lunkes et al., 2002; Ratovitski et al., 2007; Scherzinger et al., 1999) and decreased mutant huntingtin fragment length correlates with increased disease progression and aggregate formation (Kim et al., 2001; Martindale et al., 1998; Schilling et al., 2007; Weiss et al., 2008). Further work focused on characterizing the HN10-exon1-Q72 cell line as it expresses the shortest aminoterminal mutant fragment which is most prone to aggregate. Since mutant huntingtin aggregation and impairment of cell viability is most pronounced in differentiated adult neuronal cells (DiFiglia et al., 1997; Fennema-Notestine et al., 2004; Li et al., 2000; Macdonald and Halliday, 2002; Rosas et al., 2003), it was important that our cellular model can be cultured under mitotic and post-mitotic

conditions (Figure 13), therefore allowing for analysis of exon1-72Q expression effects under proliferating as well as differentiating conditions.

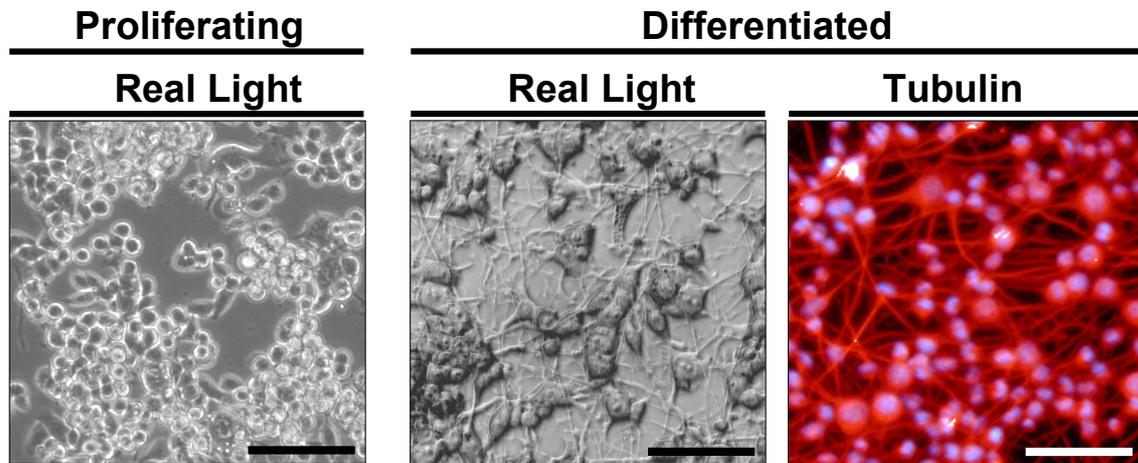


**Figure 13: HN10 cells can be grown under proliferating and differentiated conditions.** Adjusting the culture conditions allows for controlled differentiation of the normally proliferating HN10 cells. Staining with tubulin (red) and Hoechst nuclei stain (blue) reveals the dense neurite network formed after 7 days of differentiation. (representative pictures, all bars=100  $\mu$ m).

### **Exon1-72Q expression decreases PGC1-alpha levels and impairs cellular viability**

One of the major characteristics of HD is transcriptional dysregulation. Transcription factors such as specificity protein 1 (SP1) (Dunah et al., 2002; Hodges et al., 2006; Luthi-Carter et al., 2002a) and cAMP response element binding (CREB) protein (Jiang et al., 2006; Nucifora et al., 2001; Wyttenbach et al., 2001) can interact with mutant huntingtin and get sequestered into intranuclear aggregates, resulting in a decreased transcription of their target genes. To examine the relevance of our model for transcriptional dysregulation as a result of mutant huntingtin expression, we analyzed the expression levels of several genes which are under the promoter control of SP1 or CREB. First, we compared gene expression in noninduced proliferating versus differentiating HN10-exon1-72Q cells. As expected, keeping the cells in a proliferative active or in differentiated state resulted in different gene expression patterns (Figure 14A). Expression of transcriptional coactivator peroxisome proliferator-activated receptor-gamma coactivator 1 (PGC-1alpha), a CREB dependent master regulator of mitochondriogenesis (Puigserver and Spiegelman, 2003), was found to be upregulated in noninduced differentiating cells, possibly reflecting the increased energetic demand of differentiating cells due to extensive neurite formation. Differences in basal PGC-1alpha expression levels were of special interest for establishing a valid cellular HD model, as human PGC-1alpha is one of the key genes found to be constantly downregulated in HD patients (Cui et al., 2006; Weydt et al., 2006). When analyzing the effect of induced exon1-72Q on gene

expression we detected a downregulation of PGC-1alpha in proliferating (Figure 14B) as well as in differentiating cells (Figure 14C).

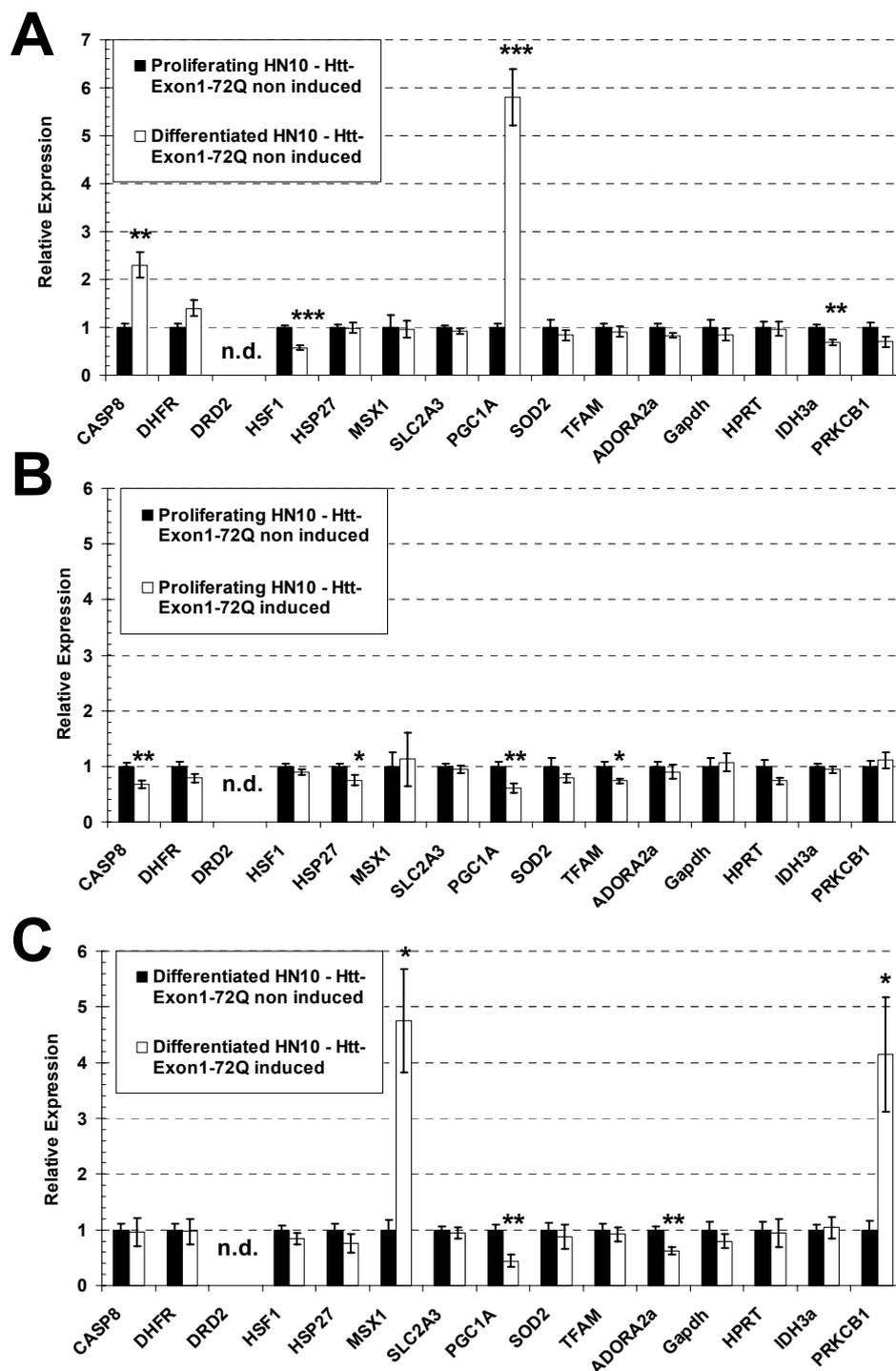


**Figure 14: Differences in transcriptional dysregulation in proliferating and differentiated HN10 cells with or without exon1-72Q induction.** A: Real-time PCR for 15 genes of interest in Huntington’s Disease reveals influence of culture conditions on gene expression in noninduced HN10 exon1-72Q clone with pronounced upregulation of PGC1A expression (~6-fold) upon differentiation. B: Induced expression of exon1-72Q in proliferating cells results in significant downregulation of PGC1A and TFAM, genes known to be also decreased in Huntington’s Disease patients. C: Expression of exon1-72Q in differentiated cells reproduces the significant downregulation of PGC1A. (All graphs: n=3, p<0.05=\*, p<0.01=\*\*, p<0.001=\*\*\*).

Next, we examined whether expression of mutant Htt fragment and the downregulation of PGC-1alpha influenced cell viability or mitochondrial function. For this, cells were cultured under proliferating or differentiating conditions with or without induction of exon1-72Q for three days and cellular protein levels were measured to determine general cell viability. Cellular protein amounts increased with time when culturing the cells under proliferating conditions, reflecting the mitotic nature of the cells (Figure 15A, upper graph). A small but not significant decrease in cellular protein levels was detected after 3 days in the proliferating clones with exon1-72Q expression compared to proliferating noninduced clones. The influence of exon1-72Q expression increased when keeping the clone under differentiating, non-dividing conditions. Significant decrease of cellular protein levels between noninduced and induced cells were detected already after 2 days of exon1-72Q expression and differences increased after 3 days of induction, indicating a general impairment of cell viability as a result of mutant Htt expression (Figure 15A, lower graph).

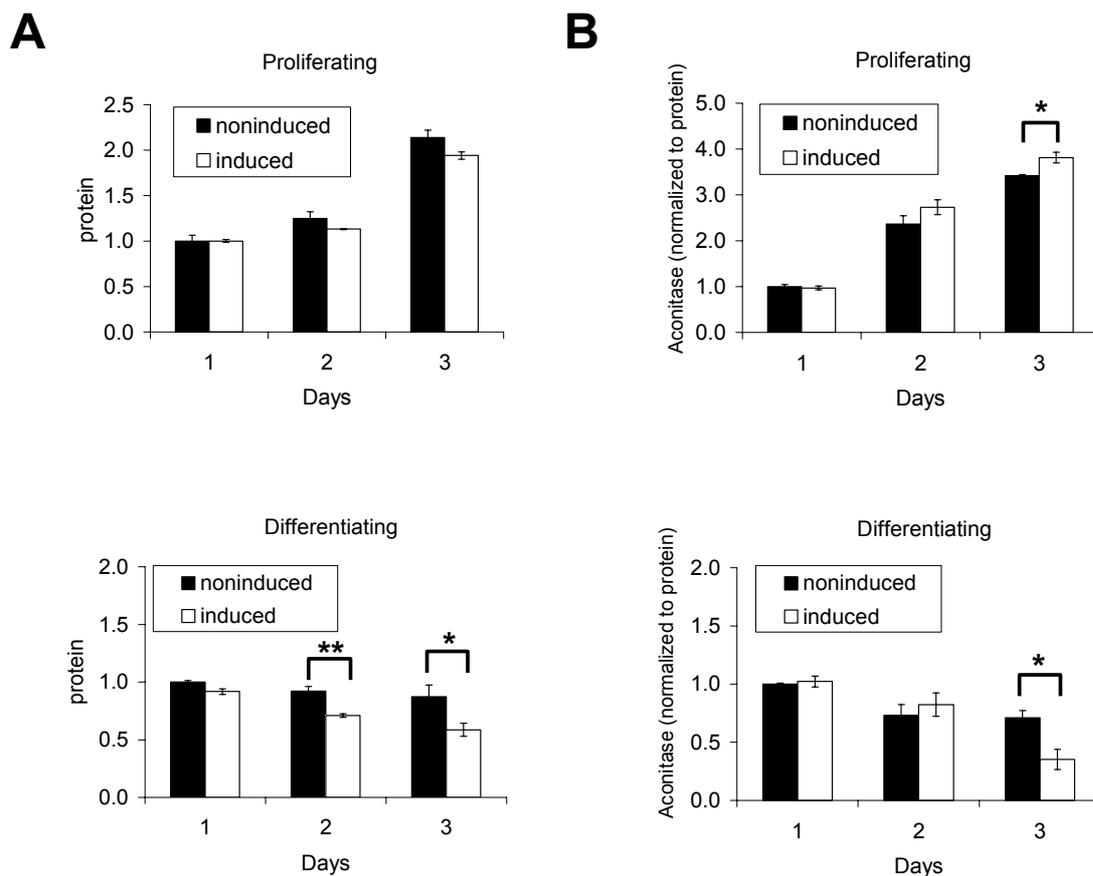


**Figure 15: Impaired cell viability and aconitase activity as a result of exon1-Q72 expression in differentiated HN10 cells.** A: Induction of exon1-72Q expression in proliferating (upper graph) and differentiating cells (lower graph) leads to decreased cell viability as measured by cellular protein expression levels only in differentiating cells. B: Aconitase activity as a measure for mitochondrial function and presence of radical oxygen species reveals impaired mitochondria function after 3 days of exon1-72Q expression in differentiated but not proliferating cells. (All graphs: n=4, p<0.05=\*, p<0.01=\*\*).

Since PGC1-alpha, a key regulator of mitochondriogenesis, was downregulated in proliferating and in differentiated cells upon exon1-72Q expression but only differentiated cells displayed a significant impairment in cell viability, we examined the influence of exon1-72Q expression on mitochondria in noninduced and induced cells under proliferating and differentiating conditions. Using aconitase activity as a marker for mitochondrial function and oxidative damage (Bulteau et al., 2003; Gardner et al., 1994; Yan et al., 1997), we found a significant mitochondrial impairment in differentiating cells after 3 days of exon1-72Q expression (Figure 15B, lower graph) but not in proliferating cells (Figure 15B, upper graph) when compared to noninduced control.

To validate that the observed effects of exon1-72Q in differentiated cells are a direct result of the mutated polyQ stretch in the exon1 fragment and not due to the expression of a Htt fragment per se, we compared the effects of wild-type exon1-25Q and mutant exon1-72Q expression on cell viability (Figure 16). Measuring caspase 3/7 activity as a generic marker for apoptosis showed an increased caspase activity in differentiated cells upon exon1-72Q expression whereas expression of the wild-type exon1-25Q fragment resulted in decreased caspase 3/7 activity (Figure 16A). Using neurite outgrowth as an orthogonal readout for the different effects of wild-type and mutant huntingtin fragments in differentiating cells verified the protective effect of exon1-25Q expression whereas expression of exon1-72Q construct resulted in a significantly decreased neurite outgrowth (Figure 16B).

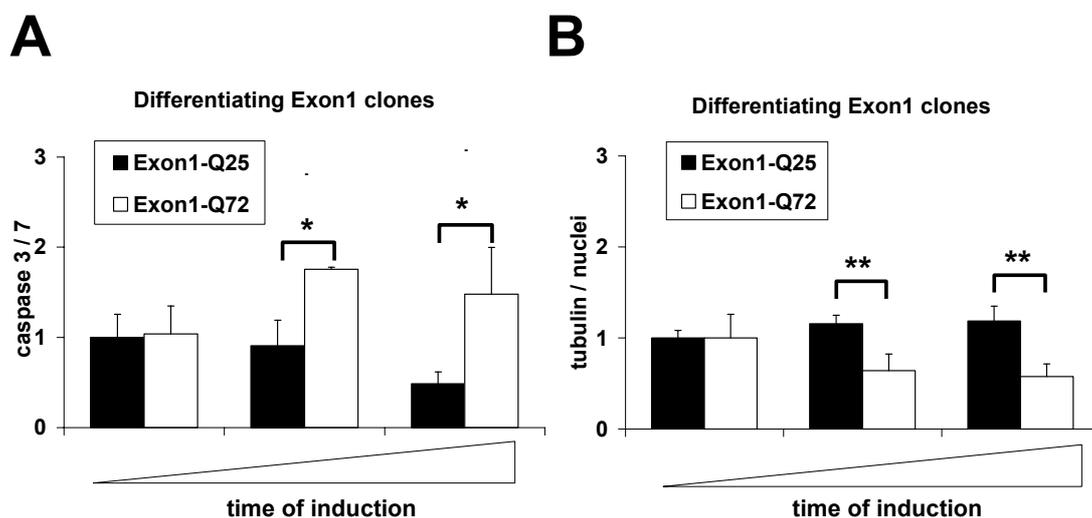


**Figure 16: Effects of wild-type and mutant huntingtin exon1 expression on cell viability in differentiated cells.** **A:** Caspase 3/7 activity as a measure of cellular dysfunction reveals increased apoptosis after exon1-72Q expression in differentiated cells. Expression of the wild-type construct exon1-25Q protects the differentiated cells from caspase 3/7 activity. **B:** Quantification of tubulin/nuclei ratio with in-cell western as a indicator for neurite outgrowth in differentiated HN10 clones upon exon1-25Q or exon1-72Q induction. Induced expression of wild-type exon1-25Q leads to increased neurite outgrowth over noninduced control whereas expression of mutant exon1-72Q construct leads to decreased neurite formation. (A: n=4, B: n=3, All graphs: p<0.05=\*, p<0.01=\*\*).

#### 4.1.5 DISCUSSION

Despite a remarkable progress in the understanding of HD, the most common monocausal neurodegenerative disorder (Bates et al., 2002), over the past decades, the cellular mechanisms leading to neuronal death remain elusive and various pathogenic mechanisms of action have been proposed including transcriptional dysregulation, impaired neurite function and mitochondrial dysfunction. In order to elucidate some of the open questions concerning the pathology of Huntington's Disease and to establish a valid cellular Huntington's Disease model which can be used for drug discovery purposes, we have developed a flexible expression system in a neuronal cell line in which we can control the amount and time of wild-type and mutant Htt expression (Figure 12) as well as the mitotic state of the cells (Figure 13).

The ability to culture the cells under both proliferating as well differentiating conditions is especially relevant considering that terminally differentiated cells such as neurons and adult muscle cells display the strongest aggregate formation and are most vulnerable to mutant huntingtin expression (Arenas et al., 1998; Fennema-Notestine et al., 2004; Lodi et al., 2000; Rosas et al., 2003; Sathasivam et al., 1999b). Since the rate of aggregation is dependent on the intracellular concentration of mutant huntingtin fragments (Scherzinger et al., 1999), the increased aggregate formation in these cell types is thought to be a direct result of their terminally differentiated status in which a threshold concentration of aggregation-prone mutant huntingtin precursors can be surpassed. In contrast, the continuous division of proliferating cells allows for a constant dilution of the cleaved mutant huntingtin fragments therefore making it more unlikely that the amount of intracellular huntingtin fragments can build up to a critical concentration. Indeed when comparing the effects of induced mutant huntingtin expression in the identical clone line which has been either cultured under proliferating or differentiating conditions, a different susceptibility to the mutant huntingtin became apparent with differentiating, post-mitotic cells being more vulnerable to the toxic insult from mutant huntingtin than the mitotically active proliferating cells (Figure 15).

By comparing the effects of exon1-25Q and exon1-72Q expression on cell viability, we showed that the sensitivity of differentiated HN10 cells to mutated huntingtin fragment is specific to the elongated polyglutamine stretch in the huntingtin fragment and not to the artificial expression of a short huntingtin fragment itself (Figure 16). Interestingly, the expression of a wild-type huntingtin fragment resulted in a protective effect on caspase 3 activity, a finding which is in agreement with earlier *in vitro* and *in vivo* Huntington's Disease

models (Leavitt et al., 2006; Rigamonti et al., 2000; Rigamonti et al., 2001) thus further validating the applicability of our inducible neuronal cells as a Huntington's Disease model. Some open questions which may limit the use of our model for Huntington's Disease research remain. Even though the toxic effect of mutant huntingtin expression on the cells has been verified with three orthogonal readouts (cellular protein levels, caspase activity and neurite outgrowth), none of these readouts examines a specific cellular pathway. Therefore in theory, it may be possible that the observed impairments in cell viability in our inducible neuronal clones are unrelated to the pathologic biological mechanism of action occurring in patients. While expression of aminoterminal mutated fragments results in a more aggressive toxicity and allows for an increased dynamic range of our readouts, this decision prevents our model from being used to answer biological questions that may require the expression of more carboxyterminal parts of the mutated huntingtin protein. For example, cellular pathways relevant for the development of Huntington's Disease that may interact specifically with huntingtin's nuclear export signal at the carboxyterminus (Xia et al., 2003) cannot be studied with our current setup. Hence, further studies should include the development of an inducible full length mutant huntingtin clone based on our neuronal model system as well as the more in-depth analysis of specific cellular pathways that are supposed to be affected in Huntington's Disease.

Nevertheless, the current data supports the applicability of our neuronal cells as a valid model for Huntington's Disease. Induced expression of mutated huntingtin fragment results in prominent cellular defects also found in patients such as aggregation of mutated huntingtin fragments, specific transcriptional dysregulation, impairment of cell viability and mitochondrial dysfunction. Future use of our cell model will therefore include pathway analysis of the toxic mechanisms of action and identification of compounds which may ameliorate the described effects resulting from mutant huntingtin expression.

## **4.2 Sensitive biochemical aggregate detection reveals aggregation onset before symptom development in cellular and murine models of Huntington's Disease**

**Andreas Weiss<sup>1</sup>, Corinna Klein<sup>1</sup>, Ben Woodman<sup>2</sup>, Kirupa Sathasivam<sup>2</sup>, Miriam Bibel<sup>1</sup>, Etienne Régulier<sup>1</sup>, Gillian P. Bates<sup>2</sup> and Paolo Paganetti<sup>1</sup>**

1) Neuroscience Discovery, Novartis Institutes for BioMedical Research, 4002 Basel, Switzerland

2) Department of Medical and Molecular Genetics, King's College London School of Medicine, London SE1 9RT, UK

Published in Journal of Neurochemistry, 2008 Feb;104(3):846-58

#### 4.2.1 SUMMARY

A CAG repeat gene expansion translated into a pathogenic polyglutamine stretch at the N-terminus of huntingtin triggers Huntington's Disease. Mutated huntingtin is predicted to adopt toxic properties mainly if aggregation-prone N-terminal fragments are released by proteolysis. Huntingtin-aggregates are indeed a major hallmark of this disorder and could represent useful markers of disease-onset or progression. We designed a simple method for qualitative and quantitative characterization of aggregates. For this, we analyzed samples from *in vitro* and *in vivo* Huntington's Disease models by agarose gel electrophoresis and show that in the brain of transgenic mice huntingtin-aggregates became larger as a function of disease progression. This appears to be a property of cytoplasmic but not nuclear aggregates. In cell cultures, treatment with Congo Red inhibited aggregate growth but not total load. Finally, we show that in primary striatal neurons and in brains of R6/2 and *Hdh*Q150 mice, the presence of aggregates preceded initiation of any other functional deficits. This observation argues for a pathogenic role of huntingtin-aggregation in Huntington's Disease. Our results emphasize that thorough analysis of huntingtin metabolism and aggregation is now feasible, thus significantly improving the power of studies assessing therapies designed to lower huntingtin levels or to interfere with its aggregation.

#### 4.2.2 INTRODUCTION

Huntington's Disease (HD) is a neurodegenerative disorder characterized by motor dysfunction (choreiform movements), emotional disturbance, dementia, and weight loss (Bates et al., 2002). HD is caused by an autosomal dominant expansion of a CAG repeat encoding for polyglutamine (polyQ) in exon 1 of the huntingtin (Htt) gene (Group, 1993b). Mutated Htt (mHtt) gains a neurotoxic function, leading to the onset of clinical symptoms mostly in mid-life. The progression of HD is characterized by a marked degeneration of gray and white brain matter whereby a loss of vulnerable neurons, most notably striatal medium-sized spiny neurons, is observed, while resistant populations are spared (Davies et al., 1997; DiFiglia et al., 1997; Henley et al., 2006; Rosas et al., 2006; Ruocco et al., 2006; Vonsattel and DiFiglia, 1998). HD progresses relentlessly with a lethal outcome about two decades after diagnosis.

In transgenic mouse models of HD the expression of N-terminal fragments or full-length mHtt leads to HD-like pathology and associated motor, cognitive and behavioral deficits. R6/2 mice are the first and most intensely studied mouse model of HD (Mangiarini et al., 1996). They express mHtt-exon 1 with an expansion of more than 150 glutamines under the control of the human Htt-promoter. The mice develop an early and severe phenotype with first motor deficits appearing already at 5-6 weeks (wk) after birth, behavioral deficits are observed at 8 wk and rapid lethality ensues after 14 wk of age. Because of this fast and prominent progression, R6/2 mice are often used to dissect the neurodegenerative processes causing HD or as a translational model for experimental therapeutics. Critically, neuronal dysfunction can be replicated *in vitro* by expressing N-terminal fragments of mHtt in cell lines and primary neuronal cultures (Li et al., 2000; Saudou et al., 1998).

A hallmark of neuropathology in animal HD models as well as in human patients affected by HD is the presence of intracellular mHtt-aggregates (Davies et al., 1997; Nguyen et al., 2006; van Roon-Mom et al., 2002; Woodman et al., 2007). It is an ongoing debate whether these mHtt containing aggregates are toxic to the cell, neutral byproducts of the pathogenic process or even neuroprotective by sequestering toxic polymeric forms of mHtt (Chen et al., 2001; Davies et al., 1997; DiFiglia et al., 1997; Yang et al., 2002). Even though the exact role of mHtt-aggregates in HD pathology remains unclear, it is a common observation that accumulation of aggregates in brains of HD patients and animal models increases with disease progression (DiFiglia et al., 1997; Gutekunst et al., 1999; Menalled et al., 2003; van Roon-Mom et al., 2002; Woodman et al., 2007). In R6/2 mice, histochemistry was used to show wide-spread accumulation of Htt in cytosolic and nuclear inclusions, which increased in

number and size with age and whose formation was highly correlated with the progression of neurological symptoms (Li et al., 1999). In light of these findings, detailed and sensitive mHtt-aggregate characterization is therefore required when analyzing disease onset and progression or for testing disease-modifying treatments.

As discussed, histochemistry provides access to the study of aggregate morphology, number and regional localization but does not provide the power for quantitative biochemical determinations. PolyQ-aggregates are insoluble and resistant to chemical extractions, thus they can be poorly determined by polyacrylamide gel electrophoresis because they are retained in the loading wells (Hazeki et al., 2000). More precise biochemical quantitative information can be obtained with the filter-trap assay for aggregates (Scherzinger et al., 1997). However, detailed investigation of aggregate growth or of aggregate composition depending on size is impossible by this method due to indiscriminate retention of all protein inclusions larger than the filter pores of the cellulose acetate membrane.

Here, we developed Agarose Gel Electrophoresis for Resolving Aggregates (AGERA) as a simple and sensitive biochemical detection method for quantitative and qualitative investigations of aggregate formation in *in vitro* and *in vivo* HD models. Notably, using AGERA we report that sizeable amounts of aggregates are found before the onset of other pathological dysfunctions in different *in vitro* and *in vivo* models of HD suggesting a pathogenic role of aggregates in HD.

### **4.2.3 MATERIALS AND METHODS**

#### **Cell culture, DNA transfections and lentivirus infections**

HN10 cells were grown in DMEM (Gibco), 10% FCS, penicillin and streptomycin. Plasmid transfections were performed with Lipofectamine 2000 (Invitrogen) according to the manufacturer protocol. Two days later, cells were lysed in RIPA buffer (10 mM Tris pH 7.5, 150 mM NaCl, 1 mM EDTA pH 8, 1% NP40, 0.5% SDS, Complete Protease Inhibitor) and samples were separated by electrophoresis on agarose or SDS polyacrylamide gels (Wiltfang et al., 1991). For immunohistochemistry, cells were fixed with 4% paraformaldehyde (PFA) and GFP autofluorescence was analyzed by microscopy.

Primary striatal cultures were prepared and cultured as described (Zafra et al., 1990). In short, timed-pregnant female mice were sacrificed and embryos were collected at E16.5. Ganglionic eminences were dissected and incubated for 20 min at 37°C in phosphate buffered saline (PBS) without  $\text{Ca}^{2+}/\text{Mg}^{2+}$  (Gibco), but containing 10 mM glucose, 1 mg/ml albumin (Sigma), 6 g/ml DNase (Sigma) and 0.25% trypsin (Sigma). After washing, striatal cells were dissociated with a fire polished Pasteur pipette. Cells were collected and resuspended in DMEM (Gibco), supplemented with 10% FCS and plated on culture dishes precoated with poly-DL-ornithine (0.5 mg/ml) and cultured in serum-free medium and supplements (Brewer and Cotman, 1989). One day after plating, cells were infected with lentivirus expressing Htt-exon1 with 25Q or 72Q. A virus expressing eGFP was used as control, generation and titer determination were done as previously described (Regulier et al., 2004). Briefly, 293T cells were transfected with four plasmids encoding for packaging proteins, envelope (VSV-G) protein, Rev protein and transfer vector encoding for Ex1-25Q, Ex1-72Q or GFP proteins. The viruses were resuspended in (PBS) with 1% BSA and matched for particle content in ng p24 antigen/ml as measured by ELISA (Zeptomatrix Corp; USA). The cell cultures were infected with lentiviral vectors at ratio of 100 ng of p24 antigen/ $10^5$  cells the day after plating (1 DIV).

Four and seven days after infections, cells were either lysed and analyzed by gel electrophoresis or fixed with 4% PFA and stained with mEM48 antibody (Chemicon, MAB 5374) and DAPI according to standard immunohistochemistry protocol.

#### **Generation and characterization of inducible HN10 cell line**

Rheoswitch system (New England Biolabs) was used to create a stable HN10 cell line with inducible Ex1-72Q expression. Ex1-Q72 was subcloned into the pNEBR-X1Hygro Vector according to standard molecular biology procedures. HN10 cells were transfected with

pNEBR-R1 plasmid and cultured with 1 mg/ml G418 (Invitrogen). Stable clones were first screened for normal cell morphology, transiently transfected with the pNEBR-GLuciferase reporter plasmid and induced with 500 nM Rheoswitch-ligand (RSL). Luciferase expression was measured and the clone with highest induction ratio was further expanded and subsequently transfected with pNEBR-ExQ72 plasmid. Stable clones were selected with 1 mg/ml G418 and 1 mg/ml Hygromycin (Invitrogen) and screened for normal cell morphology. Expression of Ex1Q72 in stable clones was monitored after induction with 500 nM RSL. Expression levels were analyzed with western blot. The clone with the best expression level and non detectable basal expression was chosen for further experiments (HN10-Ex1Q72V). For RSL-concentration and time-dependency of induction, HN10-Ex1Q72V clone was grown in RSL-containing media as indicated. Cell lysates were analyzed by western blot for huntingtin monomer expression or AGERA for aggregate determination.

### **Brain homogenates and subcellular fractionation**

Aggregate quantification was conducted using mouse brains homogenized in 10 volumes (w/v) TBS (100 mM Tris, pH 7.4, 150 mM NaCl) and Complete Protease Inhibitor (Roche Diagnostics) twice for 2 min at 30 Hz in a Retsch MM 300 Mill. Samples were further homogenized by 10 ultrasound pulses with a Branson sonifier and stored at -80°C.

To isolate cytoplasmic and nuclear fractions, each brain was homogenized in 5 volumes (w/v) ice-cold Buffer 1 (575 mM sucrose, 25 mM KCl, 50 mM triethanolamine, 5 mM MgCl<sub>2</sub>, 1 mM DTT, 0.5 mM PMSF, Complete Protease Inhibitor) and few strokes with Teflon pestle in a glass homogenizer. DTT concentration was adjusted to 5 mM. A crude homogenate aliquot was kept as starting material reference. The rest of the homogenate was centrifuged at 800 g for 15 min (all centrifugations were run at 4°C) to isolate a crude nuclear fraction (pellet) and a cytoplasmic fraction (supernatant). The nuclei were resuspended in Buffer 1 to 3 ml final volume and supplemented with 6 ml of Buffer 2 (2.3 M sucrose, 25 mM KCl, 50 mM triethanolamine, 5 mM MgCl<sub>2</sub>, 1 mM DTT, 0.5 mM PMSF, Complete Protease Inhibitor) and centrifuged at 124,000 g for 1 h over a cushion made of 0.5 ml Buffer 2. The pellet was resuspended in 500 µl Buffer 1 and centrifuged at 800 g for 15 min. The nuclear fraction was equivalent to the pellet dissolved in 100 µl 1% SDS in PBS and boiled for 10 min to shred the DNA. For different mice, samples were normalized after immunoblots with antibodies to  $\alpha$ -tubulin or histone 1, marker proteins for the cytoplasmic and nuclear fractions, respectively.

### **Filter-trap retardation assay**

Brain homogenate samples were diluted 1:10 v/v with 250 µl 2% SDS in PBS, corresponding to 0.15 mg of total protein per brain tissue sample. Cellulose acetate membrane (Whatman Group, OE 66, 200 nm pore size) was equilibrated in 2% SDS in PBS and samples were sucked through the membrane on a Biorad dot-blot vacuum device. Wells were washed three times with 300 µl 2% SDS in PBS. Membrane was blocked with 10% milk powder in TBS for 1 h and incubated with primary antibody overnight at 4°C. The antibodies were selective for ubiquitin (1:5000; DAKO) or for Htt (1:1000, MW1 and MW8 (Ko et al., 2001), Chemicon mEM48/MAB5374 and Nov1). Nov1 mouse monoclonal antibody was generated by custom production (GENOVAC GmbH, Germany) after DNA-vaccination with a cDNA encoding for Q25Htt1-857. The membranes were washed three times with TBST and incubated with secondary antibody (1:10000, anti-mouse or anti-rabbit IgG coupled to horse radish peroxidase). After washing, immunoblots were developed with the ECL detection reagent (Amersham Biosciences). The MCID software was used for densitometric analysis of digitalized autoradiograms.

### **AGERA**

For short 1.5% (2%) agarose gels, 1.5 g (2 g) agarose (Biorad, #161-3101) was dissolved in 100 ml 375 mM Tris-HCl, pH 8.8 brought to boiling in a microwave oven. After melting, SDS was added to a final concentration of 0.1%. Gels were poured on short Biorad DNA Sub Cell™ trays resulting in a gel thickness of 8 mm. Long 1% (1.5%) agarose gels were obtained by dissolving 2.5 g (3.75 g) agarose in 250 ml 375 mM Tris-HCl, pH 8.8, adjusting the final SDS concentration to 0.1% and pouring the gels on long Biorad DNA Sub Cell™ trays (gel thickness = 8 mm). Samples were diluted 1:1 into non-reducing Laemmli sample buffer (150 mM Tris-HCl pH 6.8, 33% glycerol, 1.2% SDS and bromophenol blue) and incubated for 5 min at 95°C. For brain tissue samples, 0.15 mg of total protein, for cellular samples 0.1 mg of total protein was loaded per AGERA lane. Purified catalase (232 kDa), ferritin (440 kDa) and thyroglobulin (669 kDa) were taken as high molecular weight size markers (all proteins included in Amersham Bioscience HMW Gel Filtration Kit, #17-0441-01). After loading, gels were run in Laemmli running buffer (192 mM glycine, 25 mM Tris-base, 0.1% SDS) at 100 V, 2 A until the bromophenol blue running front reached the bottom of the gel. Semi-dry electroblotter model B (Ancos) was used to blot the gels on PDVF membranes (Millipore Immobilon-P, #IPVH00010) at 200 mA for 1 h with a Biorad 200 power supply (transfer buffer: 192 mM glycine, 25 mM Tris-base, 0.1% SDS, 15% methanol). As the thickness of

the 1% long gels decreased substantially during the 1 h transfer, a 500 g weight was centered on the electroblotter's top to guarantee constant and even contact between the gel and the electroblotter when blotting these gels. After transfer, starting with the blocking step, immunoblot membranes were then developed exactly as described for the cellulose acetate membranes.

### **Aggregate analysis**

To determine the relative mHtt-aggregate size, AGERA autoradiograms were digitalized with a Cool Snap Photometrics camera. Densitometry of aggregate signals was performed with MCID software. The peak signal intensity for each lane and the distance of this peak signal to the running front were calculated automatically with MCID. For each experiment, the largest peak distance, which represented the lane with the largest aggregates, was set to 1.

### **Immunoprecipitations**

30  $\mu$ l brain homogenate from 14 wk-old R6/2 mice was diluted in 950  $\mu$ l RIPA buffer. 2  $\mu$ g ubiquitin- or huntingtin antibodies were added and incubated on a shaker at 4°C overnight. 15  $\mu$ l Protein A/G bead mixture (1:1) was added and incubated at 4°C for 2 h. Beads were washed three times with RIPA buffer. 30  $\mu$ l Laemmli sample buffer was added and the beads were incubated for 10 min at 95°C. Supernatants were then loaded on 1.5% agarose gels, immunoblotted and analyzed with anti-ubiquitin antibody.

#### 4.2.4 RESULTS

##### **AGERA is a sensitive assay to visualize and quantify mHtt-aggregates**

The formation of mHtt containing aggregates is one of the major hallmarks of HD. The prevention of the formation of these aggregates in neurons may represent an attractive therapeutic strategy to ameliorate Huntington's disease. A sensitive and quantitative method is necessary to monitor aggregate formation and progression or when assessing the efficacy of a potential drug candidate against HD. So far the analysis of the onset and progression of Htt-aggregates in biological samples has relied on immunohistochemistry or the filter-trap retardation assay, a method that has analytical limitations due to its all-or-nothing cut-off imposed by the size of the membrane pores. We thus designed an agarose gel electrophoresis-based methodology enabling the quantitative and qualitative investigation of Htt-aggregation with high sensitivity and generating reliable values. We applied this Agarose Gel Electrophoresis for Resolving Aggregates (AGERA) to determine the load of mHtt-aggregates in the brain of 14 wk-old R6/2 mice, which display pronounced Htt-deposition and brain pathology. At 14 wk of age, R6/2 mice suffer of severe HD-like symptoms approaching the terminal stage. The presence of Htt-inclusions in the R6/2 brain extracts was first verified by the filter-trap assay (Figure 17A, upper panels) using three different Htt-specific antibodies as well as an anti-ubiquitin antibody, confirming previous findings that the presence of ubiquitin is a hallmark of Htt-aggregates in R6/2 mice (Davies et al., 1997). A weak but discernible background signal was present for all used antibodies also in brain samples from wild-type (wt) littermate controls. The same samples were then resolved using AGERA (Figure 17A, lower panels) and the dynamic range of this method was assessed by comparing the signal intensity obtained for the 14 wk-old R6/2 mice with that of wt mice. When compared to the filter-trap assay, the signal-to-background ratios were considerably improved by AGERA (Figure 17B). In fact, the mean ratio determined by AGERA was 340-fold over background and thus 18-fold larger than that produced by the filter-trap assay (each group n=6). On the AGERA immunoblots, aggregates were detected with Htt antibodies as well as with the ubiquitin antibody (Figure 17A, lower panel).

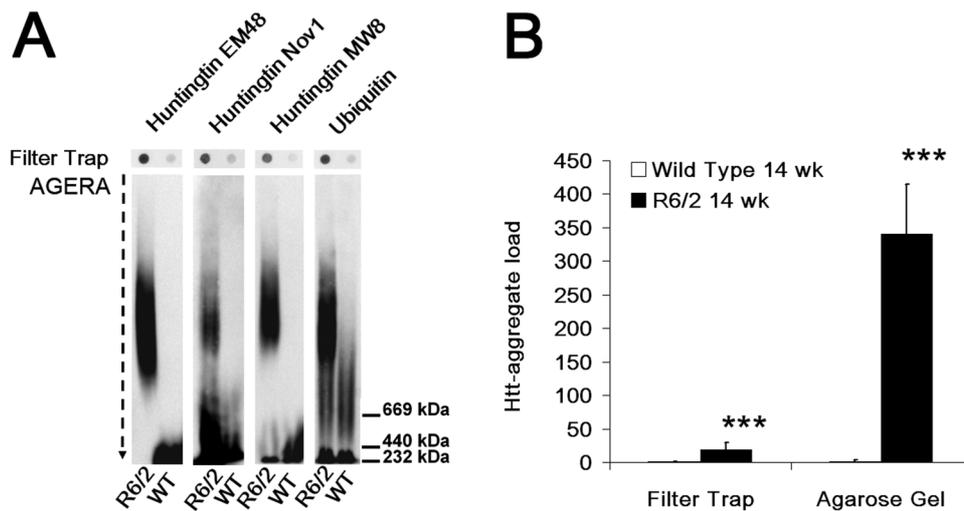


**Figure 17:** **A:** Identical samples of brain homogenates from 14 wk-old R6/2 mice or wt siblings were analyzed by filter-trap retardation assay or by AGERA on short 2% agarose gels. Both methods visualize aggregates with antibodies against huntingtin (MW8, EM48, Nov1) or ubiquitin in the transgenic but not in the wt samples. **B:** Comparison of the sensitivity of AGERA with the filter-trap assay. Signal ratios were calculated using the respective mean background signal obtained for brains of age-matched wt siblings and are shown with error bars representing standard deviations. AGERA generates a signal 340-fold  $\pm$  75 above background in 14 wk-old R6/2 brains compared to a 19-fold  $\pm$  10 signal using the filter-trap retardation assay (n=6; \*\*\*=p<0.001).

In order to demonstrate that the ubiquitin signal detected in brains of 14 wk-old R6/2 mice resulted from Htt-ubiquitination, a brain homogenate sample was first immunoprecipitated with the MW8 antibody specific for huntingtin or with the anti-ubiquitin antibody and then analyzed by ubiquitin-immunoblotting (Figure 18).



**Figure 18:** Htt-aggregates in brain homogenate of 14 wk-old R6/2 mice were immunoprecipitated with huntingtin antibody (MW8) or ubiquitin antibody (Ubi). Detection of aggregates on AGERA blots with ubiquitin antibody shows that huntingtin aggregates are ubiquitinated.

Although we can not exclude that other ubiquitinated proteins were sequestered into the aggregates, these data support the view that mHtt-aggregates were indeed ubiquitinated and that, more importantly, AGERA can reveal the extent of ubiquitination, and possibly other posttranslational modifications, of Htt-aggregates in biological samples.

### Separation of mHtt-aggregates by AGERA is based on their size

Htt-aggregates resolved by AGERA were distributed over a wide region of the gel. We analyzed whether the signal smear was caused by the presence of heterogeneous species of inclusions or due to the low resolving property of the gels. For this, brain homogenates of 14 wk-old R6/2 mice were first separated by agarose gel electrophoresis to obtain multiple gel fractions depending on their mobility on the gel. The fractions were then embedded in a second gel and again resolved by electrophoresis. We found that, as an example, Htt-aggregates isolated from the middle part of the gel retained a similar migration behavior when analyzed by AGERA and were separated from Htt-aggregates isolated from the upper or lower ends of the gel (Figure 19A). Thus, we concluded that AGERA resolved distinct, heterogeneous species of aggregates over most of the length of the gel. Supporting these data, another sample of a 14 wk-old R6/2 mice was run in two perpendicular dimensions of the agarose gel. This resulted in a 2D spatial resolution of the Htt-aggregates. The signal distributed mainly along the gel diagonal (Figure 19B) confirming that AGERA is a method suitable to separate distinct Htt-aggregate species in a reproducible manner.

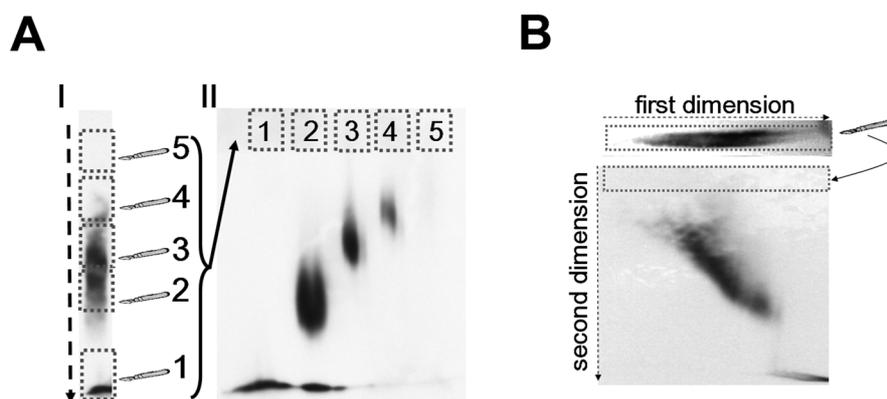


**Figure 19:** **A:** Two samples from a brain homogenate from a 14 wk-old R6/2 mouse were resolved by AGERA. The first sample was immunoblotted using the MW8 antibody (I). For the second sample, five sections were dissected from the agarose gel, embedded into a new gel and resolved again by AGERA (II). Aggregates preserve a distinct migration rate on the second gel, suggesting that Htt-aggregates are specifically and reproducibly separated in the agarose gels according to their size. **B:** A brain homogenate from a 14 wk-old R6/2 mouse was run on a short 1.5% agarose gel. The entire lane was dissected, embedded in a perpendicular direction in a new agarose gel and resolved by electrophoresis. Detection of the Htt-aggregates transferred on a PVDF membrane using MW8 reveals the two-dimensional distribution mostly along the diagonal of the second agarose gel. This indicates that separation by AGERA is reproducible and based on a heterogeneous trait of Htt-aggregates.

## Htt-aggregate formation in HN10 cells

To analyze the formation of Htt-aggregates *in vitro*, we first transiently expressed Htt-exon 1 fused to green fluorescent protein (GFP) with either 72 (Ex1-Q72GFP) or 25 glutamines (Ex1-Q25GFP) in HN10 neuroblastoma cells (Lee et al., 1990). Ex1-Q25GFP, a construct with a non-pathologic polyQ-length, was distributed diffusely throughout the cytosol as indicated by GFP-autofluorescence. Ex1-Q72GFP, a construct similar to the ones routinely used to study the aggregation-prone effect of elongated polyQ-repeat in Htt (Bodner et al., 2006; Lecerf et al., 2001; Zhang et al., 2005) formed aggregates which were located in the nucleus (Figure 20A). Equal expression of monomeric Htt was verified by polyacrylamide gel electrophoresis (Figure 20B, SDS-PAGE) and the presence of Htt-aggregates in Ex1-Q72GFP transfected cells was verified by the filter trap assay and AGERA (Figure 20B). No aggregates were detected in mock transfected cells or in cells transfected with Ex1-Q25GFP. On the other hand, aggregates were visualized with anti-Htt antibodies (Figure 20B, AGERA) or anti-GFP antibodies (not shown) in Ex1-Q72GFP transfected cell lysates. The mEM48 and Nov1 antibodies specific for soluble and aggregated Htt detected both forms of the protein by AGERA. In contrast, MW1 an antibody specific for monomeric, soluble Htt (Ko et al., 2001), failed to detect Htt-aggregates in Ex1-Q72GFP transfected cell lysates, but visualized monomers running just behind the running front of the agarose gel and which were poorly, if at all, retained by the filter-trap retardation assay. These data confirm the potential of AGERA to separate and detect in a single step soluble and aggregated Htt forms present in cells expressing mutant Htt *in vitro*.

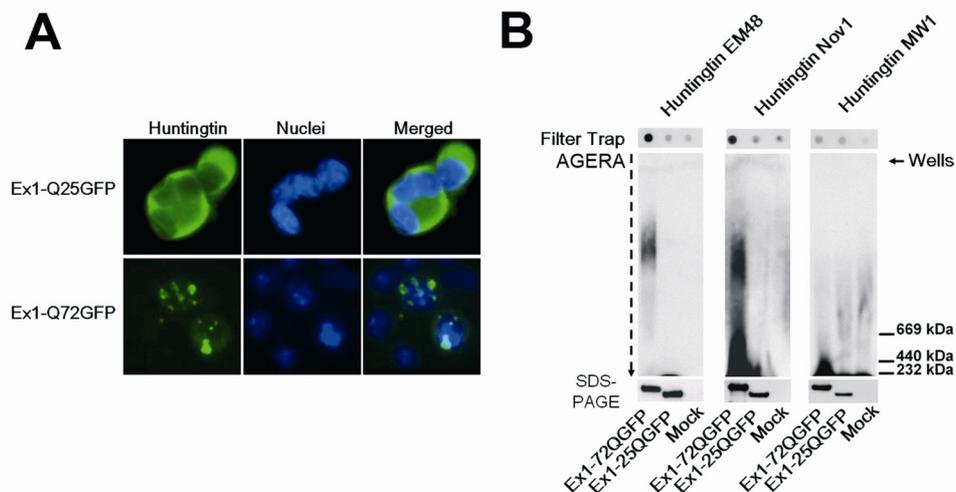


**Figure 20:** A: HN10 neuronal cells were transiently transfected with huntingtin Ex1-Q25GFP or Ex1-Q72GFP plasmids and analyzed after 2 days by GFP autofluorescence. Huntingtin Ex1-Q72GFP forms aggregates located predominantly in the nucleus, whereas Ex1-Q25GFP distributed evenly in the cytoplasm of the cells B: Identical amounts of lysates from HN10-cells transfected with Ex1-Q72GFP, Ex1-Q25GFP or with empty vector (mock) were analyzed by filter-trap, by AGERA on short 2% agarose gels or by SDS-PAGE as indicated on the left of the panels. SDS-PAGE confirms equal expression of the Htt constructs with three Htt-antibodies.

Aggregates in cells expressing the pathogenic Ex1-Q72GFP construct were detected selectively with Htt-specific antibodies. Ex1-Q25GFP-monomers running just behind the running front of the agarose gel reacted also to the MW1 antibody.

### Congo Red affects the size, not the amount, of Htt-aggregates *in vitro*

The dye Congo Red stains protein aggregates in various neurodegenerative diseases by binding to fibril proteins with enriched  $\beta$ -sheet conformation (Divry, 1927; Frid et al., 2007). Recent *in vitro* and *in vivo* studies in HD models indicate that Congo Red treatment prevents later stages of mHtt-fibrillization into larger aggregates (Poirier et al., 2002), thereby reducing mHtt- accumulation in general (Heiser et al., 2000; Sanchez et al., 2003; Smith et al., 2001). In order to study a possible effect of Congo Red, or other chemical compounds, on the formation of mHtt-aggregate *in vitro*, we created a stable HN10 clone with inducible Ex1-Q72 expression in the absence of the GFP or any other tags (Figure 21A,B). In this cell line, Htt-aggregates were detected as early as 3 days after induction (Figure 21C). Similar data were obtained with independent cell clones but not with inducible cell lines for normal polyQ-length (Ex1-Q25; data not shown).

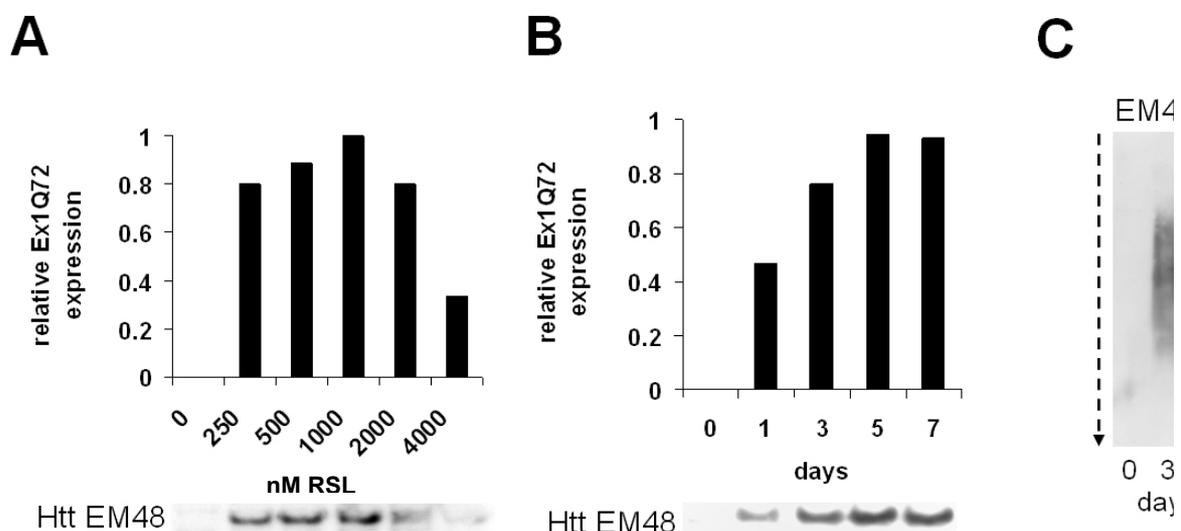


**Figure 21:** **A:** Monomer expression of Ex1-Q72 in HN10-Ex1Q72V clone was induced by adding different Rheoswitch-ligand (RSL) concentrations to the culture media. Cells were lysed after 3 days of induction and monomer expression levels were analyzed with anti-huntingtin antibody EM48 on a western blot. **B:** Monomer expression of Ex1-Q72 in HN10-Ex1Q72V clone was induced by adding 500 nM RSL to the culture media. Cells were lysed 0-7 days after induction and monomer expression levels were analyzed with anti-huntingtin antibody EM48 on a western blot. **C:** Expression of Ex1-Q72 was induced in HN10-Ex1Q72V clone by adding 500 nM RSL to the culture media. Cells were lysed after 0, 3 or 6 days of induction and equal protein levels of cell lysates were analyzed with AGERA to visualize aggregate load

Interestingly, treatment with increasing amounts of Congo Red caused the Htt-aggregates to acquire a faster mobility on the AGERA gels, indicative for decreased size of the aggregates in the presence of Congo Red (Figure 22, AGERA blot). Quantification of this effect was obtained by measuring the position of the peak signal intensity within the gel lane in relation to its distance from the running front (Figure 22, bar graph).

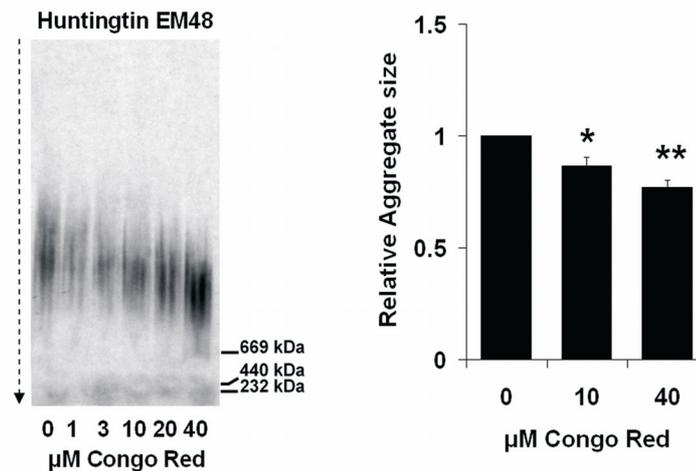


**Figure 22:** Congo Red treatment (up to 40  $\mu\text{M}$ ) of an induced Ex1-Q72 expressing HN10 clone inhibits aggregate growth as visualized by AGERA on short 1.5% agarose gels (left panel) or quantified as relative apparent mobility (right panel) using densitometric scans of the gels ( $n=3$ ;  $*=p<0.05$ ,  $**=p<0.01$ ).

The dose-dependent effect of Congo Red culminated at the maximal concentration tested (40  $\mu\text{M}$ ), whereby the peak aggregate size was reduced to a relative factor of 0.76 when compared to the vehicle control (value set to 1). Due to logarithmic dependence of Rf on molecular weight, the difference on Htt aggregate size after Congo Red treatment may even be bigger. Nevertheless, a precise determination of the Rf values on AGERA is difficult due to the paucity of adequate markers for the molecular weight range of aggregates. Our data are in good agreement with the effect of Congo Red on Htt aggregation reported using the filter-trap retardation assay (Heiser et al., 2000) but demonstrate that this effect did not relate to the total load of aggregates present in the cells. This was rather due to a change in the aggregate type in favor of smaller species, which may have escaped detection in the filter-trap assay.

### **Htt-aggregates in striatal primary cells precede appearance of polyQ-induced toxicity**

To extend our studies to a cellular model more relevant to HD, we infected primary striatal cells with a lentivirus transducing expression of Ex1-Q25 or Ex1-Q72 in the absence of the GFP-tag. As previously described (Zala et al., 2005) and using GFP-transduction as control, stable and sustained expression of the transgene was observed in more than 90% of the

cultured neurons with no sign of cytotoxicity at the viral dose used (data not shown). The same conditions were used to transduce striatal primary neurons with Ex1-25Q or Ex1-72Q. Immunocytochemistry using the mEM48 antibody revealed aggregates in most if not all nuclei of Ex1-Q72 infected striatal cells 7 days after infection. In contrast, the Ex1-Q25 construct was evenly distributed in the cytosol of cell bodies and neurites of the neurons (Figure 23).

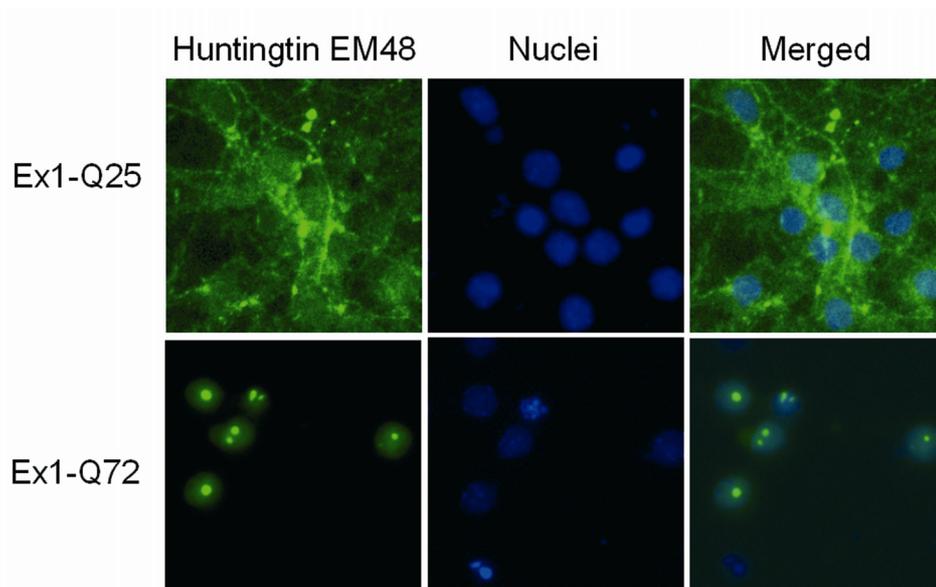


**Figure 23:** Striatal primary cells were infected with a lentivirus driving expression of Ex1-Q25 or Ex1-Q72. After seven days of infection the cells were fixed and stained with the mEM48 antibody. The Ex1-Q25 protein distributes in the cytoplasm and neurites whereas the Ex1-Q72 Htt fragment localizes to the nucleus and formed aggregates.

Consistent with previously published data (Li et al., 2000; Saudou et al., 1998; Zala et al., 2005), severe neuron degeneration and neurite collapse were observed at 7 days after infection for neurons expressing Ex1-Q72 but not for cells expressing Ex1Q25 or GFP (Figure 24).

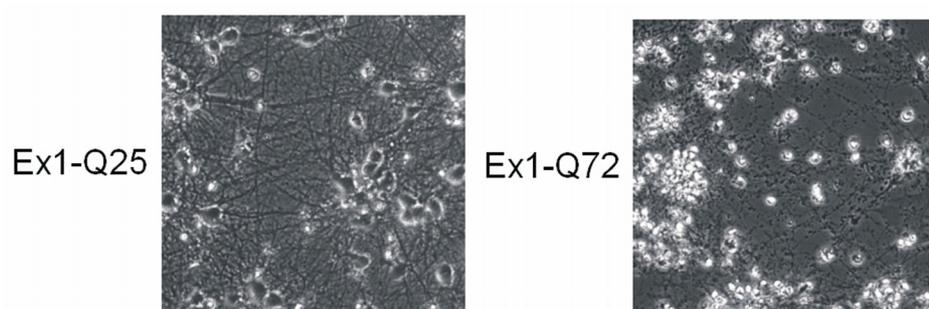


**Figure 24:** Light microscopy of transduced striatal cells 7 days after transfection reveals severe neurodegeneration in cells infected with Ex1-Q72 but not in cells infected with Ex1-Q25.

More relevantly, significant amounts of Htt-aggregates were already detected at 4 days post-transduction in lysates of Ex1-Q72 expressing primary striatal cells, thus well before the onset of visible neurite degeneration (Figure 25).

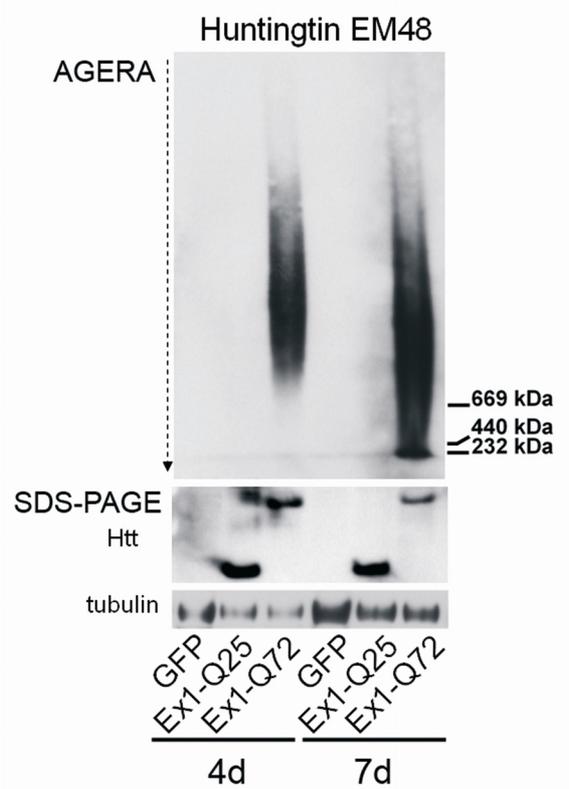


**Figure 25:** Lysates of transduced cells were analyzed by AGERA on short 1.5% agarose gels or SDS-PAGE. EM48 antibody detects Htt-monomers after SDS-PAGE and aggregates by AGERA in the Ex1-Q72 infected cells at 4 and 7 days post-infection. The data were reproduced in at least three independent experiments.

The load of aggregates increased further at the 7th day of infection. As expected, no Htt-aggregates or toxicity were detected in striatal neurons transduced with GFP or Ex1-Q25, despite the presence of huntingtin monomers at 4 and 7 days after infection (Figure 25; SDS-PAGE). Quantification of the partition of monomeric mHtt (detected after SDS PAGE) versus aggregated mHtt (detected by AGERA) demonstrated an increase of Ex1-Q72 aggregates between day 4 and 7 post-infection accompanied by a reduction in the amount of monomeric Htt (not shown).

### **Presence of presymptomatic Htt-aggregates in mouse models of HD**

Having demonstrated biochemically that Htt-aggregate formation occurred before or at the onset of neurodegeneration in a cellular model of HD, we proceeded to study Htt-aggregate

appearance in two mouse models of HD. Using AGERA, we detected a significant amount of Htt-aggregates in brains of R6/2 mice already at 2 weeks after birth (Figure 26). At this age, no behavioral differences were detectable when we compared R6/2 mice to littermate controls (data not shown and (Davies et al., 1997; Li et al., 1999)).

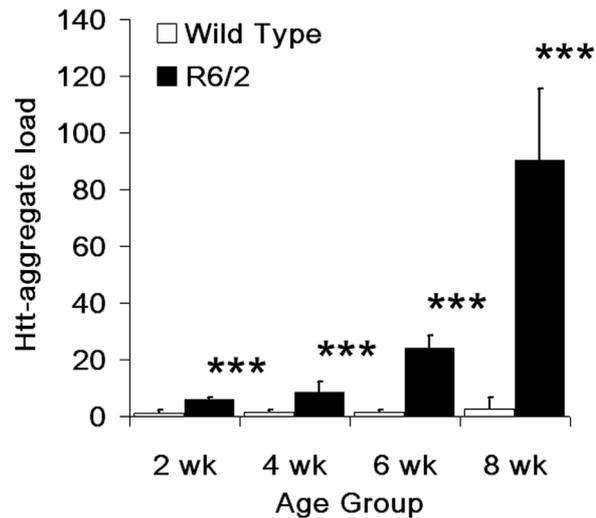


**Figure 26:** Onset and accumulation of aggregated Htt as a function of age were assessed in brain homogenates from 2, 4, 6 and 8 wk-old wt or R6/2 mice. Data are shown as signal ratios over background with error bars representing standard deviations (n=6-8; \*\*\* = p<0.001).

The aggregate signal by AGERA was 6-fold higher than that determined in age-matched wt siblings (p <0.001, each group n=6). Accumulation of Htt-aggregates progressed in a semi-exponential modus across the age groups 4 wk (8.6-fold above controls, p <0.001), 6 wk (24-fold, p <0.001) and 8 wk (90-fold, p <0.001) (Figure 26). Maximal aggregate load was measured in the 14 wk-old R6/2 mice (340-fold, Figure 17B). In contrast, when analyzing the homogenates with filter trap assay, no aggregate signal was detected at 2 wk and the signal at 4 wk was 3.3-fold (p <0.05) above background (data not shown). To assess the potential of AGERA to detect a difference in Htt-accumulation over a period of 2 wk (a typical treatment duration for subchronic drug trials), we conducted a power analysis using the values acquired at 4 and 6 wk of age. Under these conditions, a 30% reduction in the amount of Htt-aggregates accumulating over this period is predicted to be observed at 95% confidence (p = 0.05) with 10 transgenic mice per treatment arm (20% reduction would require group sizes of at least 22 animals, 40% reduction group sizes of at least 5 animals). Quantification of Htt-aggregates in distinct brain regions of 14 wk-old R6/2 mice showed the largest aggregate load is present in the hippocampus and striatum, whereas cortex and cerebellum contained 2 to 3-fold less Htt-aggregates (Figure 27).

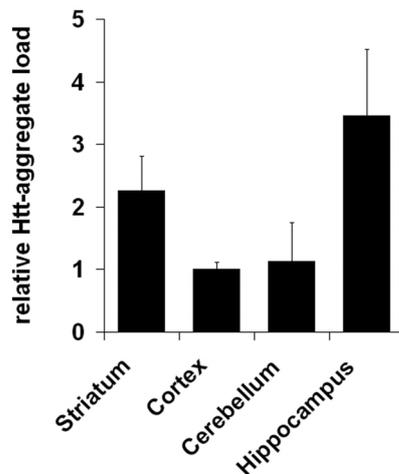


**Figure 27:** Quantification of relative Htt-aggregate load in different brain regions of 13 wk-old R6/2 mice (n=5) reveals that aggregate deposition is most pronounced in the hippocampus and striatum.

Next, we analyzed Htt-aggregate formation in the *HdhQ150* knock-in mouse model which was generated by inserting an elongated polyQ stretch of 150 glutamines in the endogenous mouse huntingtin gene (Lin et al., 2001). Typical for full-length polyQ-Htt models, in the *HdhQ150* mice disease-onset and progression is delayed when compared to Htt-fragment models such as the R6/2 mice. First phenotypic alterations in *HdhQ150* mice are observed starting from about one year of age (body weight loss) or from 18 months of age on the RotaRod (Woodman et al., 2007). In contrast, we detected Htt-aggregates in *HdhQ150* brain samples already at 6 months of age, at this age the AGERA signal was 3.4-fold above background of wt littermates (Figure 28).

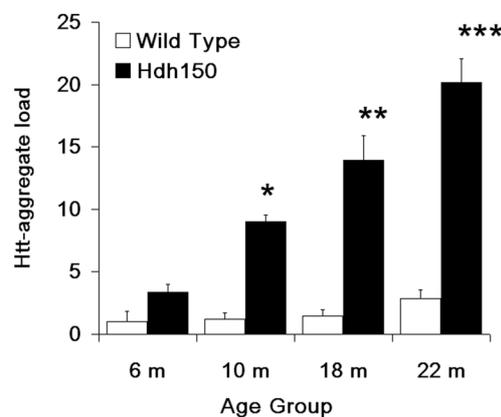


**Figure 28:** Onset and accumulation of Htt-aggregates during disease progression were confirmed in cortical samples from the full-length Htt knock-in model *HdhQ150* from 6, 10, 18 and 22 months old *HdhQ150* mice (n=3-4, \*=p<0.05, \*\*= p<0.01, \*\*\* = p<0.001)

We then found an age- and disease progression-dependent increase in the load of Htt-aggregates, reaching a 9.0-fold difference at 10 months, 13.9-fold at 18 months and 20.1-fold at 22 months of age (all groups n=4 but n=3 for the *Hdh*Q150 mice at 6 months). No aggregate signal was detected in 6 months old mice and signal failed to reach significant levels before 18 months of age with the filter trap assay (data not shown). Overall, our data demonstrate that sizable amounts of Htt-aggregates appeared before the onset of disease symptoms in two mouse models of HD.

### Age-dependent growth of brain Htt-aggregates

In our *in vitro* studies we demonstrated that AGERA is not only an accurate method to measure quantitatively the absolute amount of Htt-aggregates, but that this methodology has also the potential to reveal qualitative changes in their appearance. Age-dependent growth of Htt-deposits *in vivo* has been observed previously in immunohistochemical studies on brain sections isolated from brains of HD patients or of R6/2 mice (DiFiglia et al., 1997; Li et al., 1999). To confirm this biochemically, we analyzed brain homogenates of 4 and 14 wk-old R6/2 mice on a long 1% agarose gel in order to maximize the resolution of distinct Htt-aggregate species. This procedure established that in young mice Htt-aggregates had faster average mobility, since they were detected in the lower half of the agarose gel (Figure 29). In contrast, Htt-aggregates from brain samples of 14 wk-old mice scattered over most of the gel. This was more evident with a short exposure of the gel to compensate for the larger amount of aggregates present at 14 wk of age.

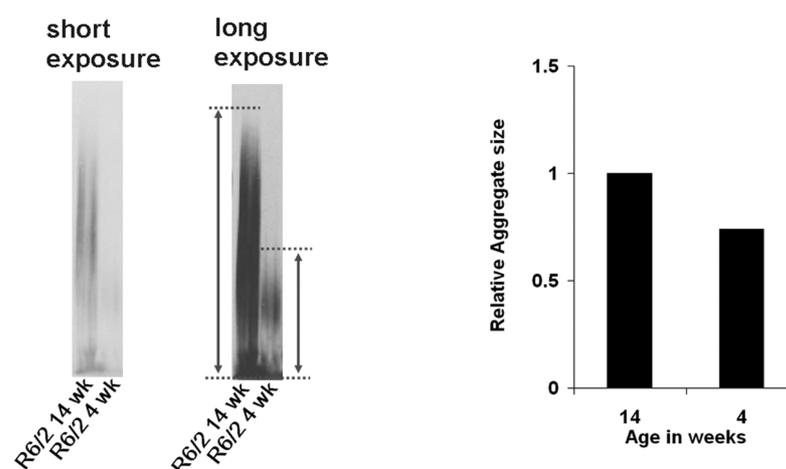


**Figure 29:** Brain homogenates from 4 or 14 wk-old mice were run on a long 1% agarose gel and immunoblotted with the MW8 antibody (left panel). A long and a short exposure of the same blot were done in order to compare signals with similar intensity for the two ages. Dotted lines indicate the distribution of the aggregates on the agarose gels in the 14 wk-old (left lane) and in the 4 wk-old (right lane) R6/2 brains. Aggregates are significantly larger in older mice, also confirmed by determining the relative apparent mobility using densitometric scans of the gels (right panel).

Histological examinations also indicated that the localization within the cell may have an effect on the size of the Htt-deposits (Gutekunst et al., 1999; Stack et al., 2005). In fact, neuropil inclusions appeared initially small but then grew faster than those observed in the nuclei of affected neurons. To revisit this finding, we isolated cytoplasmic and nuclear fractions from brains of 6, 8 and 14 wk-old R6/2 mice. The purity of the two subcellular fractions was verified using cytoplasmic and nuclear markers, respectively (Figure 30, lower panels). When using AGERA, we indeed observed that the aggregates present in the cytoplasmic fraction at 6 and 8 wk of age migrated faster than those detected in the nuclear fractions of the same samples. These data demonstrated that cytoplasmic aggregates were smaller than nuclear aggregates in brains of 6 or 8 wk-old R6/2 mice.

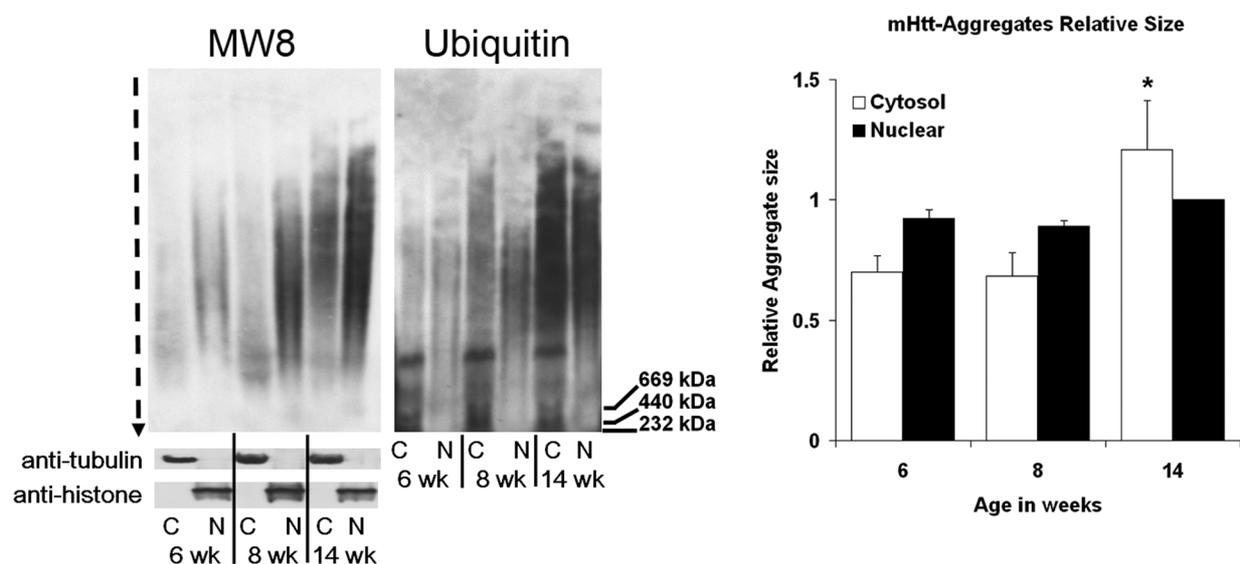


**Figure 30:** Cytoplasmic (C) and nuclear (N) fractions were isolated from brains of 6, 8 and 14 wk-old R6/2 mice. Purity of the fractions was confirmed with a cytoplasmic ( $\alpha$ -tubulin) and a nuclear marker (histone) by Western blot after SDS PAGE. Samples were resolved by AGERA on a long 1.5% agarose gel and using the MW8 or the anti-ubiquitin antibody. A clear increase in the size of cytosolic aggregates occurs between the age of 8 and 14 wk. Nuclear aggregates are larger than the cytoplasmic aggregates at 6 wk of age but their size does not change significantly with disease progression. More aggregates localize into nuclei at 14 wk of age, but ubiquitination is more prominent in the cytosolic fractions and is more pronounced for the larger aggregates.

A significant increase in the size of the cytoplasmic aggregates was observed between the age of 8 and 14 wk. In contrast to this, the size of nuclear aggregates remained constant with age. Moreover, the use of anti-ubiquitin antibodies revealed that in particular the slow-migrating aggregates were ubiquitinated. Not surprisingly, modification with ubiquitin was more prominent for cytosolic than nuclear aggregates (Figure 30), contradicting earlier histological studies (Li et al., 1999). Further studies may help understanding whether location and size of

Htt-aggregates might have differential roles in the manifestation of HD as previously suggested by others (Yang et al., 2002).

#### 4.2.5 DISCUSSION

The genetic cause for Huntington's Disease is an aberrant polyQ-expansion in Htt. PolyQ-length regulates deposition of Htt-fragments into intracellular aggregates (Chen et al., 2002; Huang et al., 1998) whose number correlates with disease progression in HD patients and animal models (DiFiglia et al., 1997; Gutekunst et al., 1999; Menalled et al., 2003; van Roon-Mom et al., 2002; Woodman et al., 2007). Precise quantification of the amount of aggregates present in biological samples has proven challenging due to analytical limitations such as high background in the filter-trap assay or indirect quantitative determination by histochemistry. For instance, the filter-trap assay often retains contaminants such as tissue debris, which may include soluble Htt-forms and adsorb unselectively antibodies, both reducing the signal specificity. AGERA overcomes this and other limitations as it is based on active electrophoretic separation of aggregates. Moreover, soluble (monomeric and oligomeric) Htt-species migrate fast through the agarose gels thereby becoming fully resolved from insoluble aggregates. The negligible background signals obtained by AGERA may indeed explain the drastic improvement in Htt-aggregate detection sensitivity, also when compared to other agarose-gel methods (Kushnirov et al., 2006). This will become critical for a comprehensive study of cellular and rodent models of HD. We showed that in cultured striatal neurons expressing mHtt-Exon 1, aggregates formed several days before onset of neurite degeneration. *In vivo*, a significant amount of Htt-aggregates was measured in the brains of R6/2 mice at two weeks of age, preceding the development of first motor impairments by weeks (Carter et al., 1999; Lione et al., 1999; Mangiarini et al., 1996). Aggregates have been previously detected in defined areas of the cortex and striatum of R6/2 mice at 3.5 and 4.5 weeks of age, respectively (Davies et al., 1997). A more recent study reported the immunohistochemical and electronmicroscopical detection of very small Htt aggregates as early as postnatal day 1 and 15 (Stack et al., 2005).

We reproduced these findings in a second HD mouse model. In *Hdh*Q150 mice, Htt-aggregates were detected at 6 months of age, about half a year earlier than the first discernible phenotype. Detection of Htt-aggregates in *Hdh*Q150 mice, which express full-length polyQ-Htt, suggests that AGERA may also be applicable for the analysis of aggregates in human tissue.

In addition to the determination of the total amount of aggregated Htt, we studied by AGERA aggregate growth and composition. We showed that disease progression correlated in R6/2 mice not only with an increase of the amount of Htt-aggregates but also with an increase in their size, and this depending on their intracellular localization. Notably, Htt-deposits in the

cytosol were smaller than those found in the nucleus in young R6/2 mice but grew dramatically between 8 and 14 weeks of age. These data suggest that the microenvironment may affect Htt-deposition and hinted that nuclear and cytosolic aggregates may differently impact specific cellular functions. Also, the ubiquitination level of Htt-aggregates was more prominent in the cytoplasmic than the nuclear fraction. In light of recent findings that hindrance of the proteasome clearance pathway by ubiquitinated Htt may induce autophagy (Bence et al., 2001; Iwata et al., 2005; Jana et al., 2001), AGERA could become a critical method to study ubiquitination or other posttranslational modifications of Htt-aggregates and their influence on cytotoxicity or induction of protective mechanisms such as autophagy. Determination of changes in aggregate size was particularly important in three aspects of this work. We first demonstrated that Congo Red inhibited mainly aggregate growth but less so their total amount. Then, we showed that deposit size correlated with disease progression. Finally, we illustrated that in this respect nuclear and cytosolic aggregates behaved differently. The role of aggregates in HD is still under debate. While some researchers argue that aggregates are toxic and lead to neurodegeneration, others have suggested that they are a mere byproduct of the pathology. Yet others discuss a neuroprotective role for aggregates as a molecular sink for putative soluble toxic Htt forms (Arrasate et al., 2004; Saudou et al., 1998). It is to be expected that aggregate localization will influence toxicity to a larger extent than aggregate size or composition. Indeed nuclear rather than cytosolic Htt-aggregates led to a very quick cell death and this independently of polyQ-length (Saudou et al., 1998, Bates, 2003; Chen et al., 2001; Chen et al., 2002; Yang et al., 2002). Also, it has been reported that the smaller, more aggregation prone fragments of mHtt were found preferentially in the nucleus (Lunkes and Mandel, 1998; Wellington et al., 2000a). Interestingly, the study of a conditional mouse model of HD demonstrated that development and progression of a HD-like pathology was dependent on the continuous expression of the transgene. In fact, switching off Htt-expression stopped disease progression, reversed aggregate load and improved motor deficits (Martin-Aparicio et al., 2001; Yamamoto et al., 2000). Most pre-clinical trials failed to show a decrease of aggregate formation in the brain of HD mouse models, although occasionally motor behavior or striatal volume loss improved (Ferrante et al., 2004; Gardian et al., 2005; Smith et al., 2006). However, assessment of aggregates in these studies was mostly limited to immunohistochemical analysis. The use of AGERA has improved sensitivity and reproducibility of our analysis and has allowed for active resolution of Htt-aggregates based on size. In light of this, although our study does not solve the problem of the role of aggregates in the pathology of HD, AGERA enables a sensitive and quantitative

assessment of aggregate load and therefore is expected to enable their detailed analysis and thus significantly improve the power of future pre-clinical HD drug trials.

As protein misfolding and deposition are hallmarks of not only HD but also most other neurodegenerative diseases, AGERA may find application for the study of the pathogenic processes in other human brain disorders and may allow for comparative studies of the many neurodegeneration models developed over the recent years. Indeed, agarose gel electrophoresis has been recently used to study prion polymerization in yeast (Kushnirov et al., 2006), to analyze fibril generated *in vitro* from synthetic  $\beta$ -amyloid peptide (Bagriantsev et al., 2006) and readily detects aggregation of other pathogenic polyQ-containing proteins (A. Weiss, unpublished results). The development and optimization of AGERA aimed at the specific analysis of protein aggregates in cellular and tissue samples. While AGERA is in principle similar to the agarose-based method described independently by Kushnirov and colleagues, in order to generate reliable data enabling comparative studies using large sample sizes and granting reproducibility among independent experiments it was critical to keep all AGERA parameters constant. It will be interesting to see if AGERA can be used to trace changes within disease specific aggregate pools, specifically for visualization of subtle differences caused by experimental drugs.

## **ACKNOWLEDGEMENTS**

We thank Dr. Holger Heine for providing the Nov1 antibody, Dr. Martin Beibel for help with power analysis, Dr. Alex Kazantsev for providing the GFP-tagged Htt-plasmids. The MW1 and MW8 Htt-antibodies developed by Dr. Paul Patterson were obtained from the Developmental Studies Hybridoma Bank developed under the auspices of the NICHD and maintained by The University of Iowa, Department of Biological Sciences, Iowa City, IA 52242. We thank Dr. Christoph Wiessner for suggestions to the manuscript. This work was funded by the Wellcome Trust (60360; 66270) to GB. A. Weiss, C. Klein, E. Regulier, M. Bibbel and P. Paganetti are employed by Novartis Pharma AG, Basel, Switzerland.

### **4.3 Development of a method for the high-throughput-quantification of cellular protein levels**

**Andreas Weiss<sup>1\*</sup> & Paolo Paganetti<sup>1\*</sup>, Monique Trapp<sup>2</sup>, Dorothee Bleckmann<sup>1</sup>, Ruth Bodner<sup>3</sup>, David Housman<sup>3</sup>, Ina Hammerl<sup>2</sup>, Christian N. Parker<sup>2#</sup>**

\* shared first authors

# correspondence author

1) Neuroscience Discovery, Novartis Institutes for BioMedical Research, Basel, Switzerland

2) Center for Proteomic Chemistry, Novartis Institutes for BioMedical Research, Basel, Switzerland

3) Center for Cancer Research, Massachusetts Institute of Technology (MIT)

Submitted

### **4.3.1 SUMMARY**

The quantification of cellular proteins is essential for the study of many different biological processes. This study describes an assay for the detection of intracellular mutant huntingtin, the causative agent of Huntington's Disease, with a method that may be generally applicable to other cellular proteins. A small recombinant protein tag was designed that is recognized by a pair of readily available, high affinity monoclonal antibodies. This tag was then added to an inducible fragment of the mutant huntingtin protein by genetic engineering. First we demonstrated that it is possible to use time resolved Förster resonance energy transfer (time resolved FRET) to detect the cellular levels of this protein by a simple lysis and detection procedure. This assay was then adapted into a homogeneous, miniaturized format suitable for screening in 1536 well plates. The use of time resolved FRET also allows the assay to be multiplexed with a standard readout of cell toxicity thus detecting conditions causing reduction of protein levels simply due to cell toxicity. Screening results demonstrated that the assay is able to identify compounds that modulate the levels of huntingtin protein both positively and negatively.

### 4.3.2 INTRODUCTION

Huntington's Disease (HD) is a fatal, autosomal-dominant neurological disorder. The disease is characterized by involuntary movements, severe emotional disturbance and cognitive decline caused by a significant degeneration of brain matter (Bates et al., 2002). In 1993, the gene IT15, later called huntingtin (Htt), was cloned and found to contain a CAG repeat encoding for polyglutamine (polyQ) in exon 1 which is expanded in patients (Group, 1993a; Gusella et al., 1983). A number of possible effects on cell physiology by this polyQ region have been suggested including the generation of cytotoxic proteolytic fragments and aggregates, transcriptional dysfunctions and several other effects. Currently, there are no approved treatments for HD (Bates, 2003; Bates and Hockly, 2003; Landles and Bates, 2004; Young, 2003).

Even though the mechanism of polyQ-Htt toxicity is unknown, it has been shown in mouse models that down-regulation of polyQ-Htt expression either by RNA interference (DiFiglia et al., 2007; Machida et al., 2006; Rodriguez-Lebron et al., 2005; Wang et al., 2005) or by conditional expression of a polyQ-Htt-fragment (Yamamoto et al., 2000) will improve HD-like symptoms significantly. Critically, polyQ-Htt and wild-type Htt are distinct in terms of posttranslational modifications (e.g. phosphorylation (Warby et al., 2005)), proteolytic cleavages (Graham et al., 2006; Wellington et al., 2002), cellular localization (Davies et al., 1997) and degradation (ubiquitin/proteasome or autophagy pathway (Ravikumar et al., 2002)). As polyQ-Htt is the sole cause for HD and as the cell metabolizes polyQ-Htt and wild-type Htt differently, we established an assay capable of detecting the intracellular levels of wild-type and polyQ-Htt. In order to develop this assay, neuronal cell lines with inducible copies of either the wild-type or polyQ-Htt, tagged with small peptide sequences were created and a method was developed to detect compounds which selectively promote the degradation of polyQ-Htt.

In general, most methods to monitor cellular protein levels require separation and detection steps e.g. Western blotting or HPLC-MS. Such methods are not suitable as assays to test multiple conditions, i.e. high throughput screening of chemicals or siRNAs as high throughput screening applications require homogeneous assays that are robust enough to allow assay automation. To circumvent these problems, we developed an alternative method using time resolved Förster resonance energy transfer (time resolved FRET), a technology that has been available for monitoring biomolecular interactions since the early 1990's (Mathis, 1993). There are many different applications of this technology utilizing several aspects of the fluorescence characteristics of lanthanide ions. The large Förster's distance of the rare earth

ions is up to 9 nm which is much larger than for many fluorescent compounds which have Förster's distances of between 4-6 nm. The effect of this larger distance is that it is possible to transfer absorbed energy over much longer distances than it is possible for many FRET pairs. This then makes it possible to use rare earth chelates as generic immunodetection reagents (Bazin et al., 2001). The second advantage of rare earth FRET pairs is that the time it takes for the fluorescence to decay is greatly delayed thus allowing time resolved fluorescence. The effect of this is to reduce the influence of background fluorescence from small molecules being tested. The third advantage is the ability to monitor ratiometric readouts allowing the correction for liquid dispensing errors, thus helping to reduce assay variability and improve data quality (Imbert et al., 2007).

Because of these advantages, time resolved FRET has been used in the past to monitor a number of different biological analytes such as small molecules (e.g. cAMP (Gabriel et al., 2003)), small secreted cytokines (e.g. IL-8 (Achard et al., 2003)) as well as the levels of phosphorylated proteins in *in vitro* assays (Riddle et al., 2006). There have also been reports of using time resolved FRET to monitor the levels of phosphorylated proteins in cell lysates using cell lines over-expressing protein substrates of interest. In this report we extend these observations by designing a small peptide tag that gives an optimal time resolved FRET signal and allows the detection of polyQ-Htt, an intracellular protein expressed at endogenous levels. As polyQ-Htt detection in this assay is based on an artificial tag, this method should be generally applicable for the detection of other proteins. Importantly, the required antibody pairs for tag detection are commercially available (see Material and Methods) making the herein described method a readily applicable generic detection method for other laboratories.

### **4.3.3 MATERIALS AND METHODS**

#### **Peptides and Antibodies**

Peptides carrying epitopes against 25H10, 32A7 or  $\beta$ 1 antibodies which are separated by different linker sequences were custom produced by MIT biopolymers laboratory (MIT, Cambridge, MA). Amyloid  $\beta$ 40 peptide was purchased from Bachem (Bubendorf, Switzerland).

25H10 antibody specific against GGVV-epitope, 32A7 antibody specific against VVIA and  $\beta$ 1 antibody directed against EFRH are described elsewhere (Paganetti et al., 1996; Weihofen et al., 2003). Commercially available unlabeled antibodies equivalent to these antibodies can be obtained through several vendors such as Cell Sciences (MA, USA), The Genetics Company (Switzerland) or Immuno-Biological Laboratories (MN, USA). Labeled antibodies ready for time-resolved Förster Resonance Energy transfer can be obtained through Cisbio Bioassays (France). 2B7 antibody was custom designed against the first 17 amino acids of Htt protein (GENOVAC, Freiburg, Germany). Custom europium cryptate and D2-fluorophore labeling were performed by Cisbio Bioassays (France). Depending on the batch used, antibodies were crosslinked to 5 to 7 mol europium cryptate or D2-fluorophore per mol antibody.

#### **Generation of Neuronal Cell Lines**

Neuronal HN10 cells (Lee et al., 1990) were used to create inducible clones with expression of Htt573-Q25 and/or Htt573-Q72. In short, cells were transfected with the rheoswitch receptor plasmid (New England Biolabs) and cultured under selection of 1 mg/ml G418 (Invitrogen). Clones were screened for cell morphology, transfected with inducible luciferase reporter construct and induced for 2 days. Clone with best induction ratio were selected and used for subsequent transfection with Htt573-Q25 or Htt573-Q72 inducible plasmid. After selection with 1 mg/ml G418 and 1 mg/ml Hygromycin (Invitrogen), inducible expression of Htt fragments in the clonal lines were monitored with herein described time resolved FRET detection method and clones with no basal expression and highest inducible expression were chosen for use in the assay format.

#### **Detection of Peptides by time resolved FRET**

Peptides were prediluted in DMSO to 800  $\mu$ g/ml. DMSO solutions were further diluted in 1 to 5 RIPA buffer to 3 ng/ml final concentration. 3 ng/ml amyloid  $\beta$ 40 peptide was used as control. 10  $\mu$ l peptide solution per low-volume 96-well were mixed with 5  $\mu$ l of antibody

solution ( $\beta$ 1-D2 20 ng/well, 25H10-K 2 ng/well in 50 mM NaH<sub>2</sub>PO<sub>4</sub>, 400 mM NaF, 0.1% BSA, 0.05% tween) and incubated at 4 °C overnight. 620 and 665 nm signals were measured with a RUBYstar (BMG Labtech) reader.

### **Adaptation to 96 Well Format**

20.000 cells/well were seeded in 100  $\mu$ l normal grow medium (DMEM (Gibco), 10% FCS, penicillin and streptomycin). After 2 h medium was removed and 200  $\mu$ l inducing medium (normal growth medium plus inducer) was added to start expression of Htt fragments. After 3 days, medium was removed and 30  $\mu$ l/well readout buffer (20  $\mu$ l of different lysis buffers and 10  $\mu$ l of  $\beta$ 1-D2 and 25H10-K or 32A7-K in 50 mM NaH<sub>2</sub>PO<sub>4</sub>, 400 mM NaF, 0.1% BSA, 0.05% tween) was added. After incubating 30 min at room temperature, lysates were transferred to low volume black bottom 96 well plate. After 3 h at 4°C 620 and 665 nm signals were measured with a RUBYstar (BMG Labtech) reader.

### **1536 Well HTS Miniaturization and Compound Screen**

A Htt573-Q72 expressing HN10 cell line was incubated for 72 h at 37°C, 5% CO<sub>2</sub> with inducing medium to facilitate expression of polyQ-Htt construct. Then 3  $\mu$ l of a 2000 cells/ $\mu$ l cell suspension were added per well in a 1536-microtiterplate (Greiner) and incubated overnight +/- compound treatment. 5  $\mu$ l of sample buffer solution (3  $\mu$ l lysis buffer [1x PBS + 1% Triton X-100, complete protease inhibitors] + 2  $\mu$ l antibody buffer [50 mM NaH<sub>2</sub>PO<sub>4</sub>, 400 mM NaF, 0.1% BSA, 0.05% tween, 60 pg/well europium labeled antibody, 800 pg/well D2-labeled antibody]) was added and incubated for 30 min at room temperature. Plates were incubated at room temperature as indicated. Measurements were performed with a View Lux machine with the following settings: Label 1 time resolved FRET\_Eu-K\_(E:800K, Xsec, BF4, GN:high,SP:slow), Label 2 time resolved FRET\_XL665\_(E:800K, Xsec, BF4, GN:high,SP:slow).

### **Data Analysis**

Time resolved FRET measurement results in two different signals. The 620 nm signal from the europium cryptate labeled antibody can be used as an internal reference for possible interfering artifacts of the assay such as signal quenching or absorption by compounds, sample turbidity as well as differences in excitation energy or sample volume. The 665 nm signal results from D2 labeled antibody which is excited by time resolved energy transfer from the europium cryptate. The calculated 665/620 nm ratio therefore is an artifact corrected

specific signal of the two antibodies bound to their antigen and hence a reflection of the amount of antigen present in the sample. For 96 well data time resolved FRET signals are given as the ratio between those two wavelengths.

For 1536 microtiter well optimization data, time resolved signals are presented as  $\Delta F$  values, a format more suitable to take day-to-day assay variations into account as it is a background corrected value:

$$\Delta F = (\text{Ratio}_{665/620\text{induced}} - \text{Ratio}_{665/620\text{non-induced}}) / \text{Ratio}_{665/620\text{non-induced}} * 100$$

Analysis of high throughput screening data was conducted using an in house data analysis software. This software is able to normalize activity to percent remaining activity with the use of high and low control samples present on a plate and to correct plate effects using a local regression algorithm that corrects for local plate effects (Gubler, 2006). Z-factor was calculated according to (Zhang et al., 1999).

#### 4.3.4 RESULTS

##### Technology Development

Time resolved FRET detection of amyloid  $\beta$  peptide in fluid biological milieu has been previously described (Clarke and Shearman, 2000) and is currently commercially available. The amyloid sandwich assay takes advantage of high-affinity antibodies directed against two well characterized epitopes in the amyloid  $\beta$  peptide. We designed a library of small peptides which carry these epitopes (Figure 31A). Our goal was to use this peptide sequence as a tag for recombinant proteins, making them suitable for time resolved FRET detection. Since the efficiency of the FRET energy transfer can be influenced by various parameters (Clegg, 1996; Förster, 1948) we tested different peptides with changing linker length and amino acid composition to determine the most suitable peptide sequence. Time resolved FRET analysis of purified peptides showed that linker length and sequence of the linker can indeed influence signal intensity significantly (Figure 31B). For example, peptides with very short linker length (peptides H2 and H3) resulted in low signals probably due to steric hindrance of the two antibodies. Peptide I6 in which the neo-epitope GGVV specific for 25H10 antibody was exchanged for VVIA (specific for 32A7 antibody) failed to result in a signal when using the 25H10 europium labeled antibody (25H10-K), verifying the specificity of the signal. For further experiments we designed two Htt-protein-fragments carrying either the exact H1 peptide sequence as a tag (polyQ-Htt/Htt573-Q72) or an alternative sequence in which the neo-epitope GGVV was exchanged for VVIA (wild-type Htt/Htt573-Q25) (Figure 31C). We created clonal neuronal HN10 cell lines (Lee et al., 1990) with inducible expression of either polyQ-Htt, wild-type Htt or polyQ-Htt and wild-type Htt together. These cell lines were subsequently used to establish a cellular high-throughput time resolved FRET assay for detection of cellular protein levels (Figure 31D).

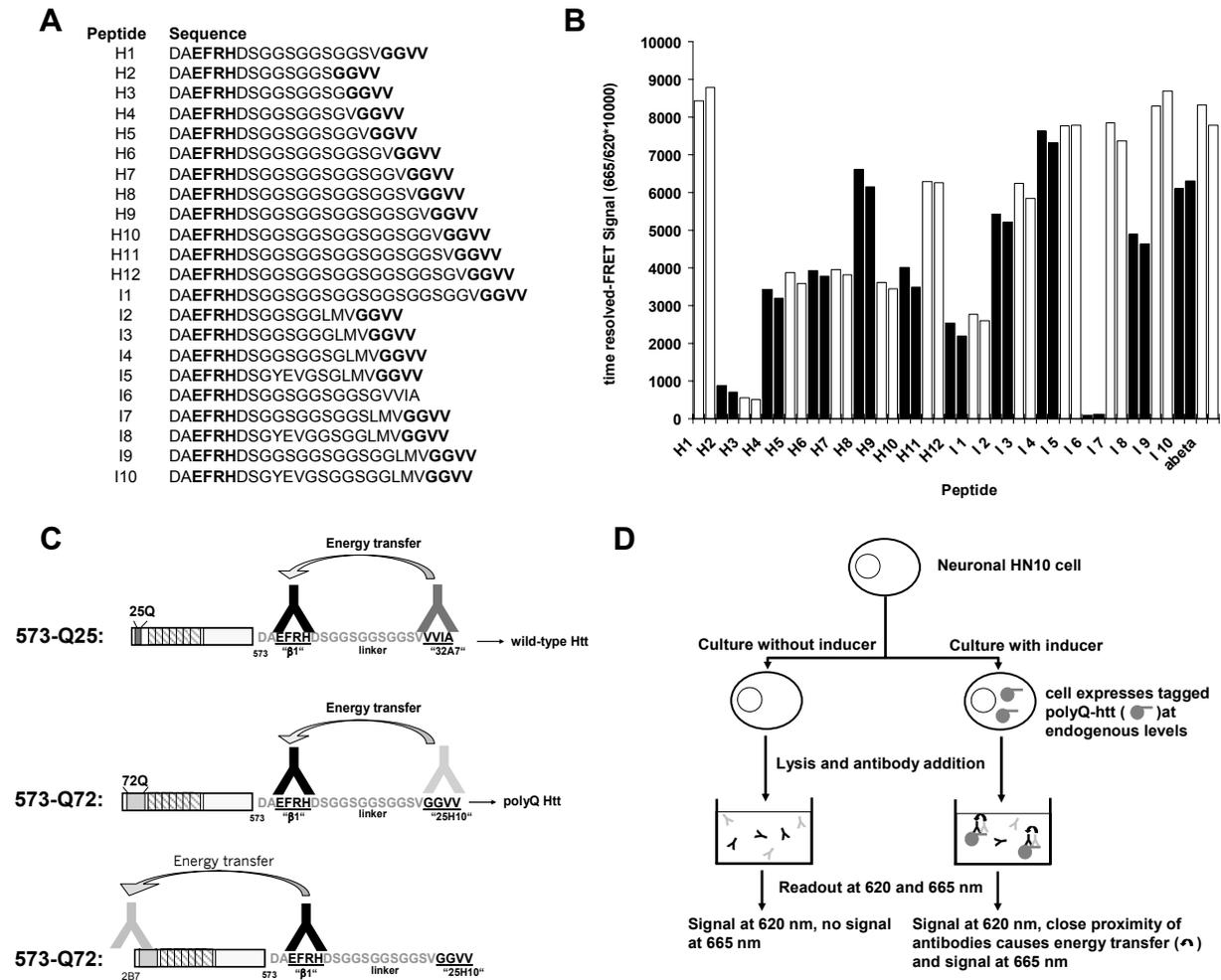


**Figure 31: Detection tag and linker optimization, protein constructs and assay principle.** **A:** Optimization of linkers. Peptide sequences analyzed with 25H10 and  $\beta$ 1 antibodies are shown with epitope sequences for antibodies in bold letters. **B:** Time Resolved FRET analysis of the peptides indicated that peptide H1 is best recognized by the antibody pair. H1 peptide sequence was subsequently chosen as an artificial tag (3 ng peptide/well loaded, duplicates for each peptide shown). **C:** Final constructs that are expressed in the clonal neuronal cell lines and detection sites of antibodies used. 25H10, 32A7 and  $\beta$ 1 antibodies detect epitopes at the carboxyterminal tag of the constructs, 2B7 antibody detects an endogenous Htt epitope at the aminotermis. Neuronal HN10 clonal cell lines with inducible expression of tagged Htt constructs were created for the assay. **D:** Concept behind the assay.

## Protein Detection and Signal Specificity

The neuronal clonal cell lines created expressed the tagged polyQ-Htt and wild-type Htt at levels corresponding to that of endogenously expressed Htt upon full induction with no detectable basal expression as demonstrated by western blot analysis (Figure 32A,B). Expression levels of the constructs after induction were stable over time (Figure 32B). Experiments using a 96-well format showed that highly specific time resolved FRET detection of either the wild-type- or polyQ-Htt-protein in a cellular context was feasible when using the antibody pairs 25H10-K +  $\beta$ 1-D2 or 32A7-K +  $\beta$ 1-D2 which detected specifically their corresponding tags. In addition, using the 2B7-K antibody specific for an aminoterminal endogenous Htt epitope in combination with the  $\beta$ 1-D2 antibody specific for an epitope at the

carboxy-terminal tag, allowed for selective detection of non-cleaved, intact Htt-protein (Figure 32C) in the cell lines expressing either wild-type or polyQ-Htt.

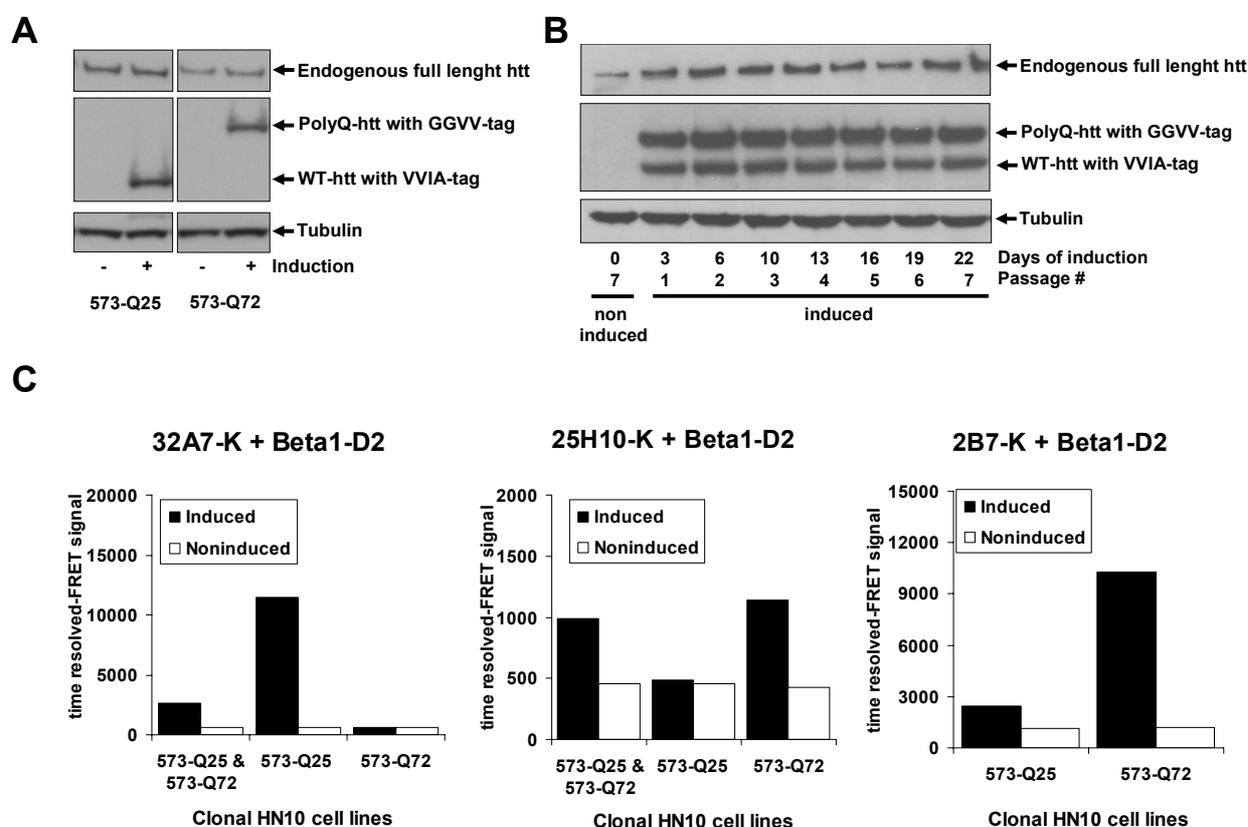


**Figure 32: Detection of induced constructs in neuronal cell lines with time resolved FRET.** A: Western blot for wild-type (Htt573-Q25) and polyQ-Htt (Htt573-Q72) shows expression levels near endogenous levels of full length Htt as well as absence of basal expression without addition of inducer. B: Western blot of cell lysates from clone with inducible co-expression of the wild-type and polyQ-Htt constructs. Expression levels are stable over passages and time. C: Detection of constructs in 96-well format with time resolved FRET method proves sensitivity and specificity of the assay. After induction of expression, wild-type and polyQ-Htt are specifically detected only by the antibody pairs corresponding to the tags.

In order to determine the maximal expression levels of polyQ-Htt-protein in the HN10 Htt573-Q72 cells, we first calibrated our assay using increasing H1 peptide concentrations diluted into PBS or cell lysates from noninduced cells (Figure 33). After determining the linear range and intensity of the time-resolved FRET signal for a given H1 peptide amount in cell lysates, we were able to calculate an expression level of polyQ-Htt-protein (which carries the H1 peptide as a tag) corresponding to 17 ng Htt per mg total cellular protein. This intracellular concentration of polyQ-Htt was significantly higher than the detection limit of the assays calculated as 3-fold standard deviation over the background signal (3.6 ng polyQ-Htt per 1 mg total cellular protein).

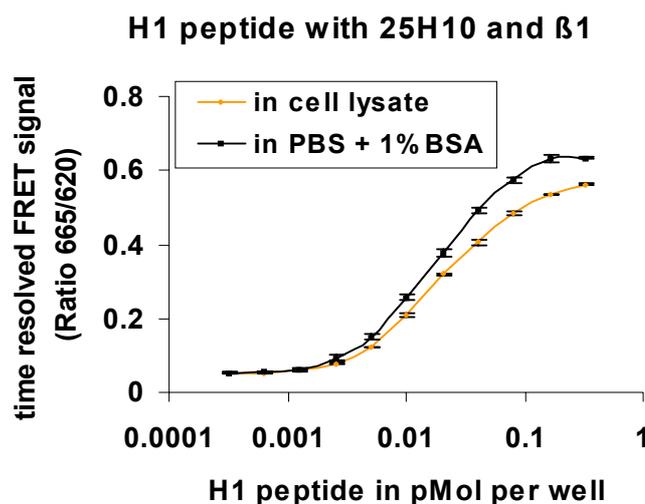


**Figure 33: Detection sensitivity of H1 peptide for 25H10-K +  $\beta$ 1-D2 antibody combination.** Increasing amounts of H1 spiked into noninduced cell lysates of Htt573-Q72 clone and time resolved FRET detection with 25H10-K +  $\beta$ 1-D2. All data points  $n=3$ , error bars =stdev.

### Assay Miniaturization

Next, we adapted the assay to a 1536 microwell format. To this end, we selected the Htt573-Q72 expressing HN10 cell line and used the 2B7-K plus  $\beta$ 1-D2 antibody combination in order to quantify uncleaved polyQ-Htt-protein. One of the advantages of using the ratiometric readout in the time resolved FRET method is that adaptation to a miniaturized assay format is readily facilitated because the assay signal is not dependent on the path length of the detection system or the absolute number of particles being detected. In addition ratiometric readout are also more robust to errors in liquid handling again facilitating assay miniaturization (Imbert et al., 2007). As liquid transfer is difficult and time consuming in a 1536 well plate format it was especially important that our detection was based on a totally homogeneous assay format whereby no liquid transfer or removing steps were necessary.

After miniaturizing the format to cells grown directly in a 1536 microwell plate, the assay protocol was optimized for lysis buffer (Figure 34A) and signal development over time (Figure 34B). Even though induced-to-non-induced signal ratio improved as a function of incubation time, the  $Z'$  value already reached a maximum of 0.86 after shorter incubation periods (Figure 34B). We proceeded to optimize the detection conditions by determining the minimal inducer concentration for maximal induction of expression. Induction of polyQ-Htt expression showed good response to changing inducer concentrations, with an EC50 corresponding to  $\sim$ 250 nM (Figure 34C) and a  $Z'$  value of 0.87 between signals at 400 nM

and 200 nM inducer, showing the reliability of the assay for a partial (~50%) reduction in polyQ-Htt.

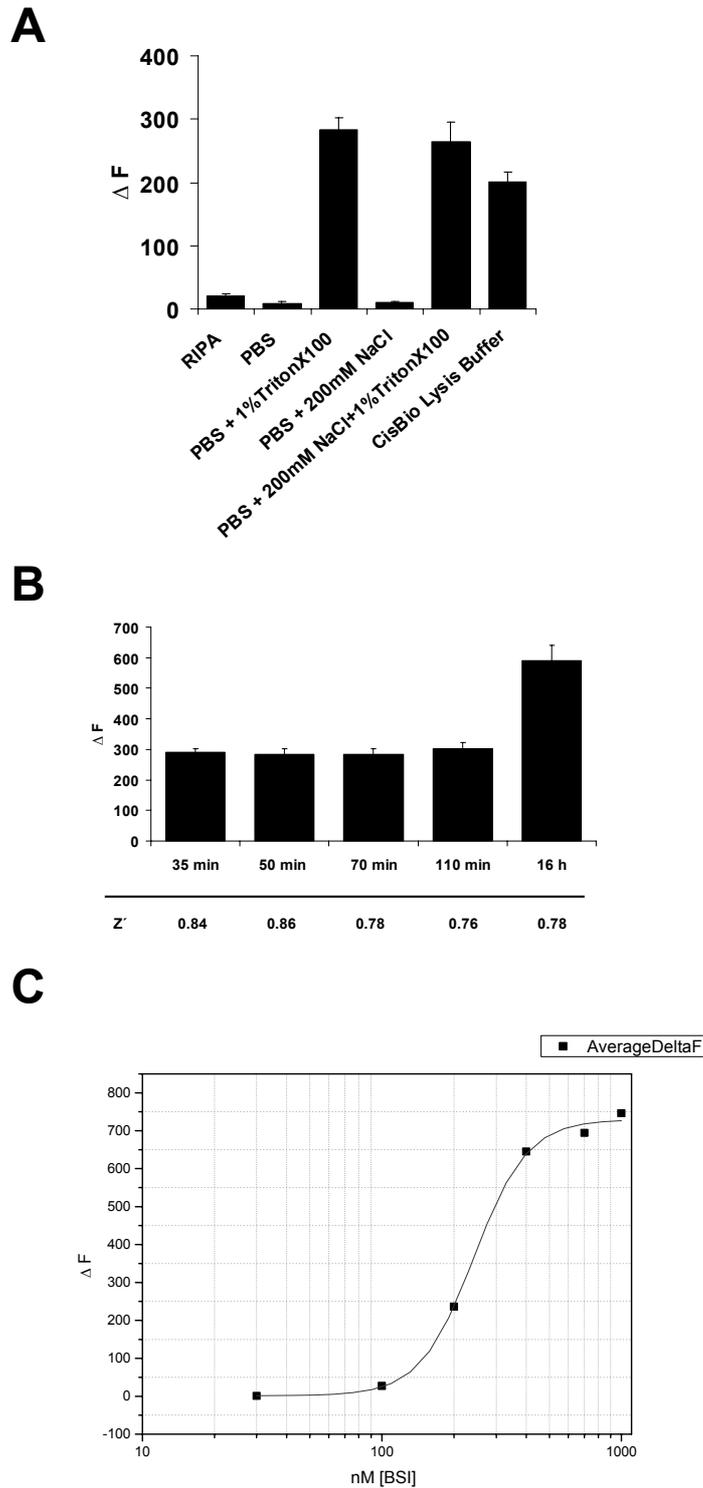


**Figure 34: Optimization of Htt construct detection in neuronal cell line with time resolved FRET.** **A:** Influence of lysis buffer on assay performance for the detection of the Htt573-Q72 construct with the 2B7-β1 antibody combination (measurement after 50 min, n=6). **B:** Time dependency of signal showed increase in induced-to-non-induced ratio but relative stability of Z' over time (Htt573-Q72 construct, n=6). **C:** Expression levels of Htt573-Q72 in response to increasing inducer concentration (n=6, IC50 ~250 nM).

Figure 35 presents some of the additional assay validation steps taken to characterize the 1536 well assay. First, the DMSO tolerance of the assay was tested to ensure that DMSO, which is used as the compound salvation agent, did not affect the assay signal by altering cell growth (Figure 35A). DMSO was well tolerated up to a concentration of 1%. The effect of cell density on the assay robustness was determined by assessing the  $Z'$  value (using induced and non-induced cells as high and low controls) at different cell densities with or without multiplexing the detection of Htt levels with a measure of cell viability (the reduction of resazurin as a measure of mitochondrial activity, Figure 35B) (O'Brien et al., 2000). The  $Z'$  values remained constant over a range between 6000 and 8000 cells/well and multiplexing with the cytotoxicity assay had no influence on the robustness of the assay. Since unbound europium cryptate labeled antibody can contribute to non-specific background signal in time resolved FRET assays, it was important to select the most appropriate dilutions of the two monoclonal antibodies used in the assay. An example of optimization of antibody concentrations is shown in Figure 35C.

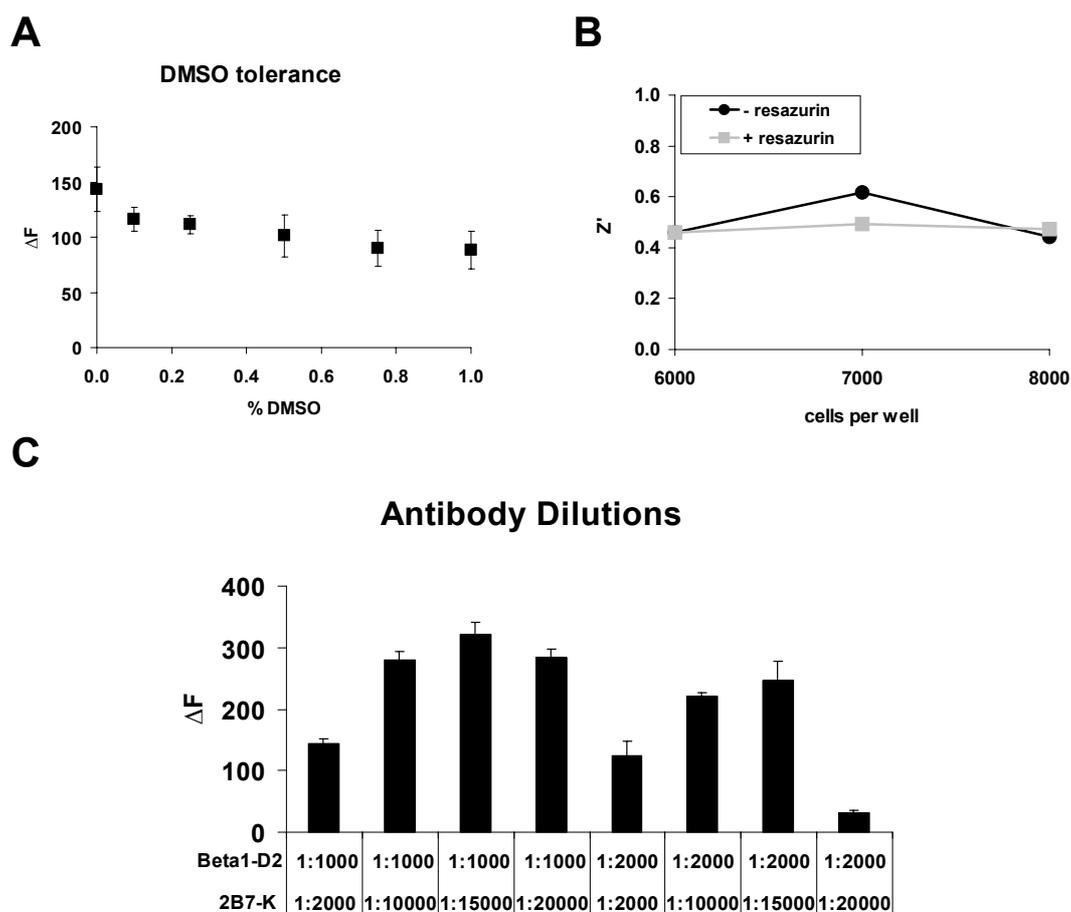


**Figure 35: Optimization of assay conditions for high-throughput-screen.** A: Shows the DMSO tolerance of the assay. B:  $Z'$  calculation at different cell densities, in the presence and absence of resazurin. C: Antibody titration to optimize the relative antibody concentrations for construct detection after induction.

## High Throughput Screening

Following miniaturization, the assay was first applied for screening a small library composed of ~10000 compounds commonly used in house for validating the assay performance before commencing screening the full deck library. This allowed to monitor the assay performance under real HTS screening conditions. Importantly, this also resulted in the identification of a small number of primary hits, which can be used to further characterize the secondary assays destined for triaging the total number of hits identified by the full primary screen.

Analysis of the prescreen values demonstrated excellent performance with  $Z'$  values averaging at ~0.6 among multiple plates. Close inspection of the primary results however did show that there was a small, but significant “edge effect” in all plates tested in the prescreen. This edge effect was more evident when viewing the correction pattern of the plates analyzed (data not shown) or when the results of this focused screen were arranged by well number (Figure 36A). This view showed a regular “saw tooth” pattern due to the plate edge effects. However, this effect was only minor and did not affect much the statistics of the assay performance, as shown in Figure 36B with the primary data presented in a Gaussian distribution.

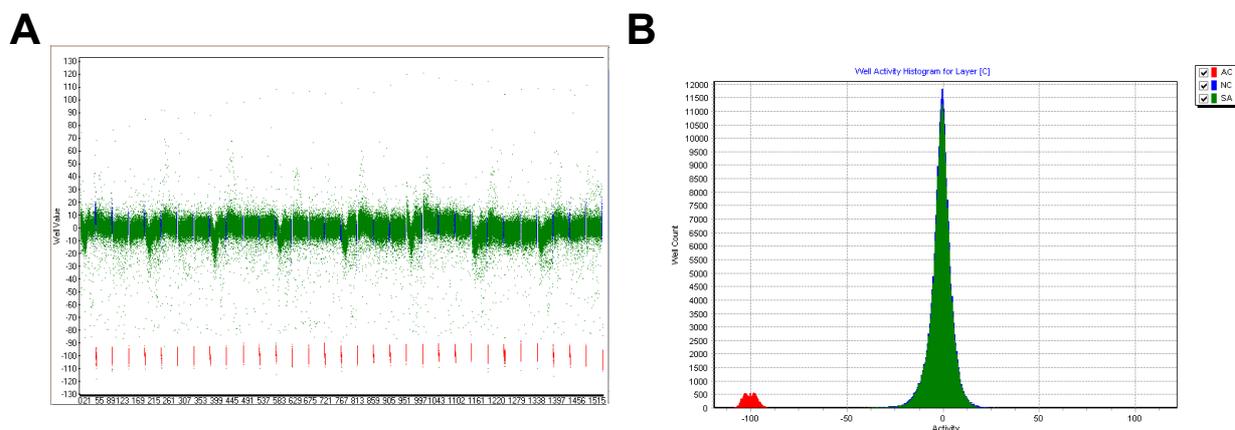


**Figure 36: Screening performance.** **A:** Scatter plot of the screening data with the x-axis being the well number for each of the samples. The slight “saw-tooth” pattern of the results show how even after “correction” of the results a slight effect of the plate effect is apparent. However, the actual magnitude of this plate effect is actually less than 20% activity. **B:** Frequency distribution of the results obtained for the samples tested (colored green) and the positive controls (noninduced cells, colored red).

## Comparison of Results Using Resazurin

In addition to testing assay performance with the standard single readout format (Figure 37A) a smaller subset of the preplated compounds were also multiplexed for cell viability, which was monitored before cell lysis, and protein detection by time resolved FRET (Figure 37B). As shown in Figure 37C, both assay formats performed equally well. If anything, the data generated by the multiplexed readout appeared less scattering. Comparison of the compound

activity in the two assay formats showed that 90% of the compounds identified as hits in the single readout format were also identified in the dual readout format with a general hit rate of ~0.4% (activity cut-off: 3-fold standard deviation over the mean signal), confirming high reproducibility and reliability of the time resolved FRET readout.

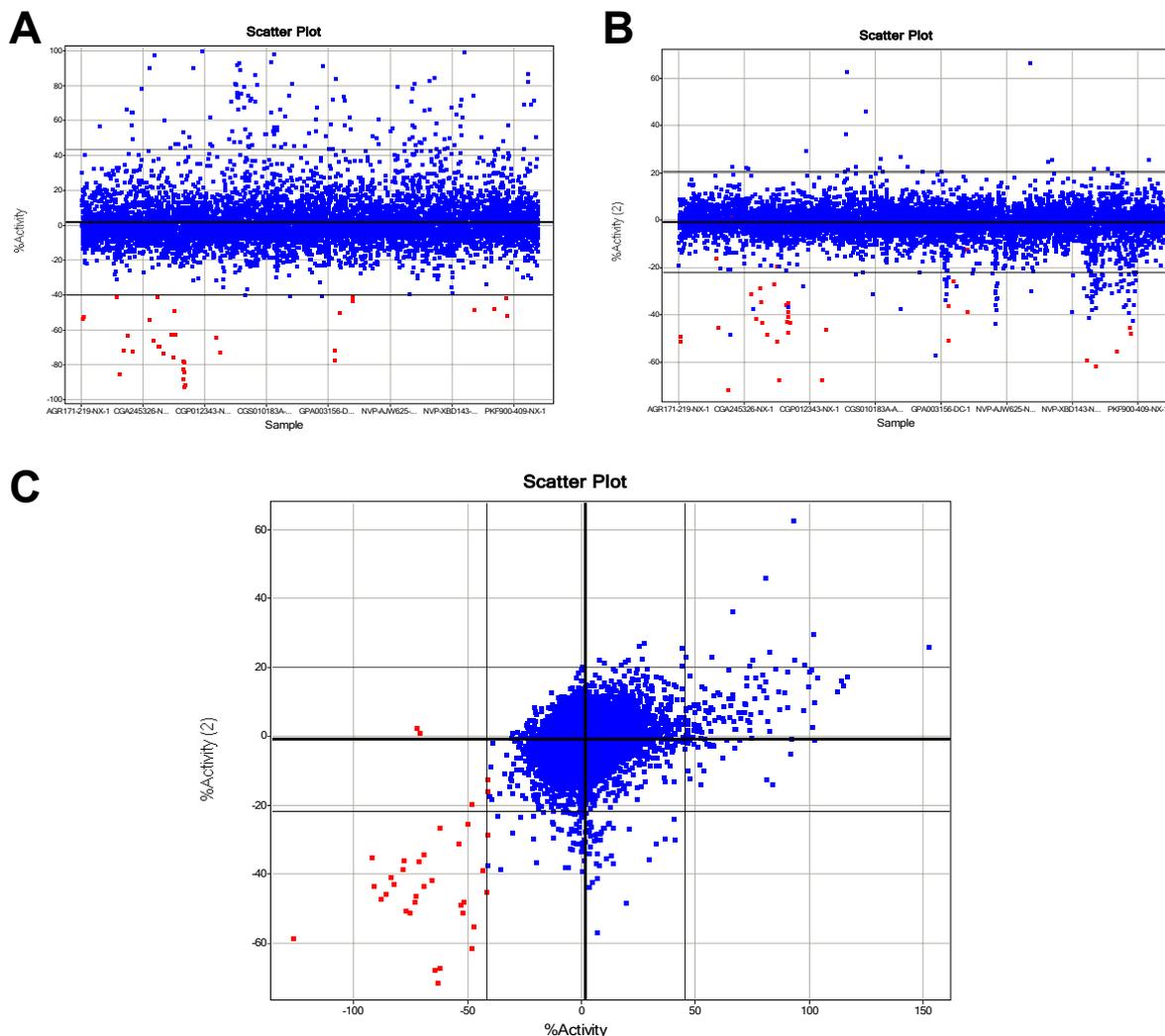


**Figure 37: Comparison of screening results in the presence or absence of resazurin.** **A:** Standard single readout format. **B:** Subset of plates tested with a multiplexed readout. Plates were tested for cell viability with resazurin and polyQ-Htt levels with time resolved FRET **C:** Comparison of single readout and multiplex readout hits. Both assay formats resulted in similar performance with 90% of the compounds identified as hits in the single readout format also being found in the multiplex readout format with a general hitrate of ~0.4%.

Both assay formats were able to identify compounds that increased the levels of polyQ-Htt protein present in the cells. Though not of primary focus in our screen, it should be noted that since we measured the levels of intact polyQ-Htt and since proteolytic cleavage of polyQ-Htt influences its toxicity (Gafni et al., 2004; Wellington et al., 2002), these compounds could potentially be of interest as Htt cleavage inhibitors or of general interest to characterize our cellular model systems.

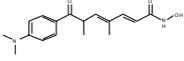
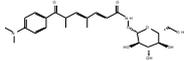
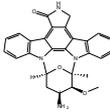
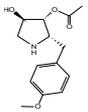
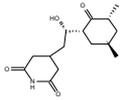
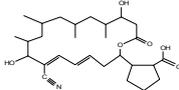
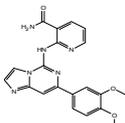
## **Characterization of Active Compounds**

The Novartis compound archive contains one of the largest collection of purified natural products. Screening of these compounds has the advantage that many of the compounds have previously reported activity and their mechanism of action is known, thus suggesting possible targets involved in the cellular regulation of polyQ-Htt expression.

As noted previously, 12 compounds out of the ~10000 compounds in the prescreen were found to increase polyQ-Htt protein in both assays. Even though Htt cleavage inhibitors of potential therapeutic use could belong to this compound group, the majority of compounds increasing polyQ-Htt levels were expected to act via unspecific pathways. Indeed, 8 of these compounds were chlamydocin or trichostatin A analogues, common HDAC inhibitors that lead to a general increase of gene expression (Table 1, #1,2) (De Schepper et al., 2003; Nishino et al., 2004; Yoshida et al., 1995).

More interesting were a number of compounds effectively lowering polyQ-Htt expression although these compounds may work by some non-specific effect or by perturbing cell viability. For example cycloheximide, borrelidin and anisomycin (Table 1, #4-6) lowered the levels of polyQ-Htt but did not influence cell viability over the incubation time of this assay. All three compounds are known to be general inhibitors of protein synthesis (Baliga et al., 1969; Grollman, 1967; Nass, 1970). Additionally, a number of staurosporine analogues (unselective protein kinase inhibitors; Table 1, #3), as well as BAY 61-3606 (a specific syk kinase inhibitor; Table 1, #7 (Yamamoto et al., 2003)) are known to interfere with various cellular pathways.

Even though many compound hits in our assay will act via unspecific pathways such as those described in the previous paragraph, the dynamic response of the assay to compounds with known mechanism of action was very encouraging. Further validation of the compounds lowering neuronal expressed polyQ-Htt by unknown biological mechanisms of action is in process as well as a full screen of the Novartis compound library.

#	Compound	Structure	Biology	Activity in assay in %
1	Trichostatin A analogue		HDAC Inhibitor	68
2	Trichostatin A analogue		HDAC Inhibitor	67
3	Staurosporine		Proteinkinase Inhibitor	-84
4	Anisomycin		Proteinsynthesis Inhibitor	-79
5	Cycloheximide		Proteinsynthesis Inhibitor	-74
6	Borrelidin		Proteinsynthesis Inhibitor	-73
7	BAY 61-3606		SYK kinase Inhibitor	-27

**Table 1: Selection of compounds with known biological mechanism of action and their activity in the assay.**

#### 4.3.5 DISCUSSION

This report describes the design and implementation of an assay that allows the quantification of proteins, even those expressed at endogenous levels. The assay format is homogenous and robust enough to allow miniaturization for high throughput screening. The assay format has been used to identify compounds that modulate the intracellular levels of the polyQ-Htt protein fragment and possibly represents the first assay that is capable of measuring the steady state levels of this protein.

There are still a number of caveats with this assay format though. First, it appears that the cell lysis conditions need to be optimized for each set of protein and antibody detection reagents (unpublished results). Second, it appears that the assay is only detecting proteins that are solubilized during cell lysis which might mean that this format would not be suitable for monitoring the levels of proteins involved in large macromolecular complexes that are not readily solubilized (e.g. proteins associated to the cell cytoskeleton or to the nuclear structure). Third, because a recombinant peptide tag has been added to facilitate detection there are a number of possible caveats including that the endogenous untagged protein levels may differ from the detected signal. Such a caveat depends on the fate of the detection tag because of potential proteolysis. The peptide tag may also have an effect on the physiology of the protein being studied. Fourth, while it is possible to multiplex this assay format with an assay to monitor cell viability, the current assay setup uses a measure of mitochondrial redox potential which may not be sensitive enough to detect changes in cell physiology that may alter relative protein levels.

One advantage of this tagging approach is that it allows not only the levels of protein expression to be monitored but readily allows detection of the protein for application to intracellular imaging assays. This would then make it possible to not only follow the levels of protein during a change in conditions but also the protein location within the cell. For Htt this is of importance as it has been reported that intracellular localization of Htt influences its toxicity (Bates, 2003; Chen et al., 2001; Chen et al., 2002; Yang et al., 2002) and may also have a bearing on the apparent protein levels (Gutekunst et al., 1999; Stack et al., 2005). While the detection method described in this report has been combined with a readout of cell viability, this readout has a tendency to underestimate the potential toxicity of compounds. However it is still possible that this assay format could be multiplexed with additional readouts such as ATP levels or even other reporter gene assays.

Finally, it should be evident that the basic strategy used to detect proteins can be extended to assays using antibodies to non-recombinant epitopes allowing endogenous and untagged protein to be detected and quantified.

#### **ACKNOWLEDGEMENTS**

We thank CisBio for providing custom labeling of antibodies and technical discussions.

#### **4.4 Single-step detection of soluble mutant huntingtin in cellular, animal and human tissue samples: a bioassay for Huntington's Disease**

**Andreas Weiss<sup>1</sup>, Corinna Klein<sup>1</sup>, Kimberly Kegel<sup>2</sup>, Ruth Bodner<sup>3</sup>, David Housman<sup>3</sup>, Marian DiFiglia<sup>2</sup>, Jonathan Fox<sup>2</sup>, Steven Hersch<sup>2</sup>, Scott Zeitlin<sup>4</sup>, Etienne Regulier<sup>1</sup>, Graeme Bilbe<sup>1</sup> and Paolo Paganetti<sup>1</sup>**

1) Neuroscience Discovery, Novartis Institutes for BioMedical Research (NIBR), Basel, Switzerland

2) MassGeneral Institute for Neurodegenerative Disease, Massachusetts General Hospital (MGH)

3) Center for Cancer Research, Massachusetts Institute of Technology (MIT)

4) Department of Neuroscience, University of Virginia School of Medicine

Submitted

#### **4.4.1 SUMMARY**

The genetic mutation causing Huntington's Disease (HD) is a polyglutamine expansion in the huntingtin protein. Expansions beyond 39 glutamines become pathogenic and appear to affect protein folding and successive formation of toxic intracellular fragments and aggregates. Innovative disease-modifying therapeutics for HD may target folding, proteolytic cleavage or degradation of mutant huntingtin. Despite the clear causative role of mutant huntingtin, assessment of huntingtin expression during disease progression or in presymptomatic HD is sparse. We established a highly sensitive detection assay, which allows for single-step quantification of soluble mutant huntingtin in biological samples. We found that mutant huntingtin levels decrease as a function of disease progression and inversely correlate with the amount of aggregates present in brains of HD mice. Specific determination of mutant huntingtin was established in blood-derived fractions and brain extracts of HD patients. This allows assessing the relevance of mutant huntingtin levels as a disease and/or pharmacodynamic biomarker in HD.

#### 4.4.2 INTRODUCTION

Huntington's Disease (HD) is the most common inherited neurodegenerative disorder with a prevalence of 5 to 8 cases per 100'000. Its main clinical manifestations include motoric dysfunction, psychiatric disturbances and dementia. Numerous symptomatic treatments have been tried for HD without any substantial success (Bonelli and Wenning, 2006) and no approved treatments for HD exist (Bates, 2003; Bates and Hockly, 2003; Landles and Bates, 2004; Young, 2003). HD is the founding member of the polyglutamine (polyQ) disease family composed of nine autosomal-dominant inherited disorders whose common characteristic is a polyQ-repeat expansion in different ubiquitously expressed proteins (Everett and Wood, 2004; Ross, 2002). The expanded polyQ repeat in the huntingtin gene (Htt) lies in exon 1 and leads to the expression of mutant Htt protein (Group, 1993a; Gusella et al., 1983). The polyQ-repeat expansion may promote a conversion from a native random-coiled to a cylindrical, parallel beta-sheet conformation tethered by hydrogen bonds between the polyglutamine strands (Perutz et al., 1994; Perutz et al., 2002b). Similar to other neurodegenerative diseases characterized by protein misfolding like Alzheimer's Disease, the proteins with helical beta-sheet conformation are prone to form non-soluble protein aggregates (Balbirnie et al., 2001; Benzinger et al., 2000; Perutz et al., 2002b).

HD-like symptoms are reversed when expression of mutant Htt is down-regulated in the brain of HD mouse models by RNA interference (DiFiglia et al., 2007; Machida et al., 2006), (Rodriguez-Lebron et al., 2005; Wang et al., 2005) or by tetracyclin-regulated conditional expression (Yamamoto et al., 2000). Interestingly, mutant and wild-type-Htt are differently metabolized by the cell and display a different pattern of posttranslational modifications (phosphorylation (Warby et al., 2005)), proteolytic cleavage (Gafni et al., 2004; Graham et al., 2006; Wellington et al., 2002), cellular localization (Davies et al., 1997; van Roon-Mom et al., 2002) and degradation (Ravikumar et al., 2002). These findings prompted discovery work for HD therapeutics aimed at influencing the misfolding or the clearance of mutant Htt e.g. through upregulation of the chaperone system or induction of the autophagy degradation pathway (King et al., 2008; Perrin et al., 2007; Yamamoto et al., 2006; Zourlidou et al., 2007). Such approaches may find application for other neurodegenerative diseases caused by protein misfolding.

Currently, there is no bioassay available to assess the effect of such therapies on mutant Htt levels in clinical trials. We recently described a new homogenous time resolved Förster resonance energy transfer method for Htt detection suitable for high-throughput screening in a neuronal cell line (Weiss et al. submitted). Here, we show that this method can be modified to

quantify endogenous, full-length soluble mutant Htt in cellular, animal and human samples. This will enable researchers to address the relevance of soluble mutant Htt as a marker for disease progression or to monitor the efficacy of drug treatments in preclinical and clinical trials. As the design of the method is highly flexible, it is in principle applicable for investigations of other diseases, especially other members of the polyQ-family.

### **4.4.3 MATERIALS AND METHODS**

#### **Antibodies**

25H10, 32A7 and 2B7 antibodies have been described previously (Paganetti et al., 1996; Weihofen et al., 2003), (Weiss et al., submitted). MW1 antibody specific against the polyglutamine stretch of Htt and developed by Dr. Paul Patterson were obtained from the Developmental Studies Hybridoma Bank developed under the auspices of the NICHD and maintained by The University of Iowa, Department of Biological Sciences, Iowa City, IA 52242. Custom europium cryptate and D2-fluorophore labeling of the antibodies were performed by CisBio (Bagnols/Seze, France). Depending on the batch used, antibodies were cross-linked to 5 to 7 mol europium cryptate or D2-fluorophore per mol antibody.

#### **Cellular Models**

Inducible, neuronal HN10 cells (Lee et al., 1990) were described elsewhere (Weiss et al., 2008), (Weiss et al., submitted). The knock-in embryonic stem cells (ES cells) were generated as described in (Wheeler et al., 1999; White et al., 1997). The neomycin selection cassette was removed by a second electroporation with a plasmid expressing cre recombinase. Embryonic stem cell-derived neurons (ES neurons) were generated using the differentiation protocol as published by (Bibel et al., 2007; Bibel et al., 2004). In brief, ES cells were cultivated on mitomycin-inactivated mouse embryonic fibroblasts for at least two passages after thawing in ES medium containing 15% foetal calf serum (FCS) and 1000 U/ml LIF (leukemia inducing factor). Subsequently, they were cultured without fibroblast feeder cells for two more passages. Embryoid bodies (EBs) were formed on bacterial dishes in EB medium containing 10% FCS but no LIF and incubated for 8 days with the addition of retinoic acid on the last four days. EBs were dissociated by trypsinisation and plated on poly-L-lysine and laminin coated plates in N2 medium and changed to neuronal differentiation medium as described by (Brewer and Cotman, 1989) two days after dissociation.

#### **Animal Models.**

Heterozygous transgenic R6/2 males of CBAxC57BL/6 strain were obtained from G. Bates laboratory (Mangiarini et al., 1996) and bred with CBAxC57BL/6 F1 females. The offspring were genotyped by PCR assay of DNA obtained from tail tissue. The animals were housed in a temperature-controlled room that was maintained on a 12 hr light/dark cycle. Food and water were available *ad libitum*. All experiments were carried out in accordance with authorization guidelines for the care and use of laboratory animals. For time resolved FRET

assay detection of huntingtin, 2-3 months old animals were anesthetized with 3-5% isofluran followed by an intraperitoneal dose of 100mg/kg Ketamin and 10mg/kg xylazine. After CSF and blood collection, animals were given a sodium pentobarbital overdose (150 mg/kg). Muscle (gastrocnemius) and brain were immediately further collected for FRET analysis.

### **Aggregate analysis by AGERA**

AGERA analysis was performed as described (Weiss et al., 2008). In short, R6/2 brains were homogenized in 10 volumes (w/v) PBS + 0,4% TritonX100 and Complete Protease Inhibitor (Roche Diagnostics). Brain samples corresponding to 0.15 mg of total protein were loaded per AGERA lane. For separation of brain homogenates into soluble and non-soluble fractions, homogenates were centrifuged at 124 000 g for 1 h, supernatant was aliquoted (soluble fraction) and pellet was resuspended in equal to starting volume PBS + 0,4% TritonX100 (non-soluble fraction).

### **Human samples**

HD patient identification was based on the presence of movement disorders, a positive family history and known CAG repeat expansion. Patients were categorized by using the total functional capacity (TFC) score assessed by experienced clinical raters. Control subjects showed no history of neurological or psychiatric symptoms. Consent of patients was obtained according to the Declaration of Helsinki (Br Med J 1991; 302: 1194). Blood samples were taken in EDTA-Vacutainer tubes (BD, Oxford) and fractionated by density gradient centrifugation using a standard technique to obtain red blood cell and buffy coat (> 90% lymphocytes) fractions.

### **Time resolved-FRET: Cellular models**

Detection of polyQ huntingtin in cell lysates was performed as described (Weiss et al. submitted).

### **Time resolved-FRET: BioAssay**

Brain and muscle tissue were homogenized in 10x volume sample buffer (PBS + 1% Triton X-100 + complete protease inhibitor). Blood, plasma and corticospinal fluid samples were prediluted 1:1 in sample buffer. 10 µl sample and 5 µl antibody dilution (europium cryptate and D2 labeled antibodies in 50mM NaH<sub>2</sub>PO<sub>4</sub>, 400mM NaF, 0.1% BSA, 0.05% Tween) was added to each well to a final dilution of 1.5 ng/well 2B7-europium labeled antibody and 30

ng/well MW1-D2-labeled antibody. Plates were incubated at 4°C for 1h. Measurements were performed with a Xenon-lamp Envision Reader for 620 and 665 nm wavelengths after excitation at 320 nm (time delay 100  $\mu$ s, window 400  $\mu$ s, 100 flashes per well).

### **Data analysis**

The time resolved-FRET readouts are performed at 620 and 665 nm wavelength. The signal obtained from the 620 nm wavelength is a huntingtin unspecific signal and results from the emission of the europium labeled antibody. It is possible to use the 620 nm signal as a control reference signal for possible artifacts caused by scattering, quenching, absorption or general turbidity resulting from the analyzed sample. The huntingtin specific signal at 665 nm wavelength is caused by the time delayed excitation of the D2 labeled antibody by the 620 nm emission of the europium labeled antibody. Therefore, 665/620 nm ratio calculation results in an artifact corrected specific determination of the amount of the two antibodies binding in close proximity of each other on the huntingtin protein. As the antibodies are present in excess, 665/620 ratio is a precise reflection of the amount of antigen present in the sample.

### **Statistical analysis**

Quantification of cellular and mouse values are presented as averages with standard deviations. Significances were calculated by students' t-test.

#### 4.4.4 RESULTS

##### Time-resolved Förster resonance energy transfer assay for detection of endogenous huntingtin

Aminoterminal fragments of mutant Htt are neurotoxic *in vitro* and *in vivo* (Arrasate et al., 2004; Li et al., 2000; Varma et al., 2007). Mutant Htt toxicity and aggregation are dependent on polyQ length, Htt fragment length, and level of mutant Htt expression (Colby et al., 2006; King et al., 2008; Machida et al., 2006; Scherzinger et al., 1999; Wang et al., 2005). We recently demonstrated the feasibility to measure in one step intracellular mutant Htt using a time resolved-FRET assay. In this assay, an antibody pair recognizes a short artificial tag fused to a Htt fragment. (Weiss et al. 2008, submitted) (Figure 38).

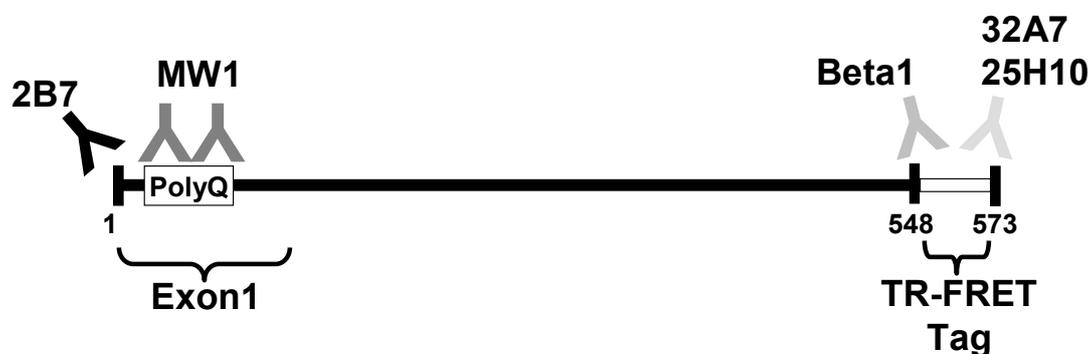


**Figure 38: Binding sites of antibodies used in this study to the 573-Htt construct.** While 2B7 and MW1 detect endogenous Htt epitopes, Beta1, 32A7 and 25H10 are specific against the artificial tag added at the C-terminus (Weiss et al, submitted). Note: as MW1 is specific against the polyQ-stretch, increasing polyQ-length will result in stronger and increased MW1 binding (represented by the two antibodies displayed in the figure) (Li et al., 2007).

With the aim of detecting untagged mutant Htt, it was necessary to use a different antibody pair. In order to measure fragments as well as full-length mutant Htt, we used the monoclonal antibody 2B7, which binds to the 17 amino acids preceding the polyQ-repeat at the aminoterminal of Htt. We selected MW1, a polyQ-specific antibody (Ko et al., 2001) as second antibody. The combination of 2B7 and MW1 antibodies resulted in specific detection of all Htt-fragments expressed in HN10 cells, including untagged Htt-exon1 (Figure 39A, Exon1-Q25 and -Q72). As expected, using other antibody combinations which included one or both of the epitopes against the artificial tag failed to detect the untagged Htt-exon1 constructs (Figure 39A, Exon1-Q25 and -Q72) but readily detected the Htt constructs carrying the tags (Figure 39A, 573-Q25 and -Q72).

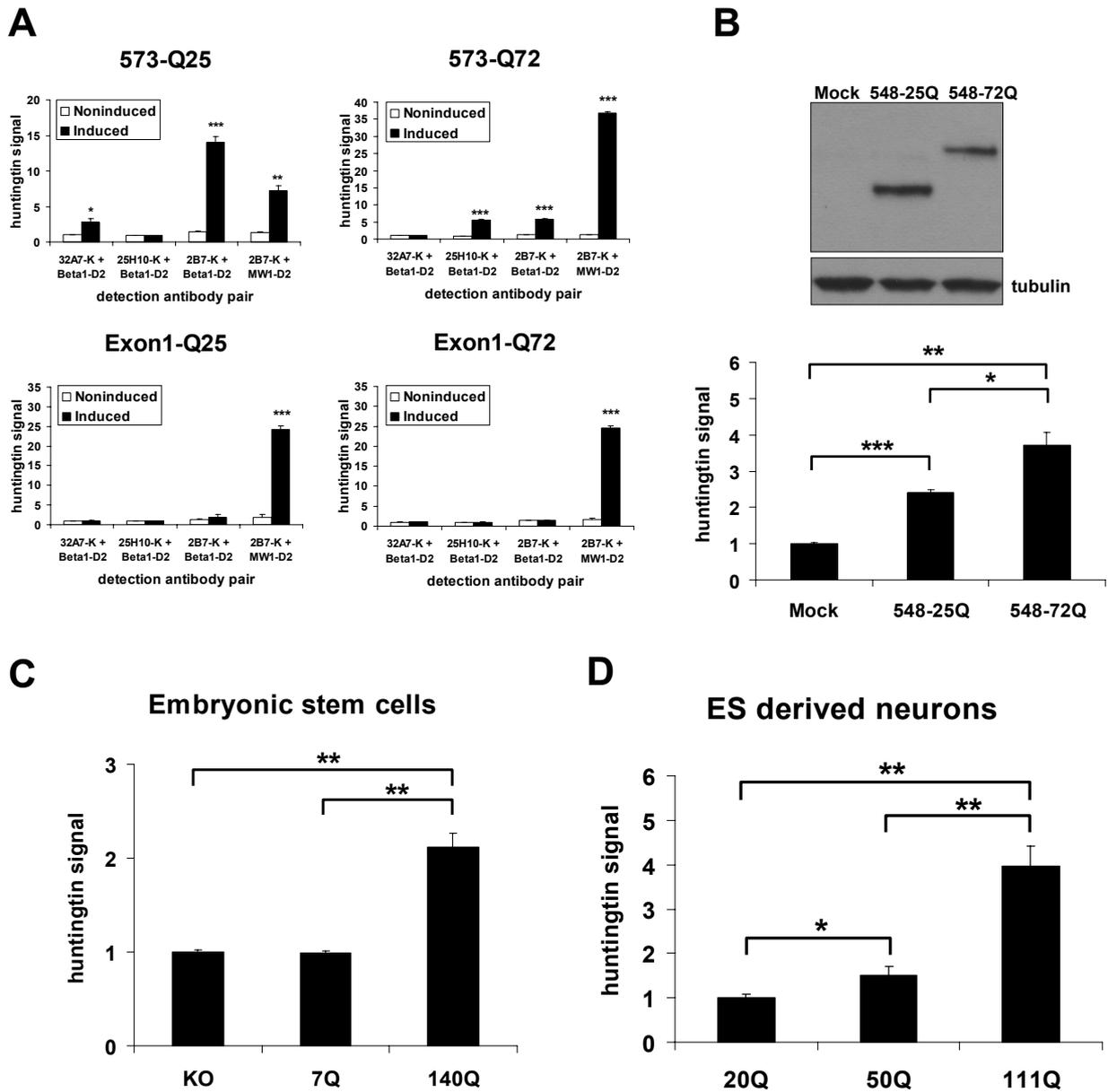


**Figure 39: Mutant huntingtin detection in cellular models of Huntington's disease.** **A:** Time resolved-FRET detection of Htt constructs upon inducible expression in neuronal HN10 clones. Specific detection of 573-Htt-constructs by different antibody combinations. Using antibody combinations that included one of the epitope against the artificial tag which is included in the 573-constructs fails to detect untagged exon1 constructs. Using antibody combination 2B7 and MW1 both specific against Htt-endogenous epitopes, results in a Htt specific signal for all constructs tested, including the untagged exon1 constructs. **B:** Time resolved-FRET signal for 2B7-MW1 detection is polyQ-dependent. Lentiviral expression of untagged Htt-constructs with varying polyQ-length with a fixed virus titer resulted in equal expression of all the constructs as shown by western blot. Time resolved-FRET detection showed a clear dependency of the signal strength on the polyQ-length. Loading: 7 ug total protein per sample. **C:** Detection of full length Htt expressed at endogenous levels. A notable and significant signal difference was observed for lysates from ES cells expression full-length Htt with 140 polyQ repeats over lysates from Htt knock-out ES cells or ES cells expressing full length Htt with the mice wild-type polyQ length of 7 glutamines. Loading: 10 ug total protein per sample. **D:** Detection of full length Htt expressed at endogenous levels in neurons in a polyQ-dependent manner. Detection of full-length huntingtin expressed at endogenous, neuronal levels is possible as shown by lysates from ES-derived neurons. In addition, as shown for lentiviral system, signal strength is polyQ-dependent. Loading: 40 ug protein per sample. (All figures: n=3, stdev, \*= $p < 0.05$ , \*\*= $p < 0.01$ , \*\*\*= $p < 0.001$ ).

Clone to clone variations may contribute to different expression levels in the HN10 cell lines, thereby possibly complicating efforts to compare polyQ-dependent detection sensitivity when analyzing wild-type and mutant huntingtin expression from different clones. To circumvent this limitation, we opted for a lentiviral approach for expression of untagged Htt-constructs with 25 or 72 glutamines in a homogenous population of mouse embryonic stem cells (ESC; (Bibel et al., 2004)). A predefined virus titer led to equal expression of the constructs as demonstrated by western blot. Signal strength in time resolved-FRET increased with polyQ-length (Figure 39B). This was expected, since expansion of the polyQ-repeat would increase binding of MW1 relative to wild-type Htt (Ko et al., 2001; Li et al., 2007). These data demonstrated specific detection of Htt fragments in a polyQ-dependent manner by the antibody pair 2B7-MW1.

For evaluating the use of the time resolved-FRET assay to detect endogenous, full-length Htt, we selected ESC with the Htt gene deleted (Htt knock-out as negative control) or modified by a polyQ insertion (polyQ knock-in as positive control). A significant signal was obtained in samples from the 140Q knock-in ESC when compared to samples from the Htt knock-out ESC (Figure 39C). In contrast, we did not observe a signal above background (mock condition) when using normal ESC. This is consistent with the fact that normal mouse Htt has a polyQ-stretch of only 7 glutamines, evidently too short for recognition by the MW1 monoclonal (Figure 39C) (Ko et al., 2001). In cell lysates obtained from ESC-derived glutamatergic neurons in which varying polyQ-lengths were knocked-in in the endogenous Htt gene, neuronal Htt was detected in a polyQ-length dependent manner (Figure 39D). Notably, a significant amount of Htt was detected also for 20Q-Htt, a polyQ length representing the majority of the normal human alleles. These data demonstrate that our single-step detection method can be used for rapid, quantitative and polyQ-length dependent detection of endogenous Htt protein in neuronal cells.

### **Detection of soluble mutant Htt in central and peripheral tissues of murine HD models and significant changes in soluble brain Htt as a function of disease progression**

The single-step bioassay for Htt was next used to analyze brain homogenates obtained from 4 and 12 week-old R6/2 mice and aged-matched wild-type mice. R6/2 mice develop an aggressive HD-like phenotype because of the ubiquitous expression of mutant Htt exon1 driven by the human Htt promoter (Mangiarini et al., 1996). Figure 40 summarizes the data obtained for the HD mice. Robust signals were observed in all transgenic animals analyzed. The mutant Htt specific signal in young, presymptomatic mice was about 25-fold above that

measured in wild-type animals (Figure 40A), which is likely to represent the background noise as endogenous mouse Htt was not detected in ESC Htt-knock out cells (see above). Interestingly, the level of mutant Htt detected in the brain of the older mouse group, which have an advanced HD-like phenotype, was about 45% less than that in young R6/2 mice (Figure 40A). This decrease in mutant Htt was surprising, as the Htt-aggregate load measured in the same brain samples by AGERA increased as a function of age (Weiss et al., 2008) (Figure 40A; AGERA blot). One possible explanation for these results was that the time resolved-FRET assay using the 2B7-MW1 antibody pair was specific for a mutant Htt fraction distinct from mutant Htt aggregates. To further investigate this possibility, we separated by ultracentrifugation R6/2 brain homogenates into two fractions, one containing only soluble Htt species and one containing Htt aggregates sedimented as an insoluble pellet. Analysis of the supernatant and pellet fractions by AGERA demonstrated successful separation of the insoluble aggregates into the pellet fraction whereby no aggregates were present in the supernatant fractions (Figure 40B, AGERA blot). In contrast, we found that the amount of Htt detected by time resolved-FRET was predominantly enriched (most likely in a soluble monomeric and oligomeric form) in the supernatant fractions. These data indicated that the time resolved-FRET assay was specific for soluble mutant Htt forms. Thus, the decrease in the time resolved-FRET signal may indicate recruitment of soluble Htt species into aggregates accumulating as a function of age and disease progression, a mechanism also suggested for other neurodegenerative disorders such as Alzheimer's Disease (Sjogren et al., 2002; Strozyk et al., 2003).

We extended our analysis to include muscle and plasma samples from 6 week old as well as corticospinal fluid samples from 9 to 12 week old R6/2 or WT mice. We found significant detectable amounts of mutant Htt in the R6/2 mice when compared to their normal siblings in all tissue samples analyzed, although the signals in the body fluids were significantly lower than those detected in cortical extracts (Figure 40C).

In the context of a bioassay for mutant Htt, the R6/2 mouse model of HD based on the expression of a short fragment of Htt may have only a limited value as a model of the human situation in which mutated full-length Htt is expressed. As an alternative, we applied the time resolved-FRET assay for the analysis of mutant Htt in a knock-in mouse model expressing endogenous mouse full-length Htt with a polyQ-stretch of 140 glutamines (Menalled et al., 2003). Similar to the R6/2 mouse samples, significant amounts of mutant Htt were detected in every brain area analyzed as well as in full blood samples (Figure 40D) obtained from the polyQ-knock-in mice.

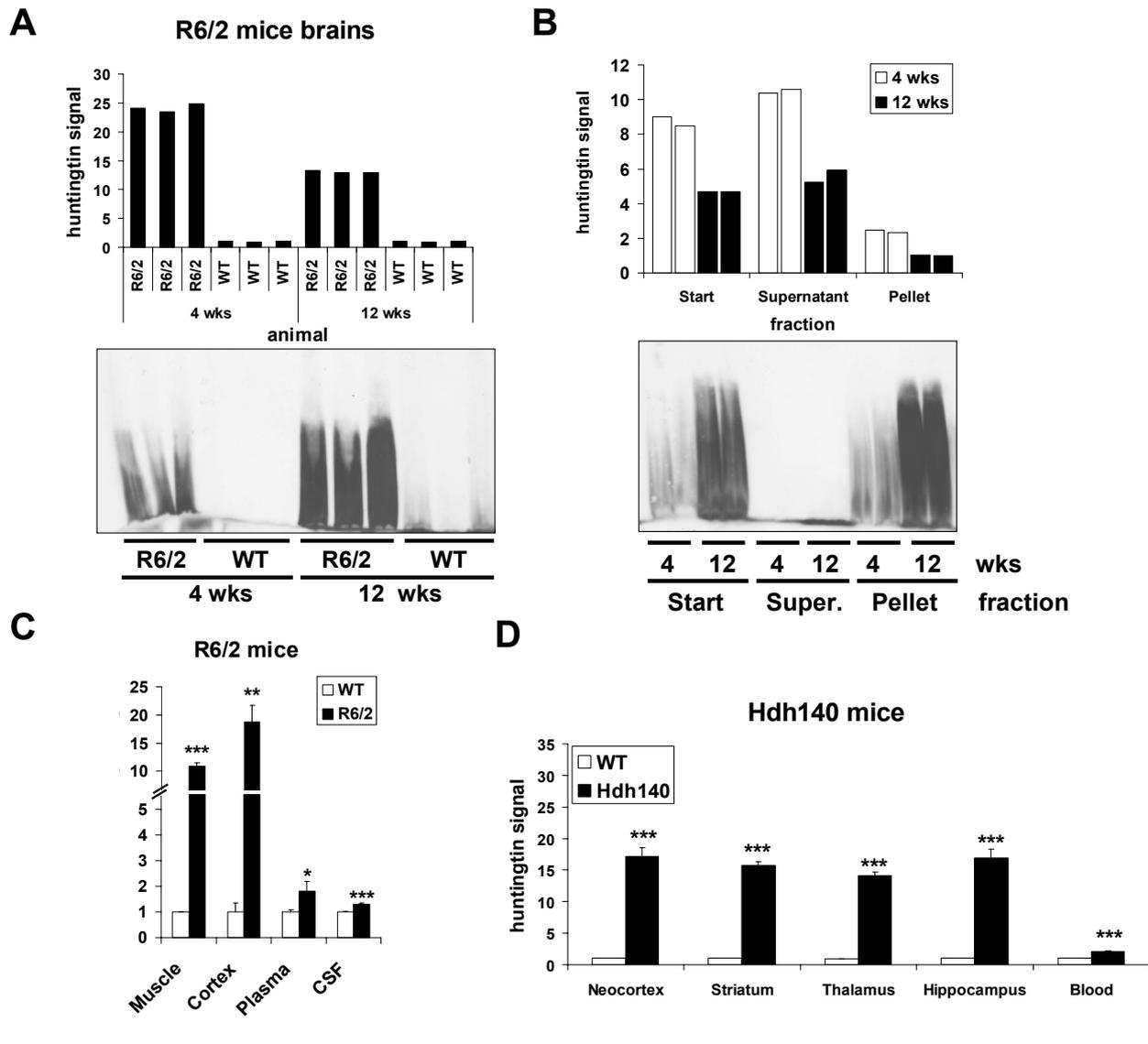


**Figure 40: Detection of soluble mutant huntingtin in mice HD models.** **A:** Time resolved-FRET signal in brains of R6/2 decreases with age. Full-brain homogenates of 4 and 12 week-old wild-type (WT) or R6/2 mice were analyzed with time resolved-FRET using the 2B7-K-MW1-D2 antibody combination. The sensitive time resolved-FRET detection resulted in a highly significant signal difference between not only WT and R6/2 mice ( $p < 0.001$ ) but also between 4 and 12 week-old R6/2 mice ( $p < 0.001$ ). Time resolved-FRET signal in R6/2 brain decreased with age (upper graph) whereas the aggregate load in these samples increases with age (lower AGERA blot), indicating that the time resolved-FRET method based on 2B7-MW1 does detect a mutant Htt subspecies different from insoluble aggregates. **B:** Time resolved-FRET detects soluble fraction and not insoluble aggregates. Ultracentrifugation (1h at 124000g) of four R6/2 full-brain homogenates separated the insoluble Htt aggregates from soluble monomeric/oligomeric species. Analysis of supernatant and pellet fractions showed that ultracentrifugation successfully separated the insoluble aggregates into the pellet fractions whereas no aggregates were detected in the supernatant fractions (lower AGERA blot). In contrast we found that the Htt signal detected by time resolved-FRET is found in the supernatant fractions and thus specific for soluble mutant Htt. **C:** Quantification of mutant Htt-exon1 in R6/2 mice. Cortex, muscle and plasma samples from 6 week old R6/2 or WT mice showed a significant signal difference between R6/2 and WT in all samples analyzed ( $n=3$ , stdev,  $*=p < 0.05$ ,  $**=p < 0.01$ ,  $***=p < 0.001$ ). Analysis of corticospinal fluid from 9 to 12 week old R6/2 mice ( $n=9$ ) and WT mice ( $n=4$ ) showed a small but highly significant signal difference between R6/2 and WT CSF. **D:** Endogenous full-length mutant Htt detection in Hdh140 mice. Detection in a knock-in mouse model that expresses full-length mutant Htt at endogenous levels is possible with the time resolved-FRET method. Highly significant quantification was possible in every tissue sample analyzed. ( $n=3$ , stdev,  $*=p < 0.05$ ,  $**=p < 0.01$ ,  $***=p < 0.001$ )

## Sensitive and polyQ-dependent huntingtin detection in human tissue samples

Next, we analyzed post-mortem cortex tissue from three HD and three control patients. A significant signal difference was observed for all HD patients over the healthy controls, demonstrating the feasibility of our method for sensitive and polyQ-length dependent detection of soluble Htt levels in human tissue (Figure 41A). To our knowledge, this is the first time that the specific pool of potentially toxic soluble mutant Htt can be accurately quantified in human samples.

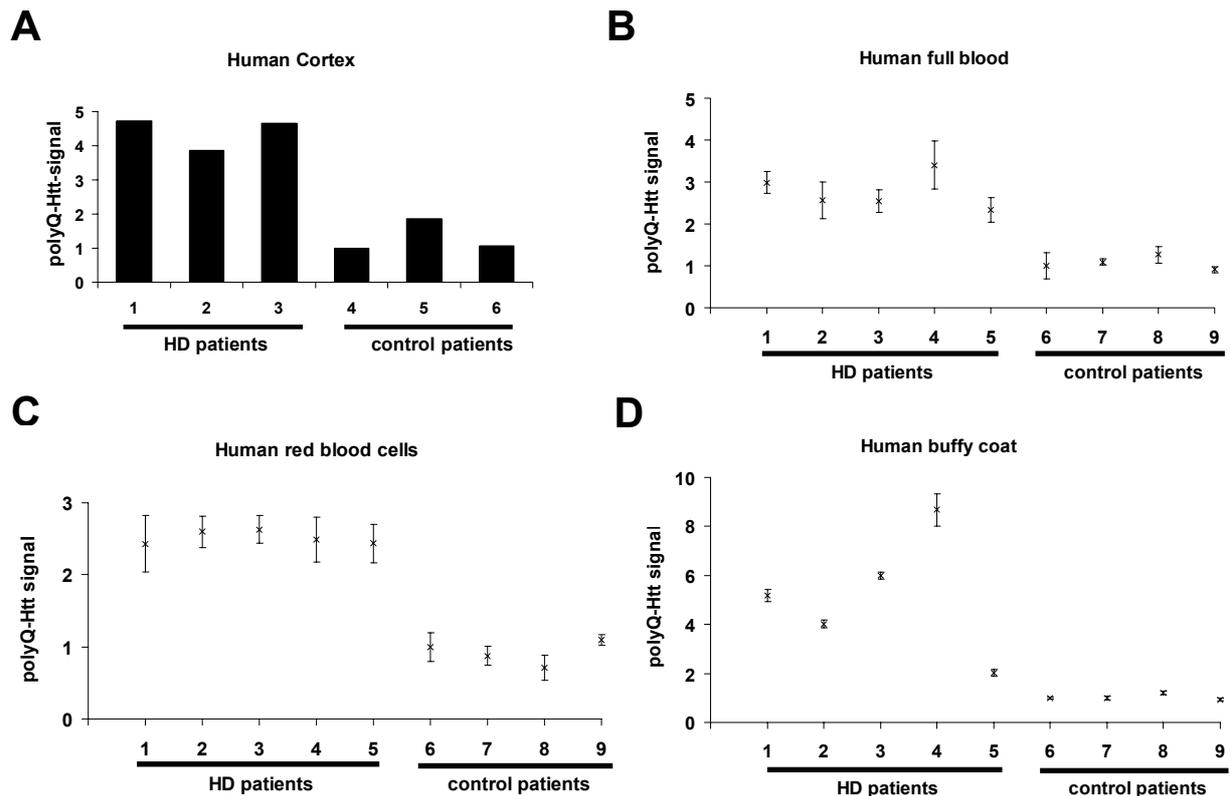


**Figure 41: Sensitive and polyQ-dependent huntingtin detection in human tissue samples.** **A:** PolyQ-dependent Htt detection in post-mortem human cortex. Analysis of cortex homogenates from three Huntington's Disease and three control patients revealed a polyQ-length dependent signal intensity allowing for clear distinction of human tissue from a diseased versus a healthy patient. **B:** Detection of mutant huntingtin in human snap frozen full blood samples. Human full blood samples from five living Huntington's Disease patients and four living control patients were analyzed. A clear distinction of the diseased patients from the healthy patients based on the polyQ-length dependent detection of Htt was possible. Averages of technical triplicates with standard deviation are shown for each patient. **C-D:** Separation of EDTA treated full blood into red blood cells and buffy coat fraction revealed polyQ-dependent detection of mutant Htt in erythrocytes and buffy coat cells of Huntington's Disease patients. Average of technical triplicates with standard deviation are shown for each patient.

We proceeded to test human full blood, red blood cells (erythrocytes) and human buffy coat samples from five living HD and four control patients (Table 2). As in the post-mortem cortex tissue analyzed, we were able to identify all five living HD patients based on their increased

time resolved-FRET polyQ-Htt-dependent signal in full blood, erythrocytes and buffy coat over the signal of the four healthy control patients (Figure 41B-D).

<b>Patient</b>	<b>Sex</b>	<b>Age</b>	<b>TFC</b>	
1	F	42	10	<b>Huntington's Disease patient</b>
2	F	62	5	
3	F	46	10	
4	M	50	9	
5	F	45	6	
6	M	30	13	<b>Healthy control patient</b>
7	M	23	13	
8	M	24	13	
9	F	54	13	

**Table 2: Patients providing blood samples.** The age, sex and total functional capacity (TFC) score (13=normal; 0=severe disability) for each patient are shown.

#### 4.4.5 DISCUSSION

We have developed a bioassay for determination of soluble mutant Htt and demonstrated its use to measure mutant Htt levels in cell lysates, animal and human tissues. The time resolved-FRET assay is a simple, one-step methodology that requires only small sample volumes. Quantitative determination of mutant Htt levels are therefore possible with as little as 5  $\mu$ l human full blood, providing the possibility to determine soluble mutant Htt protein levels multiple times over a longer clinical trial period without affecting the patient as obtaining the sample is minimally invasive. In addition, the ability to correct for artifacts using the time resolved-FRET method allows for a very reliable quantification of mutant Htt even in small sample sizes (Imbert et al., 2007).

To verify the specificity of our detection method for soluble mutant Htt, several experimental steps were taken. Importantly, we based our bioassay on a method that has been recently described to detect intracellular levels of tagged Htt fragments in a sensitive, robust and reliable manner as indicated by a high Z-factor value, a common statistical parameter that reflects assay quality in terms of reliability and robustness (Zhang et al., 1999, Weiss et al. submitted). By exchanging the detection antibodies of the high-throughput screen to an antibody pair that recognizes endogenous Htt epitopes, we were able to show detection of untagged Htt fragments in a stable neuronal cell line with inducible expression of tagged Htt. In order to specifically detect mutant Htt levels over wild-type Htt, one of the antibodies is directed against the polyQ-repeat that is elongated in Huntington's Disease. We showed that the signal intensity directly correlates with the polyQ length in lentiviral infected embryonic stem cells as well as in cell lysates obtained from wild-type and polyQ-knock-in embryonic stem cells and embryonic stem cell derived neurons. Critically, using knock-out embryonic stem cell lysates void of any Htt protein expression, we were able to prove the Htt specificity of our signal. As the detection method is polyQ-length dependent, it should be noted that while wild-type Htt is not detected in murine cells or tissue due to the WT-polyQ-length of only 7 glutamines, human healthy polyQ length normally resides around ~20 glutamines (Myers, 2004), a length that is also detected by our method. However, the intensity of this healthy Htt derived signal only contributes little to the total signal that is largely comprised of mutant polyQ Htt detection with polyQ-length >39 glutamines.

We proceeded to analyze mouse models of HD and for the first time were able to quantifiably determine soluble, non-aggregated mutant Htt levels in various tissue samples of two different HD mouse models. Notably, we found that the levels of soluble mutant Htt decrease while the amount of insoluble Htt aggregates increase in the brains of aging R6/2 mice. This decrease of

an aggregation prone monomeric species upon aging resembles similar findings in Alzheimer Disease whereby a decrease in Abeta42 levels is a marker for disease progression (likely to be caused by recruitment of soluble Abeta as a function of increased plaque burden).

Finally, we tested human post-mortem cortex samples as well as full blood and blood-derived human samples from living control and HD patients. We were able to clearly distinguish between healthy and HD patient samples by the intensity of the signal alone. This quantitative detection of soluble Htt in readily available human tissue samples opens up the possibility to determine the value of this soluble mutant Htt quantification for use as a potential biomarker for HD disease progression. In that regard, it is interesting that the signal measured in buffy coat fraction tends to correlate with severity of disease progression as determined by the total function capacity score in the analyzed HD patients. This trend was not observed in full blood or erythrocytes. However, erythrocytes represent the vast majority of cells found in full blood. Erythrocytes display a shorter lifespan than some of the lymphocytes found in the buffy coat fraction. In addition, mature erythrocytes differ from other cells as they are void of a nuclei and mitochondrial respiration. The difference in time resolved FRET signals could therefore be due to the longer lifespan and different cellular characteristics of a lymphocyte subpopulation in which effects of mutant huntingtin monomer expression, e.g. huntingtin aggregation, can accumulate over time, leading to a decreased signal of soluble mutant huntingtin similar to what we observed in R6/2 mice with advanced disease progression. Further longitudinal studies with a larger HD patient population could help to elucidate this intriguing possibility. In addition, since potential HD therapies could be aimed at influencing the soluble mutant Htt pool directly (e.g. RNAi knockdown of mutant huntingtin, compounds that alter aggregation, compounds that act on the chaperone system or compounds that act on autophagy) the precise quantification of soluble mutant Htt could also find application as a marker for treatment success in human clinical trials.

In summary, our bioassay is a very simple, one-step methodology that requires only small sample volumes. In addition, the artifact corrected nature of time resolved-FRET allows for very reliable Htt-quantification with a single small sample per subject, making the method useful for experiments that are limited by sample numbers or sample volume as it is often found in human clinical trials. Because signal specificity of the method depends on the antibody pair used, the method could also find further application not only for HD but also for other diseases, especially other polyQ-diseases like the spinocerebellar ataxias.

## **ACKNOWLEDGMENTS**

We thank Christian Parker for helpful tips and discussions.

## **AUTHOR CONTRIBUTIONS**

A.W. designed the research and developed method described, provided neuronal inducible HN10 cells, provided R6/2 aggregate data, provided western blot of lentiviral lysates, analyzed all samples by time resolved-FRET and provided statistical analysis. C.K. provided lentiviral infected embryonic stem cell derived neurons as well as knock-in embryonic stem cell derived neurons. K.K and M.D. provided knock-out embryonic stem cells and provided western blot of embryonic stem cells. R.B. and D.H. provided knock-out embryonic stem cells and provided western blot of embryonic stem cells. E.R. provided R6/2 samples. J.F. provided Hdh140 mouse samples. S.H. provided human samples. P.P. is the principle investigator and proposed and oversaw all studies. A.W. and P.P. wrote the manuscript. All authors edited the manuscript.

## 5 GENERAL DISCUSSION AND OUTLOOK

This thesis focused on the development and application of new models, methods and therapeutic approaches for the investigation of Huntington's Disease, a fatal neurodegenerative disorder caused by the expression of mutated huntingtin protein (Bates et al., 2002). Currently, no cure for this devastating disease exists (Bonelli and Hofmann, 2007). To help in elucidating the open questions about the affected cellular mechanism in Huntington's Disease, we developed an inducible neuronal model and established readouts to measure the effects of mutant huntingtin expression (Chapter 4.1.). The observed effects on cell viability, transcriptional dysregulation and neurite formation are consistent with earlier reports (Borrell-Pages et al., 2006; Hodges et al., 2006; Landles and Bates, 2004). We made use of our model to develop two new methods for the detection of aggregated and soluble mutant huntingtin protein (AGERA method: Chapter 4.2; TR-FRET method: Chapter 4.4). Since these methods are specific for huntingtin protein because of the use of anti-huntingtin antibodies, these methods can in principle be applied to a variety of other targets of interest by using alternative antibodies directed against other proteins.

The presented results focused solely on the mutated huntingtin protein while leaving the question of a potential RNA toxicity in Huntington's Disease untouched. Understanding the potential role of RNA toxicity in disease development is important as numerous nucleotide expansion diseases are thought to be caused by pathogenic RNA and not pathogenic protein. So far, almost 30 hereditary diseases are known to result from nucleotide repeat expansions (Mirkin, 2007; Pearson et al., 2005). Interestingly, nucleotide expansions in exons can only be found in approximately 50% of these diseases. In the rest of the known nucleotide expansion disorders, elongation of the DNA are found in the 5' or 3' untranslated regions or in introns. Consequently, these nucleotide expansions do not result in expression of mutated proteins but in transcription of altered RNAs or changed levels of protein expression.

The mechanisms how RNA with expanded nucleotide repeats can become toxic in these diseases are not yet fully understood. Studies in myotonic dystrophy, a disorder caused by nucleotide expansion in an untranslated gene region (Brook et al., 1992), showed that expanded RNA can form hairpin structures and distinct RNA foci inside the nucleus (Davis et al., 1997). These foci seem to sequester proteins like muscleblind-like protein 1 (MBNL1) or CUG RNA-binding protein 1 (CUG-BP1) which play a role in alternative RNA splicing (Fardaei et al., 2002; Ho et al., 2004; Miller et al., 2000). In good agreement with these *in vitro* observations are studies which show that deregulation of RNA splicing during development is a key pathogenic event leading to myotonic dystrophy (Philips et al., 1998).

An alternative interesting theory for mRNA toxicity is based on recent studies reporting that CNG-triplet mRNA hairpins are not only recognized and cleaved by Dicer protein (Handa et al., 2003; Malinina, 2005) but that these resulting (CNG)<sub>n</sub> fragments seem to have gene silencing effects normally reserved for siRNA (Krol et al., 2007).

In contrast to myotonic dystrophy, Huntington's Disease and the other eight members of the polyglutamine disease family are characterized by an expansion of a CAG repeat in an exon coding region leading to a polyglutamine repeat length above a critical threshold in an expressed protein. Since the dominating characteristic of all these polyglutamine diseases are the visible protein aggregations in the central nervous system, it has been mostly believed that these disorders are caused by the mutated proteins and not by the subjacent, altered mRNA.

Interestingly, a recent study demonstrated that mRNA toxicity contributes significantly to the onset and progression of SCA3 and Huntington's Disease in a drosophila model (Li et al., 2008). However, several observations speak against toxicity of the huntingtin mRNA. Firstly, it has been shown that the amino acid flanking sequences of the polyglutamine repeat have a significant influence on the tendency of the protein to aggregate and the overall toxicity (Darnell et al., 2007; Dehay and Bertolotti, 2006; Rockabrand et al., 2007). Secondly, numerous studies reported that subcellular localization of the mutated protein influences disease progression substantially (Benn et al., 2005; Hackam et al., 1999; Martindale et al., 1998; Perez et al., 1998; Saudou et al., 1998; Wheeler et al., 2000; Yang et al., 2002). In addition, posttranslational modifications of the mutant huntingtin protein such as cleavage or phosphorylation have been shown to influence the overall disease progression (Graham et al., 2006; Ratovitski et al., 2007; Warby et al., 2005; Wellington et al., 2002). Notably, expression of anti-huntingtin-intrabodies results in specific binding of the huntingtin protein and reduces symptoms in cellular and mouse models of Huntington's Disease (Wang et al., 2008). Finally, earlier studies in other drosophila Huntington's Disease models argue specifically for the polyglutamine repeat in the protein itself as the toxic agent (Marsh et al., 2000; McLeod et al., 2005). All these findings connect the expression, localization and posttranslational modifications of the mutated protein directly with disease onset and progression, questioning the role of a potential mRNA toxicity in Huntington's Disease. Nevertheless, a potential minor contribution of mRNA toxicity to disease development should not be ruled out and further experiments will be needed on this subject. The in the process of this thesis developed detection methods for the different conformational subspecies of mutant huntingtin protein could complement the already available sensitive detection methods for mRNA in such

studies, helping to find a more definitive answer to the possibility of an additional RNA toxicity in Huntington's Disease.

Because of the above described arguments against a potential RNA toxicity in Huntington's Disease, we were confident that applying our TR-FRET method to screen a small-molecule library comprised of 10000 molecules with the aim to identify compounds which lower specifically the levels of mutant huntingtin protein will help in approaching an alternative therapeutic treatment against Huntington's Disease (Chapter 4.3). Even though the screen identified mostly compounds which influence generic cellular pathways, the specificity of the readout for mutant huntingtin and the dynamic response of the assay encouraged us to proceed with the analysis of a larger compound library (>1 million compounds). This screen is currently in progress and it is expected to be finished by the end of this year. If a verified compound hit list can be established, it will be interesting to test the effect of these compounds in our readouts for cell viability (Chapter 4.1) and aggregate formation (Chapter 4.2) in our inducible neuronal model but also other established cellular and animal models of Huntington's Disease (Bates and Hockly, 2003; Sathasivam et al., 1999a).

A key finding when using the herein described methods was that the levels of soluble and aggregated mutant huntingtin seem to display an inverse correlation in aging Huntington's Disease mice (Chapter 4.4). This could be explained by a "sink"-hypothesis-model which postulates that the levels of soluble cellular mutant huntingtin protein decrease as they get sequestered into a growing number of intracellular mutant huntingtin aggregates associated with disease progression. Indeed, a similar observation has been put forward for patients suffering of Alzheimer's Disease, another neurodegenerative disorder characterized by misfolded protein fragments prone for aggregation (Sjogren et al., 2002; Strozyk et al., 2003). Since we readily detect soluble mutant huntingtin in human samples with our time resolved FRET assay and since we observe a correlating trend of advanced human disease progression and lower time resolved FRET signals in buffy coat fractions of HD patients (Chapter 4.4), it is intriguing to speculate that our finding from the Huntington's Disease mouse model can be translated into humans. If studies with a larger human sample size verify this correlation between a decrease of soluble huntingtin and the state of disease progression, our method may find use as a diagnostic clinical readout for treatment success of Huntington's Disease therapies and the monitoring of disease progression. Future planned experiments will therefore include the analysis of a larger collection of longitudinal patient samples to elucidate this intriguing application possibility.

## 6 REFERENCES

- Achard, S., Jean, A., Lorphelin, D., Amoravain, M. and Claret, E. J.** (2003). Homogeneous assays allow direct "in well" cytokine level quantification. *Assay Drug Dev Technol* **1**, 181-5.
- Alcantara, S., Frisen, J., del Rio, J. A., Soriano, E., Barbacid, M. and Silos-Santiago, I.** (1997). TrkB signaling is required for postnatal survival of CNS neurons and protects hippocampal and motor neurons from axotomy-induced cell death. *J Neurosci* **17**, 3623-33.
- Alexander, G. E.** (1994). Basal ganglia-thalamocortical circuits: their role in control of movements. *J Clin Neurophysiol* **11**, 420-31.
- Alexander, G. E. and Crutcher, M. D.** (1990). Functional architecture of basal ganglia circuits: neural substrates of parallel processing. *Trends Neurosci* **13**, 266-71.
- Alexander, G. M., Kurukulasuriya, N. C., Mu, J. and Godwin, D. W.** (2006). Cortical feedback to the thalamus is selectively enhanced by nitric oxide. *Neuroscience* **142**, 223-34.
- Alpha, B., Lehn, J. and Mathis, G.** (1987). Energy transfer luminescence of Eu(III) and Tb(III) cryptates of macrobicyclic polypyridine ligands. *Angew. Chem. Int. Ed. Engl.*
- Andrade, M. A. and Bork, P.** (1995). HEAT repeats in the Huntington's disease protein. *Nat Genet* **11**, 115-6.
- Andrew, S. E., Goldberg, Y. P., Kremer, B., Telenius, H., Theilmann, J., Adam, S., Starr, E., Squitieri, F., Lin, B., Kalchman, M. A. et al.** (1993). The relationship between trinucleotide (CAG) repeat length and clinical features of Huntington's disease. *Nat Genet* **4**, 398-403.
- Andrich, J., Saft, C., Ostholt, N. and Muller, T.** (2007). Complex movement behaviour and progression of Huntington's disease. *Neurosci Lett* **416**, 272-4.
- Arenas, J., Campos, Y., Ribacoba, R., Martin, M. A., Rubio, J. C., Ablanado, P. and Cabello, A.** (1998). Complex I defect in muscle from patients with Huntington's disease. *Ann Neurol* **43**, 397-400.
- Arning, L., Kraus, P. H., Valentin, S., Saft, C., Andrich, J. and Epplen, J. T.** (2005). NR2A and NR2B receptor gene variations modify age at onset in Huntington disease. *Neurogenetics* **6**, 25-8.
- Arrasate, M., Mitra, S., Schweitzer, E. S., Segal, M. R. and Finkbeiner, S.** (2004). Inclusion body formation reduces levels of mutant huntingtin and the risk of neuronal death. *Nature* **431**, 805-10.
- Bagriantsev, S. N., Kushnirov, V. V. and Liebman, S. W.** (2006). Analysis of amyloid aggregates using agarose gel electrophoresis. *Methods Enzymol* **412**, 33-48.
- Balbirnie, M., Grothe, R. and Eisenberg, D. S.** (2001). An amyloid-forming peptide from the yeast prion Sup35 reveals a dehydrated beta-sheet structure for amyloid. *Proc Natl Acad Sci U S A* **98**, 2375-80.
- Baliga, B. S., Pronczuk, A. W. and Munro, H. N.** (1969). Mechanism of cycloheximide inhibition of protein synthesis in a cell-free system prepared from rat liver. *J Biol Chem* **244**, 4480-9.
- Barbeau, A.** (1970). Parental ascent in the juvenile form of Huntington's chorea. *Lancet* **2**, 937.
- Barr, A. N., Fischer, J. H., Koller, W. C., Spunt, A. L. and Singhal, A.** (1988). Serum haloperidol concentration and choreiform movements in Huntington's disease. *Neurology* **38**, 84-8.
- Bateman, D., Boughey, A. M., Scaravilli, F., Marsden, C. D. and Harding, A. E.** (1992). A follow-up study of isolated cases of suspected Huntington's disease. *Ann Neurol* **31**, 293-8.
- Bates, G.** (2003). Huntingtin aggregation and toxicity in Huntington's disease. *Lancet* **361**, 1642-4.
- Bates, G. P., Harper, P. and Jones, L.** (2002). Huntington's Disease. Oxford: Oxford University Press.

- Bates, G. P. and Hockly, E.** (2003). Experimental therapeutics in Huntington's disease: are models useful for therapeutic trials? *Curr Opin Neurol* **16**, 465-70.
- Bazin, H., Preaudat, M., Trinquet, E. and Mathis, G.** (2001). Homogeneous time resolved fluorescence resonance energy transfer using rare earth cryptates as a tool for probing molecular interactions in biology. *Spectrochim Acta A Mol Biomol Spectrosc* **57**, 2197-211.
- Bence, N. F., Sampat, R. M. and Kopito, R. R.** (2001). Impairment of the ubiquitin-proteasome system by protein aggregation. *Science* **292**, 1552-5.
- Benn, C. L., Landles, C., Li, H., Strand, A. D., Woodman, B., Sathasivam, K., Li, S. H., Ghazi-Noori, S., Hockly, E., Faruque, S. M. et al.** (2005). Contribution of nuclear and extranuclear polyQ to neurological phenotypes in mouse models of Huntington's disease. *Hum Mol Genet* **14**, 3065-78.
- Bennett, E. J., Shaler, T. A., Woodman, B., Ryu, K. Y., Zaitseva, T. S., Becker, C. H., Bates, G. P., Schulman, H. and Kopito, R. R.** (2007). Global changes to the ubiquitin system in Huntington's disease. *Nature* **448**, 704-8.
- Benzinger, T. L., Gregory, D. M., Burkoth, T. S., Miller-Auer, H., Lynn, D. G., Botto, R. E. and Meredith, S. C.** (2000). Two-dimensional structure of beta-amyloid(10-35) fibrils. *Biochemistry* **39**, 3491-9.
- Bibel, M., Richter, J., Lacroix, E. and Barde, Y. A.** (2007). Generation of a defined and uniform population of CNS progenitors and neurons from mouse embryonic stem cells. *Nat Protoc* **2**, 1034-43.
- Bibel, M., Richter, J., Schrenk, K., Tucker, K. L., Staiger, V., Korte, M., Goetz, M. and Barde, Y. A.** (2004). Differentiation of mouse embryonic stem cells into a defined neuronal lineage. *Nat Neurosci* **7**, 1003-9.
- Bird, E. D., Caro, A. J. and Pilling, J. B.** (1974). A sex related factor in the inheritance of Huntington's chorea. *Ann Hum Genet* **37**, 255-60.
- Bittenbender, J. B. and Quadfasel, F. A.** (1962). Rigid and akinetic forms of Huntington's chorea. *Arch Neurol* **7**, 275-88.
- Bodner, R. A., Outeiro, T. F., Altmann, S., Maxwell, M. M., Cho, S. H., Hyman, B. T., McLean, P. J., Young, A. B., Housman, D. E. and Kazantsev, A. G.** (2006). Pharmacological promotion of inclusion formation: a therapeutic approach for Huntington's and Parkinson's diseases. *Proc Natl Acad Sci U S A* **103**, 4246-51.
- Bodner, T., Jenner, C., Benke, T., Ober, A., Seppi, K. and Fleischhacker, W. W.** (2001). Intoxication with riluzole in Huntington's disease. *Neurology* **57**, 1141-3.
- Bonelli, R. M., Heuberger, C. and Reisecker, F.** (2003). Minocycline for Huntington's disease: an open label study. *Neurology* **60**, 883-4.
- Bonelli, R. M. and Hofmann, P.** (2007). A systematic review of the treatment studies in Huntington's disease since 1990. *Expert Opin Pharmacother* **8**, 141-53.
- Bonelli, R. M. and Wenning, G. K.** (2006). Pharmacological management of Huntington's disease: an evidence-based review. *Curr Pharm Des* **12**, 2701-20.
- Bonelli, R. M., Wenning, G. K. and Kapfhammer, H. P.** (2004). Huntington's disease: present treatments and future therapeutic modalities. *Int Clin Psychopharmacol* **19**, 51-62.
- Bonuccelli, U., Ceravolo, R., Maremmani, C., Nuti, A., Rossi, G. and Muratorio, A.** (1994). Clozapine in Huntington's chorea. *Neurology* **44**, 821-3.
- Borrell-Pages, M., Zala, D., Humbert, S. and Saudou, F.** (2006). Huntington's disease: from huntingtin function and dysfunction to therapeutic strategies. *Cell Mol Life Sci* **63**, 2642-60.
- Brewer, G. J. and Cotman, C. W.** (1989). Survival and growth of hippocampal neurons in defined medium at low density: advantages of a sandwich culture technique or low oxygen. *Brain Res* **494**, 65-74.

- Brewer, G. J., Torricelli, J. R., Evege, E. K. and Price, P. J.** (1993). Optimized survival of hippocampal neurons in B27-supplemented Neurobasal, a new serum-free medium combination. *J Neurosci Res* **35**, 567-76.
- Brinkman, R. R., Mezei, M. M., Theilmann, J., Almqvist, E. and Hayden, M. R.** (1997). The likelihood of being affected with Huntington disease by a particular age, for a specific CAG size. *Am J Hum Genet* **60**, 1202-10.
- Brook, J. D., McCurrach, M. E., Harley, H. G., Buckler, A. J., Church, D., Aburatani, H., Hunter, K., Stanton, V. P., Thirion, J. P., Hudson, T. et al.** (1992). Molecular basis of myotonic dystrophy: expansion of a trinucleotide (CTG) repeat at the 3' end of a transcript encoding a protein kinase family member. *Cell* **68**, 799-808.
- Bruyn, G. W.** (1979). [Huntington's chorea]. *Tijdschr Ziekenverpl* **32**, 101-5.
- Bruyn, G. W. and von Wolfereen, W. J.** (1973). Pathogenesis of Huntington's chorea. *Lancet* **1**, 1382.
- Bulteau, A. L., Ikeda-Saito, M. and Szweda, L. I.** (2003). Redox-dependent modulation of aconitase activity in intact mitochondria. *Biochemistry* **42**, 14846-55.
- Carter, R. J., Lione, L. A., Humby, T., Mangiarini, L., Mahal, A., Bates, G. P., Dunnett, S. B. and Morton, A. J.** (1999). Characterization of progressive motor deficits in mice transgenic for the human Huntington's disease mutation. *J Neurosci* **19**, 3248-57.
- Chattopadhyay, B., Bakshi, K., Mukhopadhyay, S. and Bhattacharyya, N. P.** (2005). Modulation of age at onset of Huntington disease patients by variations in TP53 and human caspase activated DNase (hCAD) genes. *Neurosci Lett* **374**, 81-6.
- Chattopadhyay, B., Ghosh, S., Gangopadhyay, P. K., Das, S. K., Roy, T., Sinha, K. K., Jha, D. K., Mukherjee, S. C., Chakraborty, A., Singhal, B. S. et al.** (2003). Modulation of age at onset in Huntington's disease and spinocerebellar ataxia type 2 patients originated from eastern India. *Neurosci Lett* **345**, 93-6.
- Chen, M., Ona, V. O., Li, M., Ferrante, R. J., Fink, K. B., Zhu, S., Bian, J., Guo, L., Farrell, L. A., Hersch, S. M. et al.** (2000). Minocycline inhibits caspase-1 and caspase-3 expression and delays mortality in a transgenic mouse model of Huntington disease. *Nat Med* **6**, 797-801.
- Chen, S., Berthelie, V., Yang, W. and Wetzel, R.** (2001). Polyglutamine aggregation behavior in vitro supports a recruitment mechanism of cytotoxicity. *J Mol Biol* **311**, 173-82.
- Chen, S., Ferrone, F. A. and Wetzel, R.** (2002). Huntington's disease age-of-onset linked to polyglutamine aggregation nucleation. *Proc Natl Acad Sci U S A* **99**, 11884-9.
- Cicchetti, F., Prensa, L., Wu, Y. and Parent, A.** (2000). Chemical anatomy of striatal interneurons in normal individuals and in patients with Huntington's disease. *Brain Res Brain Res Rev* **34**, 80-101.
- Clarke, E. E. and Shearman, M. S.** (2000). Quantitation of amyloid-beta peptides in biological milieu using a novel homogeneous time-resolved fluorescence (HTRF) assay. *J Neurosci Methods* **102**, 61-8.
- Clegg, R. M.** (1996). Fluorescence resonance energy transfer. In *Fluorescence Imaging Spectroscopy and Microscopy*, (ed. X. F. W. a. B. Herman), pp. 179-252: John Wiley & Sons.
- Colby, D. W., Cassady, J. P., Lin, G. C., Ingram, V. M. and Wittrup, K. D.** (2006). Stochastic kinetics of intracellular huntingtin aggregate formation. *Nat Chem Biol* **2**, 319-23.
- Colosimo, C., Cassetta, E., Bentivoglio, A. R. and Albanese, A.** (1995). Clozapine in Huntington's disease. *Neurology* **45**, 1023-4.
- Como, P. G., Rubin, A. J., O'Brien, C. F., Lawler, K., Hickey, C., Rubin, A. E., Henderson, R., McDermott, M. P., McDermott, M., Steinberg, K. et al.** (1997). A controlled trial of fluoxetine in nondepressed patients with Huntington's disease. *Mov Disord* **12**, 397-401.
- Conneally, P. M.** (1984). Huntington disease: genetics and epidemiology. *Am J Hum Genet* **36**, 506-26.

- Cooper, J. K., Schilling, G., Peters, M. F., Herring, W. J., Sharp, A. H., Kaminsky, Z., Masone, J., Khan, F. A., Delanoy, M., Borchelt, D. R. et al.** (1998). Truncated N-terminal fragments of huntingtin with expanded glutamine repeats form nuclear and cytoplasmic aggregates in cell culture. *Hum Mol Genet* **7**, 783-90.
- Crane, F. L., Hatefi, Y., Lester, R. L. and Widmer, C.** (1957). Isolation of a quinone from beef heart mitochondria. *Biochim Biophys Acta* **25**, 220-1.
- Cui, L., Jeong, H., Borovecki, F., Parkhurst, C. N., Tanese, N. and Krainc, D.** (2006). Transcriptional repression of PGC-1alpha by mutant huntingtin leads to mitochondrial dysfunction and neurodegeneration. *Cell* **127**, 59-69.
- Darnell, G., Orgel, J. P., Pahl, R. and Meredith, S. C.** (2007). Flanking polyproline sequences inhibit beta-sheet structure in polyglutamine segments by inducing PPII-like helix structure. *J Mol Biol* **374**, 688-704.
- Davies, S. W., Turmaine, M., Cozens, B. A., DiFiglia, M., Sharp, A. H., Ross, C. A., Scherzinger, E., Wanker, E. E., Mangiarini, L. and Bates, G. P.** (1997). Formation of neuronal intranuclear inclusions underlies the neurological dysfunction in mice transgenic for the HD mutation. *Cell* **90**, 537-48.
- Davis, B. M., McCurrach, M. E., Taneja, K. L., Singer, R. H. and Housman, D. E.** (1997). Expansion of a CUG trinucleotide repeat in the 3' untranslated region of myotonic dystrophy protein kinase transcripts results in nuclear retention of transcripts. *Proc Natl Acad Sci U S A* **94**, 7388-93.
- de Almeida, L. P., Ross, C. A., Zala, D., Aebischer, P. and Deglon, N.** (2002). Lentiviral-mediated delivery of mutant huntingtin in the striatum of rats induces a selective neuropathology modulated by polyglutamine repeat size, huntingtin expression levels, and protein length. *J Neurosci* **22**, 3473-83.
- De Marchi, N., Daniele, F. and Ragone, M. A.** (2001). Fluoxetine in the treatment of Huntington's disease. *Psychopharmacology (Berl)* **153**, 264-6.
- De Schepper, S., Bruwiere, H., Verhulst, T., Steller, U., Andries, L., Wouters, W., Janicot, M., Arts, J. and Van Heusden, J.** (2003). Inhibition of histone deacetylases by chlamydocin induces apoptosis and proteasome-mediated degradation of survivin. *J Pharmacol Exp Ther* **304**, 881-8.
- Dehay, B. and Bertolotti, A.** (2006). Critical role of the proline-rich region in Huntingtin for aggregation and cytotoxicity in yeast. *J Biol Chem* **281**, 35608-15.
- Diaz-Hernandez, M., Moreno-Herrero, F., Gomez-Ramos, P., Moran, M. A., Ferrer, I., Baro, A. M., Avila, J., Hernandez, F. and Lucas, J. J.** (2004). Biochemical, ultrastructural, and reversibility studies on huntingtin filaments isolated from mouse and human brain. *J Neurosci* **24**, 9361-71.
- DiFiglia, M.** (1990). Excitotoxic injury of the neostriatum: a model for Huntington's disease. *Trends Neurosci* **13**, 286-9.
- DiFiglia, M., Sapp, E., Chase, K., Schwarz, C., Meloni, A., Young, C., Martin, E., Vonsattel, J. P., Carraway, R., Reeves, S. A. et al.** (1995). Huntingtin is a cytoplasmic protein associated with vesicles in human and rat brain neurons. *Neuron* **14**, 1075-81.
- DiFiglia, M., Sapp, E., Chase, K. O., Davies, S. W., Bates, G. P., Vonsattel, J. P. and Aronin, N.** (1997). Aggregation of huntingtin in neuronal intranuclear inclusions and dystrophic neurites in brain. *Science* **277**, 1990-3.
- DiFiglia, M., Sena-Esteves, M., Chase, K., Sapp, E., Pfister, E., Sass, M., Yoder, J., Reeves, P., Pandey, R. K., Rajeev, K. G. et al.** (2007). Therapeutic silencing of mutant huntingtin with siRNA attenuates striatal and cortical neuropathology and behavioral deficits. *Proc Natl Acad Sci U S A* **104**, 17204-9.
- DiProspero, N. A., Chen, E. Y., Charles, V., Plomann, M., Kordower, J. H. and Tagle, D. A.** (2004). Early changes in Huntington's disease patient brains involve alterations in cytoskeletal and synaptic elements. *J Neurocytol* **33**, 517-33.

- Divry, P.** (1927). Etude histochimique des plaques seniles. *J. Belge Neurol. Psychiatr.*, 643–657.
- Djousse, L., Knowlton, B., Hayden, M. R., Almqvist, E. W., Brinkman, R. R., Ross, C. A., Margolis, R. L., Rosenblatt, A., Durr, A., Dode, C. et al.** (2004). Evidence for a modifier of onset age in Huntington disease linked to the HD gene in 4p16. *Neurogenetics* **5**, 109-14.
- Dunah, A. W., Jeong, H., Griffin, A., Kim, Y. M., Standaert, D. G., Hersch, S. M., Mouradian, M. M., Young, A. B., Tanese, N. and Krainc, D.** (2002). Sp1 and TAFII130 transcriptional activity disrupted in early Huntington's disease. *Science* **296**, 2238-43.
- Dunglison, R.** (1848). *Practice of medicine* 3rd Edition.
- Duyao, M., Ambrose, C., Myers, R., Novelletto, A., Persichetti, F., Frontali, M., Folstein, S., Ross, C., Franz, M., Abbott, M. et al.** (1993). Trinucleotide repeat length instability and age of onset in Huntington's disease. *Nat Genet* **4**, 387-92.
- Duyao, M. P., Auerbach, A. B., Ryan, A., Persichetti, F., Barnes, G. T., McNeil, S. M., Ge, P., Vonsattel, J. P., Gusella, J. F., Joyner, A. L. et al.** (1995). Inactivation of the mouse Huntington's disease gene homolog Hdh. *Science* **269**, 407-10.
- Everett, C. M. and Wood, N. W.** (2004). Trinucleotide repeats and neurodegenerative disease. *Brain* **127**, 2385-405.
- Fardaei, M., Rogers, M. T., Thorpe, H. M., Larkin, K., Hamshere, M. G., Harper, P. S. and Brook, J. D.** (2002). Three proteins, MBNL, MBLL and MBXL, co-localize in vivo with nuclear foci of expanded-repeat transcripts in DM1 and DM2 cells. *Hum Mol Genet* **11**, 805-14.
- Farrer, L. A.** (1985). Diabetes mellitus in Huntington disease. *Clin Genet* **27**, 62-7.
- Farrer, L. A. and Meaney, F. J.** (1985). An anthropometric assessment of Huntington's disease patients and families. *Am J Phys Anthropol* **67**, 185-94.
- Fennema-Notestine, C., Archibald, S. L., Jacobson, M. W., Corey-Bloom, J., Paulsen, J. S., Peavy, G. M., Gamst, A. C., Hamilton, J. M., Salmon, D. P. and Jernigan, T. L.** (2004). In vivo evidence of cerebellar atrophy and cerebral white matter loss in Huntington disease. *Neurology* **63**, 989-95.
- Ferrante, R. J., Beal, M. F., Kowall, N. W., Richardson, E. P., Jr. and Martin, J. B.** (1987a). Sparring of acetylcholinesterase-containing striatal neurons in Huntington's disease. *Brain Res* **411**, 162-6.
- Ferrante, R. J., Kowall, N. W., Beal, M. F., Martin, J. B., Bird, E. D. and Richardson, E. P., Jr.** (1987b). Morphologic and histochemical characteristics of a spared subset of striatal neurons in Huntington's disease. *J Neuropathol Exp Neurol* **46**, 12-27.
- Ferrante, R. J., Ryu, H., Kubilus, J. K., D'Mello, S., Sugars, K. L., Lee, J., Lu, P., Smith, K., Browne, S., Beal, M. F. et al.** (2004). Chemotherapy for the brain: the antitumor antibiotic mithramycin prolongs survival in a mouse model of Huntington's disease. *J Neurosci* **24**, 10335-42.
- Fleischer, B.** (1918). Ueber Myotonische Dystrophie mit Katarak. *Arch Klin Exp Ophthalmol* **46**, 442-447.
- Folstein, S. E., Leigh, R. J., Parhad, I. M. and Folstein, M. F.** (1986). The diagnosis of Huntington's disease. *Neurology* **36**, 1279-83.
- Foroud, T., Gray, J., Ivashina, J. and Conneally, P. M.** (1999). Differences in duration of Huntington's disease based on age at onset. *J Neurol Neurosurg Psychiatry* **66**, 52-6.
- Förster, Th.** (1948). Zwischenmolekulare Energiewanderung und Fluoreszenz. *Annalen der Physik* **437**, 55-75.
- Frid, P., Anisimov, S. V. and Popovic, N.** (2007). Congo red and protein aggregation in neurodegenerative diseases. *Brain Res Rev* **53**, 135-60.
- Friedman, M. J., Wang, C. E., Li, X. J. and Li, S.** (2008). Polyglutamine expansion reduces the association of TATA-binding protein with DNA and induces DNA binding-independent neurotoxicity. *J Biol Chem* **283**, 8283-90.

- Fu, Y. H., Pizzuti, A., Fenwick, R. G., Jr., King, J., Rajnarayan, S., Dunne, P. W., Dubel, J., Nasser, G. A., Ashizawa, T., de Jong, P. et al.** (1992). An unstable triplet repeat in a gene related to myotonic muscular dystrophy. *Science* **255**, 1256-8.
- Fusco, F. R., Zuccato, C., Tartari, M., Martorana, A., De March, Z., Giampa, C., Cattaneo, E. and Bernardi, G.** (2003). Co-localization of brain-derived neurotrophic factor (BDNF) and wild-type huntingtin in normal and quinolinic acid-lesioned rat brain. *Eur J Neurosci* **18**, 1093-102.
- Gabriel, D., Vernier, M., Pfeifer, M. J., Dasen, B., Tenaillon, L. and Bouhelal, R.** (2003). High throughput screening technologies for direct cyclic AMP measurement. *Assay Drug Dev Technol* **1**, 291-303.
- Gafni, J. and Ellerby, L. M.** (2002). Calpain activation in Huntington's disease. *J Neurosci* **22**, 4842-9.
- Gafni, J., Hermel, E., Young, J. E., Wellington, C. L., Hayden, M. R. and Ellerby, L. M.** (2004). Inhibition of calpain cleavage of huntingtin reduces toxicity: accumulation of calpain/caspase fragments in the nucleus. *J Biol Chem* **279**, 20211-20.
- Gardian, G., Browne, S. E., Choi, D. K., Klivenyi, P., Gregorio, J., Kubilus, J. K., Ryu, H., Langley, B., Ratan, R. R., Ferrante, R. J. et al.** (2005). Neuroprotective effects of phenylbutyrate in the N171-82Q transgenic mouse model of Huntington's disease. *J Biol Chem* **280**, 556-63.
- Gardner, P. R., Nguyen, D. D. and White, C. W.** (1994). Aconitase is a sensitive and critical target of oxygen poisoning in cultured mammalian cells and in rat lungs. *Proc Natl Acad Sci U S A* **91**, 12248-52.
- Gauthier, L. R., Charrin, B. C., Borrell-Pages, M., Dompierre, J. P., Rangone, H., Cordelieres, F. P., De Mey, J., MacDonald, M. E., Lessmann, V., Humbert, S. et al.** (2004). Huntingtin controls neurotrophic support and survival of neurons by enhancing BDNF vesicular transport along microtubules. *Cell* **118**, 127-38.
- Girotti, F., Carella, F., Scigliano, G., Grassi, M. P., Soliveri, P., Giovannini, P., Parati, E. and Caraceni, T.** (1984). Effect of neuroleptic treatment on involuntary movements and motor performances in Huntington's disease. *J Neurol Neurosurg Psychiatry* **47**, 848-52.
- Glass, M., Dragunow, M. and Faull, R. L.** (2000). The pattern of neurodegeneration in Huntington's disease: a comparative study of cannabinoid, dopamine, adenosine and GABA(A) receptor alterations in the human basal ganglia in Huntington's disease. *Neuroscience* **97**, 505-19.
- Goldberg, Y. P., Nicholson, D. W., Rasper, D. M., Kalchman, M. A., Koide, H. B., Graham, R. K., Bromm, M., Kazemi-Esfarjani, P., Thornberry, N. A., Vaillancourt, J. P. et al.** (1996). Cleavage of huntingtin by apopain, a proapoptotic cysteine protease, is modulated by the polyglutamine tract. *Nat Genet* **13**, 442-9.
- Gonitel, R., Moffitt, H., Sathasivam, K., Woodman, B., Detloff, P. J., Faull, R. L. and Bates, G. P.** (2008). DNA instability in postmitotic neurons. *Proc Natl Acad Sci U S A* **105**, 3467-72.
- Gouw, L. G., Digre, K. B., Harris, C. P., Haines, J. H. and Ptacek, L. J.** (1994). Autosomal dominant cerebellar ataxia with retinal degeneration: clinical, neuropathologic, and genetic analysis of a large kindred. *Neurology* **44**, 1441-7.
- Graham, R. K., Deng, Y., Slow, E. J., Haigh, B., Bissada, N., Lu, G., Pearson, J., Shehadeh, J., Bertram, L., Murphy, Z. et al.** (2006). Cleavage at the caspase-6 site is required for neuronal dysfunction and degeneration due to mutant huntingtin. *Cell* **125**, 1179-91.
- Greenstein, P. E., Vonsattel, J. P., Margolis, R. L. and Joseph, J. T.** (2007). Huntington's disease like-2 neuropathology. *Mov Disord* **22**, 1416-23.
- Grollman, A. P.** (1967). Inhibitors of protein biosynthesis. II. Mode of action of anisomycin. *J Biol Chem* **242**, 3226-33.

**Group, T. H. s. D. C. R.** (1993a). A novel gene containing a trinucleotide repeat that is expanded and unstable on Huntington's disease chromosomes. The Huntington's Disease Collaborative Research Group. *Cell* **72**, 971-83.

**Group, T. H. s. D. C. R.** (1993b). A novel gene containing a trinucleotide repeat that is expanded and unstable on Huntington's disease chromosomes. *Cell* **72**, 971-83.

**Group, T. H. s. D. C. R.** (2003). Dosage effects of riluzole in Huntington's disease: a multicenter placebo-controlled study. *Neurology* **61**, 1551-6.

**Gubler, H.** (2006). *Methods for Statistical Analysis, Quality Assurance and Management of Primary HTS Data*: Wiley-VCH.

**Gunawardena, S., Her, L. S., Bruschi, R. G., Laymon, R. A., Niesman, I. R., Gordesky-Gold, B., Sintasath, L., Bonini, N. M. and Goldstein, L. S.** (2003). Disruption of axonal transport by loss of huntingtin or expression of pathogenic polyQ proteins in *Drosophila*. *Neuron* **40**, 25-40.

**Gusella, J. F., Wexler, N. S., Conneally, P. M., Naylor, S. L., Anderson, M. A., Tanzi, R. E., Watkins, P. C., Ottina, K., Wallace, M. R., Sakaguchi, A. Y. et al.** (1983). A polymorphic DNA marker genetically linked to Huntington's disease. *Nature* **306**, 234-8.

**Gutekunst, C. A., Li, S. H., Yi, H., Mulroy, J. S., Kuemmerle, S., Jones, R., Rye, D., Ferrante, R. J., Hersch, S. M. and Li, X. J.** (1999). Nuclear and neuropil aggregates in Huntington's disease: relationship to neuropathology. *J Neurosci* **19**, 2522-34.

**Hackam, A. S., Hodgson, J. G., Singaraja, R., Zhang, T., Gan, L., Gutekunst, C. A., Hersch, S. M. and Hayden, M. R.** (1999). Evidence for both the nucleus and cytoplasm as subcellular sites of pathogenesis in Huntington's disease in cell culture and in transgenic mice expressing mutant huntingtin. *Philos Trans R Soc Lond B Biol Sci* **354**, 1047-55.

**Handa, V., Saha, T. and Usdin, K.** (2003). The fragile X syndrome repeats form RNA hairpins that do not activate the interferon-inducible protein kinase, PKR, but are cut by Dicer. *Nucleic Acids Res* **31**, 6243-8.

**Hansotia, P., Wall, R. and Berendes, J.** (1985). Sleep disturbances and severity of Huntington's disease. *Neurology* **35**, 1672-4.

**Harper, S. Q., Staber, P. D., He, X., Eliason, S. L., Martins, I. H., Mao, Q., Yang, L., Kotin, R. M., Paulson, H. L. and Davidson, B. L.** (2005). RNA interference improves motor and neuropathological abnormalities in a Huntington's disease mouse model. *Proc Natl Acad Sci U S A* **102**, 5820-5.

**Hausladen, A. and Fridovich, I.** (1996). Measuring nitric oxide and superoxide: rate constants for aconitase reactivity. *Methods Enzymol* **269**, 37-41.

**Hayden, M. R., Hewitt, J., Stoessl, A. J., Clark, C., Ammann, W. and Martin, W. R.** (1987). The combined use of positron emission tomography and DNA polymorphisms for preclinical detection of Huntington's disease. *Neurology* **37**, 1441-7.

**Hazeki, N., Tukamoto, T., Goto, J. and Kanazawa, I.** (2000). Formic acid dissolves aggregates of an N-terminal huntingtin fragment containing an expanded polyglutamine tract: applying to quantification of protein components of the aggregates. *Biochem Biophys Res Commun* **277**, 386-93.

**Heiser, V., Scherzinger, E., Boeddrich, A., Nordhoff, E., Lurz, R., Schugar, N., Lehrach, H. and Wanker, E. E.** (2000). Inhibition of huntingtin fibrillogenesis by specific antibodies and small molecules: implications for Huntington's disease therapy. *Proc Natl Acad Sci U S A* **97**, 6739-44.

**Henley, S. M., Frost, C., MacManus, D. G., Warner, T. T., Fox, N. C. and Tabrizi, S. J.** (2006). Increased rate of whole-brain atrophy over 6 months in early Huntington disease. *Neurology* **67**, 694-6.

**Hersch, S. M., Gevorkian, S., Marder, K., Moskowitz, C., Feigin, A., Cox, M., Como, P., Zimmerman, C., Lin, M., Zhang, L. et al.** (2006). Creatine in Huntington disease is safe, tolerable, bioavailable in brain and reduces serum 8OH<sup>2</sup>dG. *Neurology* **66**, 250-2.

**Herzig, S., Long, F., Jhala, U. S., Hedrick, S., Quinn, R., Bauer, A., Rudolph, D., Schutz, G., Yoon, C., Puigserver, P. et al.** (2001). CREB regulates hepatic gluconeogenesis through the coactivator PGC-1. *Nature* **413**, 179-83.

**Hilditch-Maguire, P., Trettel, F., Passani, L. A., Auerbach, A., Persichetti, F. and MacDonald, M. E.** (2000). Huntingtin: an iron-regulated protein essential for normal nuclear and perinuclear organelles. *Hum Mol Genet* **9**, 2789-97.

**Ho, T. H., Charlet, B. N., Poulos, M. G., Singh, G., Swanson, M. S. and Cooper, T. A.** (2004). Muscleblind proteins regulate alternative splicing. *Embo J* **23**, 3103-12.

**Hodges, A., Strand, A. D., Aragaki, A. K., Kuhn, A., Sengstag, T., Hughes, G., Elliston, L. A., Hartog, C., Goldstein, D. R., Thu, D. et al.** (2006). Regional and cellular gene expression changes in human Huntington's disease brain. *Hum Mol Genet* **15**, 965-77.

**Hodgson, J. G., Agopyan, N., Gutekunst, C. A., Leavitt, B. R., LePiane, F., Singaraja, R., Smith, D. J., Bissada, N., McCutcheon, K., Nasir, J. et al.** (1999). A YAC mouse model for Huntington's disease with full-length mutant huntingtin, cytoplasmic toxicity, and selective striatal neurodegeneration. *Neuron* **23**, 181-92.

**Hoffner, G., Kahlem, P. and Djian, P.** (2002). Perinuclear localization of huntingtin as a consequence of its binding to microtubules through an interaction with beta-tubulin: relevance to Huntington's disease. *J Cell Sci* **115**, 941-8.

**Holbert, S., Denghien, I., Kiechle, T., Rosenblatt, A., Wellington, C., Hayden, M. R., Margolis, R. L., Ross, C. A., Dausset, J., Ferrante, R. J. et al.** (2001). The Gln-Ala repeat transcriptional activator CA150 interacts with huntingtin: neuropathologic and genetic evidence for a role in Huntington's disease pathogenesis. *Proc Natl Acad Sci U S A* **98**, 1811-6.

**Hoover, J. E. and Strick, P. L.** (1999). The organization of cerebellar and basal ganglia outputs to primary motor cortex as revealed by retrograde transneuronal transport of herpes simplex virus type 1. *J Neurosci* **19**, 1446-63.

**Howeler, C. J., Busch, H. F., Geraedts, J. P., Niermeijer, M. F. and Staal, A.** (1989). Anticipation in myotonic dystrophy: fact or fiction? *Brain* **112 ( Pt 3)**, 779-97.

**Huang, C. C., Faber, P. W., Persichetti, F., Mittal, V., Vonsattel, J. P., MacDonald, M. E. and Gusella, J. F.** (1998). Amyloid formation by mutant huntingtin: threshold, progressivity and recruitment of normal polyglutamine proteins. *Somat Cell Mol Genet* **24**, 217-33.

**Huntington, G.** (1872). On Chorea. *Medical and Surgical Reporter* **26**, 320-321.

**HuntingtonStudyGroup.** (2001). A randomized, placebo-controlled trial of coenzyme Q10 and remacemide in Huntington's disease. *Neurology* **57**, 397-404.

**HuntingtonStudyGroup.** (2004). Minocycline safety and tolerability in Huntington disease. *Neurology* **63**, 547-9.

**Hurlbert, M. S., Zhou, W., Wasmeier, C., Kaddis, F. G., Hutton, J. C. and Freed, C. R.** (1999). Mice transgenic for an expanded CAG repeat in the Huntington's disease gene develop diabetes. *Diabetes* **48**, 649-51.

**Ikeuchi, T., Onodera, O., Oyake, M., Koide, R., Tanaka, H. and Tsuji, S.** (1995). Dentatorubral-pallidolusian atrophy (DRPLA): close correlation of CAG repeat expansions with the wide spectrum of clinical presentations and prominent anticipation. *Semin Cell Biol* **6**, 37-44.

**Imbert, P. E., Unterreiner, V., Siebert, D., Gubler, H., Parker, C. and Gabriel, D.** (2007). Recommendations for the reduction of compound artifacts in time-resolved fluorescence resonance energy transfer assays. *Assay Drug Dev Technol* **5**, 363-72.

**Iwata, A., Riley, B. E., Johnston, J. A. and Kopito, R. R.** (2005). HDAC6 and microtubules are required for autophagic degradation of aggregated huntingtin. *J Biol Chem* **280**, 40282-92.

**Jana, N. R., Zemskov, E. A., Wang, G. and Nukina, N.** (2001). Altered proteasomal function due to the expression of polyglutamine-expanded truncated N-terminal huntingtin induces apoptosis by caspase activation through mitochondrial cytochrome c release. *Hum Mol Genet* **10**, 1049-59.

- Jankovic, J. and Beach, J.** (1997). Long-term effects of tetrabenazine in hyperkinetic movement disorders. *Neurology* **48**, 358-62.
- Jeste, D. V., Barban, L. and Parisi, J.** (1984). Reduced Purkinje cell density in Huntington's disease. *Exp Neurol* **85**, 78-86.
- Jiang, H., Poirier, M. A., Liang, Y., Pei, Z., Weiskittel, C. E., Smith, W. W., DeFranco, D. B. and Ross, C. A.** (2006). Depletion of CBP is directly linked with cellular toxicity caused by mutant huntingtin. *Neurobiol Dis* **23**, 543-51.
- Jones, E. G.** (2002). Thalamic circuitry and thalamocortical synchrony. *Philos Trans R Soc Lond B Biol Sci* **357**, 1659-73.
- Kassubek, J., Juengling, F. D., Kioschies, T., Henkel, K., Karitzky, J., Kramer, B., Ecker, D., Andrich, J., Saft, C., Kraus, P. et al.** (2004). Topography of cerebral atrophy in early Huntington's disease: a voxel based morphometric MRI study. *J Neurol Neurosurg Psychiatry* **75**, 213-20.
- Kegel, K. B., Meloni, A. R., Yi, Y., Kim, Y. J., Doyle, E., Cuiffo, B. G., Sapp, E., Wang, Y., Qin, Z. H., Chen, J. D. et al.** (2002). Huntingtin is present in the nucleus, interacts with the transcriptional corepressor C-terminal binding protein, and represses transcription. *J Biol Chem* **277**, 7466-76.
- Kehoe, P., Krawczak, M., Harper, P. S., Owen, M. J. and Jones, A. L.** (1999). Age of onset in Huntington disease: sex specific influence of apolipoprotein E genotype and normal CAG repeat length. *J Med Genet* **36**, 108-11.
- Kennedy, L., Evans, E., Chen, C. M., Craven, L., Detloff, P. J., Ennis, M. and Shelbourne, P. F.** (2003). Dramatic tissue-specific mutation length increases are an early molecular event in Huntington disease pathogenesis. *Hum Mol Genet* **12**, 3359-67.
- Kim, S., Nollen, E. A., Kitagawa, K., Bindokas, V. P. and Morimoto, R. I.** (2002). Polyglutamine protein aggregates are dynamic. *Nat Cell Biol* **4**, 826-31.
- Kim, Y. J., Sapp, E., Cuiffo, B. G., Sobin, L., Yoder, J., Kegel, K. B., Qin, Z. H., Detloff, P., Aronin, N. and DiFiglia, M.** (2006). Lysosomal proteases are involved in generation of N-terminal huntingtin fragments. *Neurobiol Dis* **22**, 346-56.
- Kim, Y. J., Yi, Y., Sapp, E., Wang, Y., Cuiffo, B., Kegel, K. B., Qin, Z. H., Aronin, N. and DiFiglia, M.** (2001). Caspase 3-cleaved N-terminal fragments of wild-type and mutant huntingtin are present in normal and Huntington's disease brains, associate with membranes, and undergo calpain-dependent proteolysis. *Proc Natl Acad Sci U S A* **98**, 12784-9.
- King, M. A., Hands, S., Hafiz, F., Mizushima, N., Tolkovsky, A. M. and Wytenbach, A.** (2008). Rapamycin inhibits polyglutamine aggregation independently of autophagy by reducing protein synthesis. *Mol Pharmacol* **73**, 1052-63.
- Kirkwood, S. C., Siemers, E., Hodes, M. E., Conneally, P. M., Christian, J. C. and Foroud, T.** (2000). Subtle changes among presymptomatic carriers of the Huntington's disease gene. *J Neurol Neurosurg Psychiatry* **69**, 773-9.
- Kirkwood, S. C., Su, J. L., Conneally, P. and Foroud, T.** (2001). Progression of symptoms in the early and middle stages of Huntington disease. *Arch Neurol* **58**, 273-8.
- Ko, J., Ou, S. and Patterson, P. H.** (2001). New anti-huntingtin monoclonal antibodies: implications for huntingtin conformation and its binding proteins. *Brain Res Bull* **56**, 319-29.
- Koide, R., Ikeuchi, T., Onodera, O., Tanaka, H., Igarashi, S., Endo, K., Takahashi, H., Kondo, R., Ishikawa, A., Hayashi, T. et al.** (1994). Unstable expansion of CAG repeat in hereditary dentatorubral-pallidoluysian atrophy (DRPLA). *Nat Genet* **6**, 9-13.
- Kovtun, I. V., Liu, Y., Bjoras, M., Klungland, A., Wilson, S. H. and McMurray, C. T.** (2007). OGG1 initiates age-dependent CAG trinucleotide expansion in somatic cells. *Nature* **447**, 447-52.
- Kovtun, I. V. and McMurray, C. T.** (2001). Trinucleotide expansion in haploid germ cells by gap repair. *Nat Genet* **27**, 407-11.

- Kremer, B., Goldberg, P., Andrew, S. E., Theilmann, J., Telenius, H., Zeisler, J., Squitieri, F., Lin, B., Bassett, A., Almqvist, E. et al.** (1994). A worldwide study of the Huntington's disease mutation. The sensitivity and specificity of measuring CAG repeats. *N Engl J Med* **330**, 1401-6.
- Kremer, H. P. and Roos, R. A.** (1992). Weight loss in Huntington's disease. *Arch Neurol* **49**, 349.
- Kremer, H. P., Roos, R. A., Dingjan, G. M., Bots, G. T., Bruyn, G. W. and Hofman, M. A.** (1991). The hypothalamic lateral tuberal nucleus and the characteristics of neuronal loss in Huntington's disease. *Neurosci Lett* **132**, 101-4.
- Krol, J., Fiszer, A., Mykowska, A., Sobczak, K., de Mezer, M. and Krzyzosiak, W. J.** (2007). Ribonuclease dicer cleaves triplet repeat hairpins into shorter repeats that silence specific targets. *Mol Cell* **25**, 575-86.
- Kushnirov, V. V., Alexandrov, I. M., Mitkevich, O. V., Shkundina, I. S. and Ter-Avanesyan, M. D.** (2006). Purification and analysis of prion and amyloid aggregates. *Methods* **39**, 50-5.
- Landles, C. and Bates, G. P.** (2004). Huntingtin and the molecular pathogenesis of Huntington's disease. Fourth in molecular medicine review series. *EMBO Rep* **5**, 958-63.
- Landwehrmeyer, G. B., Dubois, B., de Yebenes, J. G., Kremer, B., Gaus, W., Kraus, P. H., Przuntek, H., Dib, M., Doble, A., Fischer, W. et al.** (2007). Riluzole in Huntington's disease: a 3-year, randomized controlled study. *Ann Neurol* **62**, 262-72.
- Lang, W. W. a. A.** (1989). Movement disorders: a comprehensive survey. New York: Futura Publishing Company.
- Lanska, D. J., Lanska, M. J., Lavine, L. and Schoenberg, B. S.** (1988a). Conditions associated with Huntington's disease at death. A case-control study. *Arch Neurol* **45**, 878-80.
- Lanska, D. J., Lavine, L., Lanska, M. J. and Schoenberg, B. S.** (1988b). Huntington's disease mortality in the United States. *Neurology* **38**, 769-72.
- Leavitt, B. R., van Raamsdonk, J. M., Shehadeh, J., Fernandes, H., Murphy, Z., Graham, R. K., Wellington, C. L., Raymond, L. A. and Hayden, M. R.** (2006). Wild-type huntingtin protects neurons from excitotoxicity. *J Neurochem* **96**, 1121-9.
- Lecerf, J. M., Shirley, T. L., Zhu, Q., Kazantsev, A., Amersdorfer, P., Housman, D. E., Messer, A. and Huston, J. S.** (2001). Human single-chain Fv intrabodies counteract in situ huntingtin aggregation in cellular models of Huntington's disease. *Proc Natl Acad Sci U S A* **98**, 4764-9.
- Lee, H. J., Hammond, D. N., Large, T. H. and Wainer, B. H.** (1990). Immortalized young adult neurons from the septal region: generation and characterization. *Brain Res Dev Brain Res* **52**, 219-28.
- Leefflang, E. P., Zhang, L., Tavare, S., Hubert, R., Srinidhi, J., MacDonald, M. E., Myers, R. H., de Young, M., Wexler, N. S., Gusella, J. F. et al.** (1995). Single sperm analysis of the trinucleotide repeats in the Huntington's disease gene: quantification of the mutation frequency spectrum. *Hum Mol Genet* **4**, 1519-26.
- Leonard, D. P., Kidson, M. A., Brown, J. G., Shannon, P. J. and Taryan, S.** (1975). A double blind trial of lithium carbonate and haloperidol in Huntington's chorea. *Aust N Z J Psychiatry* **9**, 115-8.
- Leone, T. C., Lehman, J. J., Finck, B. N., Schaeffer, P. J., Wende, A. R., Boudina, S., Courtois, M., Wozniak, D. F., Sambandam, N., Bernal-Mizrachi, C. et al.** (2005). PGC-1alpha deficiency causes multi-system energy metabolic derangements: muscle dysfunction, abnormal weight control and hepatic steatosis. *PLoS Biol* **3**, e101.
- Li, H., Li, S. H., Cheng, A. L., Mangiarini, L., Bates, G. P. and Li, X. J.** (1999). Ultrastructural localization and progressive formation of neuropil aggregates in Huntington's disease transgenic mice. *Hum Mol Genet* **8**, 1227-36.

- Li, H., Li, S. H., Johnston, H., Shelbourne, P. F. and Li, X. J.** (2000). Amino-terminal fragments of mutant huntingtin show selective accumulation in striatal neurons and synaptic toxicity. *Nat Genet* **25**, 385-9.
- Li, L. B., Yu, Z., Teng, X. and Bonini, N. M.** (2008). RNA toxicity is a component of ataxin-3 degeneration in *Drosophila*. *Nature*.
- Li, P., Huey-Tubman, K. E., Gao, T., Li, X., West, A. P., Jr., Bennett, M. J. and Bjorkman, P. J.** (2007). The structure of a polyQ-anti-polyQ complex reveals binding according to a linear lattice model. *Nat Struct Mol Biol* **14**, 381-7.
- Lin, C. H., Tallaksen-Greene, S., Chien, W. M., Cearley, J. A., Jackson, W. S., Crouse, A. B., Ren, S., Li, X. J., Albin, R. L. and Detloff, P. J.** (2001). Neurological abnormalities in a knock-in mouse model of Huntington's disease. *Hum Mol Genet* **10**, 137-44.
- Lin, J., Wu, P. H., Tarr, P. T., Lindenberg, K. S., St-Pierre, J., Zhang, C. Y., Mootha, V. K., Jager, S., Vianna, C. R., Reznick, R. M. et al.** (2004). Defects in adaptive energy metabolism with CNS-linked hyperactivity in PGC-1alpha null mice. *Cell* **119**, 121-35.
- Lione, L. A., Carter, R. J., Hunt, M. J., Bates, G. P., Morton, A. J. and Dunnett, S. B.** (1999). Selective discrimination learning impairments in mice expressing the human Huntington's disease mutation. *J Neurosci* **19**, 10428-37.
- Lodi, R., Schapira, A. H., Manners, D., Styles, P., Wood, N. W., Taylor, D. J. and Warner, T. T.** (2000). Abnormal in vivo skeletal muscle energy metabolism in Huntington's disease and dentatorubropallidoluysian atrophy. *Ann Neurol* **48**, 72-6.
- Lund, J.** (1860). Chorea St. Vitus dance in Saetersdalen. Report of health and medicine and medical conditions in Norway in 1860. 137.
- Lunkes, A., Lindenberg, K. S., Ben-Haiem, L., Weber, C., Devys, D., Landwehrmeyer, G. B., Mandel, J. L. and Trottier, Y.** (2002). Proteases acting on mutant huntingtin generate cleaved products that differentially build up cytoplasmic and nuclear inclusions. *Mol Cell* **10**, 259-69.
- Lunkes, A. and Mandel, J. L.** (1998). A cellular model that recapitulates major pathogenic steps of Huntington's disease. *Hum Mol Genet* **7**, 1355-61.
- Luthi-Carter, R., Hanson, S. A., Strand, A. D., Bergstrom, D. A., Chun, W., Peters, N. L., Woods, A. M., Chan, E. Y., Kooperberg, C., Krainc, D. et al.** (2002a). Dysregulation of gene expression in the R6/2 model of polyglutamine disease: parallel changes in muscle and brain. *Hum Mol Genet* **11**, 1911-26.
- Luthi-Carter, R., Strand, A. D., Hanson, S. A., Kooperberg, C., Schilling, G., La Spada, A. R., Merry, D. E., Young, A. B., Ross, C. A., Borchelt, D. R. et al.** (2002b). Polyglutamine and transcription: gene expression changes shared by DRPLA and Huntington's disease mouse models reveal context-independent effects. *Hum Mol Genet* **11**, 1927-37.
- MacDonald, M. E., Barnes, G., Srinidhi, J., Duyao, M. P., Ambrose, C. M., Myers, R. H., Gray, J., Conneally, P. M., Young, A., Penney, J. et al.** (1993). Gametic but not somatic instability of CAG repeat length in Huntington's disease. *J Med Genet* **30**, 982-6.
- Macdonald, V. and Halliday, G.** (2002). Pyramidal cell loss in motor cortices in Huntington's disease. *Neurobiol Dis* **10**, 378-86.
- Machida, Y., Okada, T., Kurosawa, M., Oyama, F., Ozawa, K. and Nukina, N.** (2006). rAAV-mediated shRNA ameliorated neuropathology in Huntington disease model mouse. *Biochem Biophys Res Commun* **343**, 190-7.
- Mahant, N., McCusker, E. A., Byth, K. and Graham, S.** (2003). Huntington's disease: clinical correlates of disability and progression. *Neurology* **61**, 1085-92.
- Malinina, L.** (2005). Possible involvement of the RNAi pathway in trinucleotide repeat expansion diseases. *J Biomol Struct Dyn* **23**, 233-5.
- Mangiarini, L., Sathasivam, K., Seller, M., Cozens, B., Harper, A., Hetherington, C., Lawton, M., Trottier, Y., Lehrach, H., Davies, S. W. et al.** (1996). Exon 1 of the HD gene

with an expanded CAG repeat is sufficient to cause a progressive neurological phenotype in transgenic mice. *Cell* **87**, 493-506.

**Manley, K., Pugh, J. and Messer, A.** (1999a). Instability of the CAG repeat in immortalized fibroblast cell cultures from Huntington's disease transgenic mice. *Brain Res* **835**, 74-9.

**Manley, K., Shirley, T. L., Flaherty, L. and Messer, A.** (1999b). Msh2 deficiency prevents in vivo somatic instability of the CAG repeat in Huntington disease transgenic mice. *Nat Genet* **23**, 471-3.

**Margolis, R. L., Holmes, S. E., Rosenblatt, A., Gourley, L., O'Hearn, E., Ross, C. A., Seltzer, W. K., Walker, R. H., Ashizawa, T., Rasmussen, A. et al.** (2004). Huntington's Disease-like 2 (HDL2) in North America and Japan. *Ann Neurol* **56**, 670-4.

**Marsh, J. L., Walker, H., Theisen, H., Zhu, Y. Z., Fielder, T., Purcell, J. and Thompson, L. M.** (2000). Expanded polyglutamine peptides alone are intrinsically cytotoxic and cause neurodegeneration in *Drosophila*. *Hum Mol Genet* **9**, 13-25.

**Martin-Aparicio, E., Yamamoto, A., Hernandez, F., Hen, R., Avila, J. and Lucas, J. J.** (2001). Proteasomal-dependent aggregate reversal and absence of cell death in a conditional mouse model of Huntington's disease. *J Neurosci* **21**, 8772-81.

**Martindale, D., Hackam, A., Wieczorek, A., Ellerby, L., Wellington, C., McCutcheon, K., Singaraja, R., Kazemi-Esfarjani, P., Devon, R., Kim, S. U. et al.** (1998). Length of huntingtin and its polyglutamine tract influences localization and frequency of intracellular aggregates. *Nat Genet* **18**, 150-4.

**Mathis, G.** (1993). Rare earth cryptates and homogeneous fluoroimmunoassays with human sera. *Clin Chem* **39**, 1953-9.

**McCampbell, A., Taylor, J. P., Taye, A. A., Robitschek, J., Li, M., Walcott, J., Merry, D., Chai, Y., Paulson, H., Sobue, G. et al.** (2000). CREB-binding protein sequestration by expanded polyglutamine. *Hum Mol Genet* **9**, 2197-202.

**McLeod, C. J., O'Keefe, L. V. and Richards, R. I.** (2005). The pathogenic agent in *Drosophila* models of 'polyglutamine' diseases. *Hum Mol Genet* **14**, 1041-8.

**Menalled, L. B., Sison, J. D., Dragatsis, I., Zeitlin, S. and Chesselet, M. F.** (2003). Time course of early motor and neuropathological anomalies in a knock-in mouse model of Huntington's disease with 140 CAG repeats. *J Comp Neurol* **465**, 11-26.

**Metzger, S., Bauer, P., Tomiuk, J., Laccone, F., Didonato, S., Gellera, C., Mariotti, C., Lange, H. W., Weirich-Schwaiger, H., Wenning, G. K. et al.** (2006a). Genetic analysis of candidate genes modifying the age-at-onset in Huntington's disease. *Hum Genet* **120**, 285-92.

**Metzger, S., Bauer, P., Tomiuk, J., Laccone, F., Didonato, S., Gellera, C., Soliveri, P., Lange, H. W., Weirich-Schwaiger, H., Wenning, G. K. et al.** (2006b). The S18Y polymorphism in the UCHL1 gene is a genetic modifier in Huntington's disease. *Neurogenetics* **7**, 27-30.

**Miller, J. W., Urbinati, C. R., Teng-Umuay, P., Stenberg, M. G., Byrne, B. J., Thornton, C. A. and Swanson, M. S.** (2000). Recruitment of human muscleblind proteins to (CUG)(n) expansions associated with myotonic dystrophy. *Embo J* **19**, 4439-48.

**Mirkin, S. M.** (2007). Expandable DNA repeats and human disease. *Nature* **447**, 932-40.

**Modregger, J., DiProspero, N. A., Charles, V., Tagle, D. A. and Plomann, M.** (2002). PACSIN 1 interacts with huntingtin and is absent from synaptic varicosities in presymptomatic Huntington's disease brains. *Hum Mol Genet* **11**, 2547-58.

**Morales, L. M., Estevez, J., Suarez, H., Villalobos, R., Chacin de Bonilla, L. and Bonilla, E.** (1989). Nutritional evaluation of Huntington disease patients. *Am J Clin Nutr* **50**, 145-50.

**Morimoto, R. I.** (2008). Proteotoxic stress and inducible chaperone networks in neurodegenerative disease and aging. *Genes Dev* **22**, 1427-38.

**Murman, D. L., Giordani, B., Mellow, A. M., Johanns, J. R., Little, R. J., Hariharan, M. and Foster, N. L.** (1997). Cognitive, behavioral, and motor effects of the NMDA antagonist ketamine in Huntington's disease. *Neurology* **49**, 153-61.

- Myers, R. H.** (2004). Huntington's disease genetics. *NeuroRx* **1**, 255-62.
- Nakano, T., Iwabuchi, K., Yagishita, S., Amano, N., Akagi, M. and Yamamoto, Y.** (1985). [An autopsy case of dentatorubropallidolusian atrophy (DRPLA) clinically diagnosed as Huntington's chorea]. *No To Shinkei* **37**, 767-74.
- Nakao, N., Kokaia, Z., Odin, P. and Lindvall, O.** (1995). Protective effects of BDNF and NT-3 but not PDGF against hypoglycemic injury to cultured striatal neurons. *Exp Neurol* **131**, 1-10.
- Nance, M. A. and Sanders, G.** (1996). Characteristics of individuals with Huntington disease in long-term care. *Mov Disord* **11**, 542-8.
- Nass, G.** (1970). [Mode of action of borrelidin on protein biosynthesis and regulatory processes in microorganisms]. *Zentralbl Bakteriol [Orig]* **212**, 239-45.
- Nguyen, H. P., Kobbe, P., Rahne, H., Worpel, T., Jager, B., Stephan, M., Pabst, R., Holzmann, C., Riess, O., Korr, H. et al.** (2006). Behavioral abnormalities precede neuropathological markers in rats transgenic for Huntington's disease. *Hum Mol Genet* **15**, 3177-94.
- Nishino, N., Jose, B., Shinta, R., Kato, T., Komatsu, Y. and Yoshida, M.** (2004). Chlamydocin-hydroxamic acid analogues as histone deacetylase inhibitors. *Bioorg Med Chem* **12**, 5777-84.
- Nucifora, F. C., Jr., Sasaki, M., Peters, M. F., Huang, H., Cooper, J. K., Yamada, M., Takahashi, H., Tsuji, S., Troncoso, J., Dawson, V. L. et al.** (2001). Interference by huntingtin and atrophin-1 with cbp-mediated transcription leading to cellular toxicity. *Science* **291**, 2423-8.
- O'Brien, J., Wilson, I., Orton, T. and Pognan, F.** (2000). Investigation of the Alamar Blue (resazurin) fluorescent dye for the assessment of mammalian cell cytotoxicity. *Eur J Biochem* **267**, 5421-6.
- Ondo, W. G., Tintner, R., Thomas, M. and Jankovic, J.** (2002). Tetrabenazine treatment for Huntington's disease-associated chorea. *Clin Neuropharmacol* **25**, 300-2.
- Orr, A. L., Li, S., Wang, C. E., Li, H., Wang, J., Rong, J., Xu, X., Mastroberardino, P. G., Greenamyre, J. T. and Li, X. J.** (2008). N-terminal mutant huntingtin associates with mitochondria and impairs mitochondrial trafficking. *J Neurosci* **28**, 2783-92.
- Osborne, J. P., Munson, P. and Burman, D.** (1982). Huntington's chorea. Report of 3 cases and review of the literature. *Arch Dis Child* **57**, 99-103.
- Paganetti, P. A., Lis, M., Klafki, H. W. and Staufenbiel, M.** (1996). Amyloid precursor protein truncated at any of the gamma-secretase sites is not cleaved to beta-amyloid. *J Neurosci Res* **46**, 283-93.
- Panigrahi, G. B., Lau, R., Montgomery, S. E., Leonard, M. R. and Pearson, C. E.** (2005). Slipped (CTG)<sup>n</sup>(CAG)<sup>m</sup> repeats can be correctly repaired, escape repair or undergo error-prone repair. *Nat Struct Mol Biol* **12**, 654-62.
- Paracelsus.** (1527). Das siebente Buch in der Arznei. Von den Krankheiten, die der Vernunft berauben. S.173.
- Patterson, G. H., Piston, D. W. and Barisas, B. G.** (2000). Forster distances between green fluorescent protein pairs. *Anal Biochem* **284**, 438-40.
- Pearson, C. E., Nichol Edamura, K. and Cleary, J. D.** (2005). Repeat instability: mechanisms of dynamic mutations. *Nat Rev Genet* **6**, 729-42.
- Peinemann, A., Schuller, S., Pohl, C., Jahn, T., Weindl, A. and Kassubek, J.** (2005). Executive dysfunction in early stages of Huntington's disease is associated with striatal and insular atrophy: a neuropsychological and voxel-based morphometric study. *J Neurol Sci* **239**, 11-9.
- Penney, J. B., Jr., Young, A. B., Shoulson, I., Starosta-Rubenstein, S., Snodgrass, S. R., Sanchez-Ramos, J., Ramos-Arroyo, M., Gomez, F., Penchaszadeh, G., Alvir, J. et al.**

- (1990). Huntington's disease in Venezuela: 7 years of follow-up on symptomatic and asymptomatic individuals. *Mov Disord* **5**, 93-9.
- Penrose, L.** (1948). The problem of anticipation in pedigrees of dystrophia myotonica. *Ann Eugen* **14**, 125-132.
- Percheron, G., Francois, C., Talbi, B., Yelnik, J. and Fenelon, G.** (1996). The primate motor thalamus. *Brain Res Brain Res Rev* **22**, 93-181.
- Perez, M. K., Paulson, H. L., Pendse, S. J., Saionz, S. J., Bonini, N. M. and Pittman, R. N.** (1998). Recruitment and the role of nuclear localization in polyglutamine-mediated aggregation. *J Cell Biol* **143**, 1457-70.
- Perrin, V., Regulier, E., Abbas-Terki, T., Hassig, R., Brouillet, E., Aebischer, P., Luthi-Carter, R. and Deglon, N.** (2007). Neuroprotection by Hsp104 and Hsp27 in lentiviral-based rat models of Huntington's disease. *Mol Ther* **15**, 903-11.
- Perry, T. L., Diamond, S., Hansen, S. and Stedman, D.** (1969). Plasma-aminoacid levels in Huntington's chorea. *Lancet* **1**, 806-8.
- Perutz, M. F., Finch, J. T., Berriman, J. and Lesk, A.** (2002a). Amyloid fibers are water-filled nanotubes. *Proc Natl Acad Sci U S A* **99**, 5591-5.
- Perutz, M. F., Johnson, T., Suzuki, M. and Finch, J. T.** (1994). Glutamine repeats as polar zippers: their possible role in inherited neurodegenerative diseases. *Proc Natl Acad Sci U S A* **91**, 5355-8.
- Perutz, M. F., Pope, B. J., Owen, D., Wanker, E. E. and Scherzinger, E.** (2002b). Aggregation of proteins with expanded glutamine and alanine repeats of the glutamine-rich and asparagine-rich domains of Sup35 and of the amyloid beta-peptide of amyloid plaques. *Proc Natl Acad Sci U S A* **99**, 5596-600.
- Petrasch-Parwez, E., Nguyen, H. P., Lobbecke-Schumacher, M., Habbes, H. W., Wiczorek, S., Riess, O., Andres, K. H., Dermietzel, R. and Von Horsten, S.** (2007). Cellular and subcellular localization of Huntingtin [corrected] aggregates in the brain of a rat transgenic for Huntington disease. *J Comp Neurol* **501**, 716-30.
- Philips, A. V., Timchenko, L. T. and Cooper, T. A.** (1998). Disruption of splicing regulated by a CUG-binding protein in myotonic dystrophy. *Science* **280**, 737-41.
- Phillipson, O. T. and Bird, E. D.** (1977). Plasma glucose, non-esterified fatty acids and amino acids in Huntington's chorea. *Clin Sci Mol Med* **52**, 311-8.
- Podolsky, S. and Leopold, N. A.** (1977). Abnormal glucose tolerance and arginine tolerance tests in Huntington's disease. *Gerontology* **23**, 55-63.
- Poirier, M. A., Li, H., Macosko, J., Cai, S., Amzel, M. and Ross, C. A.** (2002). Huntingtin spheroids and protofibrils as precursors in polyglutamine fibrilization. *J Biol Chem* **277**, 41032-7.
- Prahlad, V., Cornelius, T. and Morimoto, R. I.** (2008). Regulation of the cellular heat shock response in *Caenorhabditis elegans* by thermosensory neurons. *Science* **320**, 811-4.
- Puigserver, P. and Spiegelman, B. M.** (2003). Peroxisome proliferator-activated receptor-gamma coactivator 1 alpha (PGC-1 alpha): transcriptional coactivator and metabolic regulator. *Endocr Rev* **24**, 78-90.
- Puri, B. K., Bydder, G. M., Counsell, S. J., Corridan, B. J., Richardson, A. J., Hajnal, J. V., Appel, C., McKee, H. M., Vaddadi, K. S. and Horrobin, D. F.** (2002). MRI and neuropsychological improvement in Huntington disease following ethyl-EPA treatment. *Neuroreport* **13**, 123-6.
- Puri, B. K., Leavitt, B. R., Hayden, M. R., Ross, C. A., Rosenblatt, A., Greenamyre, J. T., Hersch, S., Vaddadi, K. S., Sword, A., Horrobin, D. F. et al.** (2005). Ethyl-EPA in Huntington disease: a double-blind, randomized, placebo-controlled trial. *Neurology* **65**, 286-92.

**Ranum, L. P., Schut, L. J., Lundgren, J. K., Orr, H. T. and Livingston, D. M.** (1994). Spinocerebellar ataxia type 5 in a family descended from the grandparents of President Lincoln maps to chromosome 11. *Nat Genet* **8**, 280-4.

**Ratovitski, T., Nakamura, M., D'Ambola, J., Chighladze, E., Liang, Y., Wang, W., Graham, R., Hayden, M. R., Borchelt, D. R., Hirschhorn, R. R. et al.** (2007). N-terminal proteolysis of full-length mutant huntingtin in an inducible PC12 cell model of Huntington's disease. *Cell Cycle* **6**, 2970-81.

**Ravikumar, B., Duden, R. and Rubinsztein, D. C.** (2002). Aggregate-prone proteins with polyglutamine and polyalanine expansions are degraded by autophagy. *Hum Mol Genet* **11**, 1107-17.

**Reddy, P. H., Williams, M., Charles, V., Garrett, L., Pike-Buchanan, L., Whetsell, W. O., Jr., Miller, G. and Tagle, D. A.** (1998). Behavioural abnormalities and selective neuronal loss in HD transgenic mice expressing mutated full-length HD cDNA. *Nat Genet* **20**, 198-202.

**Regulier, E., Zala, D., Aebischer, P. and Deglon, N.** (2004). Lentiviral-mediated gene transfer to model triplet repeat disorders. *Methods Mol Biol* **277**, 199-213.

**Reynolds, N.** (2007). Revisiting safety of minocycline as neuroprotection in Huntington's disease. *Mov Disord* **22**, 292.

**Riddle, S. M., Vedvik, K. L., Hanson, G. T. and Vogel, K. W.** (2006). Time-resolved fluorescence resonance energy transfer kinase assays using physiological protein substrates: applications of terbium-fluorescein and terbium-green fluorescent protein fluorescence resonance energy transfer pairs. *Anal Biochem* **356**, 108-16.

**Ridley, R. M., Frith, C. D., Crow, T. J. and Conneally, P. M.** (1988). Anticipation in Huntington's disease is inherited through the male line but may originate in the female. *J Med Genet* **25**, 589-95.

**Ridley, R. M., Frith, C. D., Farrer, L. A. and Conneally, P. M.** (1991). Patterns of inheritance of the symptoms of Huntington's disease suggestive of an effect of genomic imprinting. *J Med Genet* **28**, 224-31.

**Rigamonti, D., Bauer, J. H., De-Fraja, C., Conti, L., Sipione, S., Sciorati, C., Clementi, E., Hackam, A., Hayden, M. R., Li, Y. et al.** (2000). Wild-type huntingtin protects from apoptosis upstream of caspase-3. *J Neurosci* **20**, 3705-13.

**Rigamonti, D., Sipione, S., Goffredo, D., Zuccato, C., Fossale, E. and Cattaneo, E.** (2001). Huntingtin's neuroprotective activity occurs via inhibition of procaspase-9 processing. *J Biol Chem* **276**, 14545-8.

**Rockabrand, E., Slepko, N., Pantalone, A., Nukala, V. N., Kazantsev, A., Marsh, J. L., Sullivan, P. G., Steffan, J. S., Sensi, S. L. and Thompson, L. M.** (2007). The first 17 amino acids of Huntingtin modulate its sub-cellular localization, aggregation and effects on calcium homeostasis. *Hum Mol Genet* **16**, 61-77.

**Rodriguez-Lebron, E., Denovan-Wright, E. M., Nash, K., Lewin, A. S. and Mandel, R. J.** (2005). Intrastriatal rAAV-mediated delivery of anti-huntingtin shRNAs induces partial reversal of disease progression in R6/1 Huntington's disease transgenic mice. *Mol Ther* **12**, 618-33.

**Roos, R. A., Pruyt, J. F., de Vries, J. and Bots, G. T.** (1985). Neuronal distribution in the putamen in Huntington's disease. *J Neurol Neurosurg Psychiatry* **48**, 422-5.

**Rosas, H. D., Goodman, J., Chen, Y. I., Jenkins, B. G., Kennedy, D. N., Makris, N., Patti, M., Seidman, L. J., Beal, M. F. and Koroshetz, W. J.** (2001). Striatal volume loss in HD as measured by MRI and the influence of CAG repeat. *Neurology* **57**, 1025-8.

**Rosas, H. D., Koroshetz, W. J., Chen, Y. I., Skeuse, C., Vangel, M., Cudkovicz, M. E., Caplan, K., Marek, K., Seidman, L. J., Makris, N. et al.** (2003). Evidence for more widespread cerebral pathology in early HD: an MRI-based morphometric analysis. *Neurology* **60**, 1615-20.

- Rosas, H. D., Koroshetz, W. J., Jenkins, B. G., Chen, Y. I., Hayden, D. L., Beal, M. F. and Cudkowicz, M. E.** (1999). Riluzole therapy in Huntington's disease (HD). *Mov Disord* **14**, 326-30.
- Rosas, H. D., Tuch, D. S., Hevelone, N. D., Zaleta, A. K., Vangel, M., Hersch, S. M. and Salat, D. H.** (2006). Diffusion tensor imaging in presymptomatic and early Huntington's disease: Selective white matter pathology and its relationship to clinical measures. *Mov Disord* **21**, 1317-25.
- Ross, C. A.** (2002). Polyglutamine pathogenesis: emergence of unifying mechanisms for Huntington's disease and related disorders. *Neuron* **35**, 819-22.
- Ruan, Q., Lesort, M., MacDonald, M. E. and Johnson, G. V.** (2004). Striatal cells from mutant huntingtin knock-in mice are selectively vulnerable to mitochondrial complex II inhibitor-induced cell death through a non-apoptotic pathway. *Hum Mol Genet* **13**, 669-81.
- Rudnicki, D. D., Pletnikova, O., Vonsattel, J. P., Ross, C. A. and Margolis, R. L.** (2008). A comparison of huntington disease and huntington disease-like 2 neuropathology. *J Neuropathol Exp Neurol* **67**, 366-74.
- Ruocco, H. H., Lopes-Cendes, I., Li, L. M., Santos-Silva, M. and Cendes, F.** (2006). Striatal and extrastriatal atrophy in Huntington's disease and its relationship with length of the CAG repeat. *Braz J Med Biol Res* **39**, 1129-36.
- Sajatovic, M., Verbanac, P., Ramirez, L. F. and Meltzer, H. Y.** (1991). Clozapine treatment of psychiatric symptoms resistant to neuroleptic treatment in patients with Huntington's chorea. *Neurology* **41**, 156.
- Sanberg, P. R., Fibiger, H. C. and Mark, R. F.** (1981). Body weight and dietary factors in Huntington's disease patients compared with matched controls. *Med J Aust* **1**, 407-9.
- Sanchez, I., Mahlke, C. and Yuan, J.** (2003). Pivotal role of oligomerization in expanded polyglutamine neurodegenerative disorders. *Nature* **421**, 373-9.
- Sathasivam, K., Hobbs, C., Mangiarini, L., Mahal, A., Turmaine, M., Doherty, P., Davies, S. W. and Bates, G. P.** (1999a). Transgenic models of Huntington's disease. *Philos Trans R Soc Lond B Biol Sci* **354**, 963-9.
- Sathasivam, K., Hobbs, C., Turmaine, M., Mangiarini, L., Mahal, A., Bertaux, F., Wanker, E. E., Doherty, P., Davies, S. W. and Bates, G. P.** (1999b). Formation of polyglutamine inclusions in non-CNS tissue. *Hum Mol Genet* **8**, 813-22.
- Saudou, F., Finkbeiner, S., Devys, D. and Greenberg, M. E.** (1998). Huntingtin acts in the nucleus to induce apoptosis but death does not correlate with the formation of intranuclear inclusions. *Cell* **95**, 55-66.
- Sawa, A., Wiegand, G. W., Cooper, J., Margolis, R. L., Sharp, A. H., Lawler, J. F., Jr., Greenamyre, J. T., Snyder, S. H. and Ross, C. A.** (1999). Increased apoptosis of Huntington disease lymphoblasts associated with repeat length-dependent mitochondrial depolarization. *Nat Med* **5**, 1194-8.
- Scarabelli, T. M., Stephanou, A., Pasini, E., Gitti, G., Townsend, P., Lawrence, K., Chen-Scarabelli, C., Saravolatz, L., Latchman, D., Knight, R. et al.** (2004). Minocycline inhibits caspase activation and reactivation, increases the ratio of XIAP to smac/DIABLO, and reduces the mitochondrial leakage of cytochrome C and smac/DIABLO. *J Am Coll Cardiol* **43**, 865-74.
- Schaffar, G., Breuer, P., Boteva, R., Behrends, C., Tzvetkov, N., Strippel, N., Sakahira, H., Siegers, K., Hayer-Hartl, M. and Hartl, F. U.** (2004). Cellular toxicity of polyglutamine expansion proteins: mechanism of transcription factor deactivation. *Mol Cell* **15**, 95-105.
- Scherzinger, E., Lurz, R., Turmaine, M., Mangiarini, L., Hollenbach, B., Hasenbank, R., Bates, G. P., Davies, S. W., Lehrach, H. and Wanker, E. E.** (1997). Huntingtin-encoded polyglutamine expansions form amyloid-like protein aggregates in vitro and in vivo. *Cell* **90**, 549-58.

**Scherzinger, E., Sittler, A., Schweiger, K., Heiser, V., Lurz, R., Hasenbank, R., Bates, G. P., Lehrach, H. and Wanker, E. E.** (1999). Self-assembly of polyglutamine-containing huntingtin fragments into amyloid-like fibrils: implications for Huntington's disease pathology. *Proc Natl Acad Sci U S A* **96**, 4604-9.

**Schilling, G., Becher, M. W., Sharp, A. H., Jinnah, H. A., Duan, K., Kotzuk, J. A., Slunt, H. H., Ratovitski, T., Cooper, J. K., Jenkins, N. A. et al.** (1999). Intranuclear inclusions and neuritic aggregates in transgenic mice expressing a mutant N-terminal fragment of huntingtin. *Hum Mol Genet* **8**, 397-407.

**Schilling, G., Klevytska, A., Tebbenkamp, A. T., Juenemann, K., Cooper, J., Gonzales, V., Slunt, H., Poirer, M., Ross, C. A. and Borchelt, D. R.** (2007). Characterization of huntingtin pathologic fragments in human Huntington disease, transgenic mice, and cell models. *J Neuropathol Exp Neurol* **66**, 313-20.

**Seppi, K., Mueller, J., Bodner, T., Brandauer, E., Benke, T., Weirich-Schwaiger, H., Poewe, W. and Wenning, G. K.** (2001). Riluzole in Huntington's disease (HD): an open label study with one year follow up. *J Neurol* **248**, 866-9.

**Shehadeh, J., Fernandes, H. B., Zeron Mullins, M. M., Graham, R. K., Leavitt, B. R., Hayden, M. R. and Raymond, L. A.** (2006). Striatal neuronal apoptosis is preferentially enhanced by NMDA receptor activation in YAC transgenic mouse model of Huntington disease. *Neurobiol Dis* **21**, 392-403.

**Shelbourne, P. F., Keller-McGandy, C., Bi, W. L., Yoon, S. R., Dubeau, L., Veitch, N. J., Vonsattel, J. P., Wexler, N. S., Arnheim, N. and Augood, S. J.** (2007). Triplet repeat mutation length gains correlate with cell-type specific vulnerability in Huntington disease brain. *Hum Mol Genet* **16**, 1133-42.

**Shelbourne, P. F., Killeen, N., Hevner, R. F., Johnston, H. M., Tecott, L., Lewandoski, M., Ennis, M., Ramirez, L., Li, Z., Iannicola, C. et al.** (1999). A Huntington's disease CAG expansion at the murine Hdh locus is unstable and associated with behavioural abnormalities in mice. *Hum Mol Genet* **8**, 763-74.

**Silvestri, R., Raffaele, M., De Domenico, P., Tisano, A., Mento, G., Casella, C., Tripoli, M. C., Serra, S. and Di Perri, R.** (1995). Sleep features in Tourette's syndrome, neuroacanthocytosis and Huntington's chorea. *Neurophysiol Clin* **25**, 66-77.

**Sjogren, M., Davidsson, P., Wallin, A., Granerus, A. K., Grundstrom, E., Askmark, H., Vanmechelen, E. and Blennow, K.** (2002). Decreased CSF-beta-amyloid 42 in Alzheimer's disease and amyotrophic lateral sclerosis may reflect mistreatment of beta-amyloid induced by disparate mechanisms. *Dement Geriatr Cogn Disord* **13**, 112-8.

**Smith, D. L., Portier, R., Woodman, B., Hockly, E., Mahal, A., Klunk, W. E., Li, X. J., Wanker, E., Murray, K. D. and Bates, G. P.** (2001). Inhibition of polyglutamine aggregation in R6/2 HD brain slices-complex dose-response profiles. *Neurobiol Dis* **8**, 1017-26.

**Smith, K. M., Matson, S., Matson, W. R., Cormier, K., Del Signore, S. J., Hagerty, S. W., Stack, E. C., Ryu, H. and Ferrante, R. J.** (2006). Dose ranging and efficacy study of high-dose coenzyme Q10 formulations in Huntington's disease mice. *Biochim Biophys Acta* **1762**, 616-26.

**Solans, A., Zambrano, A., Rodriguez, M. and Barrientos, A.** (2006). Cytotoxicity of a mutant huntingtin fragment in yeast involves early alterations in mitochondrial OXPHOS complexes II and III. *Hum Mol Genet* **15**, 3063-81.

**Sommerfeld, M. T., Schweigreiter, R., Barde, Y. A. and Hoppe, E.** (2000). Down-regulation of the neurotrophin receptor TrkB following ligand binding. Evidence for an involvement of the proteasome and differential regulation of TrkA and TrkB. *J Biol Chem* **275**, 8982-90.

- Spargo, E., Overall, I. P. and Lantos, P. L.** (1993). Neuronal loss in the hippocampus in Huntington's disease: a comparison with HIV infection. *J Neurol Neurosurg Psychiatry* **56**, 487-91.
- Stack, E. C., Kubilus, J. K., Smith, K., Cormier, K., Del Signore, S. J., Guelin, E., Ryu, H., Hersch, S. M. and Ferrante, R. J.** (2005). Chronology of behavioral symptoms and neuropathological sequela in R6/2 Huntington's disease transgenic mice. *J Comp Neurol* **490**, 354-70.
- Strozyk, D., Blennow, K., White, L. R. and Launer, L. J.** (2003). CSF Abeta 42 levels correlate with amyloid-neuropathology in a population-based autopsy study. *Neurology* **60**, 652-6.
- Stryer, L.** (1978). Fluorescence energy transfer as a spectroscopic ruler. *Annu Rev Biochem* **47**, 819-46.
- Tabrizi, S. J., Blamire, A. M., Manners, D. N., Rajagopalan, B., Styles, P., Schapira, A. H. and Warner, T. T.** (2003). Creatine therapy for Huntington's disease: clinical and MRS findings in a 1-year pilot study. *Neurology* **61**, 141-2.
- Tabrizi, S. J., Blamire, A. M., Manners, D. N., Rajagopalan, B., Styles, P., Schapira, A. H. and Warner, T. T.** (2005). High-dose creatine therapy for Huntington disease: a 2-year clinical and MRS study. *Neurology* **64**, 1655-6.
- Takiyama, Y., Sakoe, K., Amaike, M., Soutome, M., Ogawa, T., Nakano, I. and Nishizawa, M.** (1999). Single sperm analysis of the CAG repeats in the gene for dentatorubral-pallidoluysian atrophy (DRPLA): the instability of the CAG repeats in the DRPLA gene is prominent among the CAG repeat diseases. *Hum Mol Genet* **8**, 453-7.
- Telenius, H., Kremer, B., Goldberg, Y. P., Theilmann, J., Andrew, S. E., Zeisler, J., Adam, S., Greenberg, C., Ives, E. J., Clarke, L. A. et al.** (1994). Somatic and gonadal mosaicism of the Huntington disease gene CAG repeat in brain and sperm. *Nat Genet* **6**, 409-14.
- Thomas, M., Ashizawa, T. and Jankovic, J.** (2004). Minocycline in Huntington's disease: a pilot study. *Mov Disord* **19**, 692-5.
- Thompson, P. D., Berardelli, A., Rothwell, J. C., Day, B. L., Dick, J. P., Benecke, R. and Marsden, C. D.** (1988). The coexistence of bradykinesia and chorea in Huntington's disease and its implications for theories of basal ganglia control of movement. *Brain* **111** ( Pt 2), 223-44.
- Trettel, F., Rigamonti, D., Hilditch-Maguire, P., Wheeler, V. C., Sharp, A. H., Persichetti, F., Cattaneo, E. and MacDonald, M. E.** (2000). Dominant phenotypes produced by the HD mutation in STHdh(Q111) striatal cells. *Hum Mol Genet* **9**, 2799-809.
- Trushina, E., Dyer, R. B., Badger, J. D., 2nd, Ure, D., Eide, L., Tran, D. D., Vrieze, B. T., Legendre-Guillemain, V., McPherson, P. S., Mandavilli, B. S. et al.** (2004). Mutant huntingtin impairs axonal trafficking in mammalian neurons in vivo and in vitro. *Mol Cell Biol* **24**, 8195-209.
- Trushina, E., Heldebrant, M. P., Perez-Terzic, C. M., Bortolon, R., Kovtun, I. V., Badger, J. D., 2nd, Terzic, A., Estevez, A., Windebank, A. J., Dyer, R. B. et al.** (2003). Microtubule destabilization and nuclear entry are sequential steps leading to toxicity in Huntington's disease. *Proc Natl Acad Sci U S A* **100**, 12171-6.
- Underwood, B. R., Broadhurst, D., Dunn, W. B., Ellis, D. I., Michell, A. W., Vacher, C., Mosedale, D. E., Kell, D. B., Barker, R. A., Grainger, D. J. et al.** (2006). Huntington disease patients and transgenic mice have similar pro-catabolic serum metabolite profiles. *Brain* **129**, 877-86.
- Vaddadi, K. S., Soosai, E., Chiu, E. and Dingjan, P.** (2002). A randomised, placebo-controlled, double blind study of treatment of Huntington's disease with unsaturated fatty acids. *Neuroreport* **13**, 29-33.

- Vaisanen, M. L., Haataja, R. and Leisti, J.** (1996). Decrease in the CGGn trinucleotide repeat mutation of the fragile X syndrome to normal size range during paternal transmission. *Am J Hum Genet* **59**, 540-6.
- van Roon-Mom, W. M., Reid, S. J., Faull, R. L. and Snell, R. G.** (2005). TATA-binding protein in neurodegenerative disease. *Neuroscience* **133**, 863-72.
- van Roon-Mom, W. M., Reid, S. J., Jones, A. L., MacDonald, M. E., Faull, R. L. and Snell, R. G.** (2002). Insoluble TATA-binding protein accumulation in Huntington's disease cortex. *Brain Res Mol Brain Res* **109**, 1-10.
- Varma, H., Voisine, C., DeMarco, C. T., Cattaneo, E., Lo, D. C., Hart, A. C. and Stockwell, B. R.** (2007). Selective inhibitors of death in mutant huntingtin cells. *Nat Chem Biol* **3**, 99-100.
- Velier, J., Kim, M., Schwarz, C., Kim, T. W., Sapp, E., Chase, K., Aronin, N. and DiFiglia, M.** (1998). Wild-type and mutant huntingtins function in vesicle trafficking in the secretory and endocytic pathways. *Exp Neurol* **152**, 34-40.
- Verbessem, P., Lemiere, J., Eijnde, B. O., Swinnen, S., Vanhees, L., Van Leemputte, M., Hespel, P. and Dom, R.** (2003). Creatine supplementation in Huntington's disease: a placebo-controlled pilot trial. *Neurology* **61**, 925-30.
- Vonsattel, J. P. and DiFiglia, M.** (1998). Huntington disease. *J Neuropathol Exp Neurol* **57**, 369-84.
- Vonsattel, J. P., Myers, R. H., Stevens, T. J., Ferrante, R. J., Bird, E. D. and Richardson, E. P., Jr.** (1985). Neuropathological classification of Huntington's disease. *J Neuropathol Exp Neurol* **44**, 559-77.
- Walker, F. O.** (2007). Huntington's disease. *Lancet* **369**, 218-28.
- Walker, R. H., Jankovic, J., O'Hearn, E. and Margolis, R. L.** (2003). Phenotypic features of Huntington's disease-like 2. *Mov Disord* **18**, 1527-30.
- Wang, C. E., Zhou, H., McGuire, J. R., Cerullo, V., Lee, B., Li, S. H. and Li, X. J.** (2008). Suppression of neuropil aggregates and neurological symptoms by an intracellular antibody implicates the cytoplasmic toxicity of mutant huntingtin. *J Cell Biol* **181**, 803-16.
- Wang, Y. L., Liu, W., Wada, E., Murata, M., Wada, K. and Kanazawa, I.** (2005). Clinic-pathological rescue of a model mouse of Huntington's disease by siRNA. *Neurosci Res* **53**, 241-9.
- Warby, S. C., Chan, E. Y., Metzler, M., Gan, L., Singaraja, R. R., Crocker, S. F., Robertson, H. A. and Hayden, M. R.** (2005). Huntingtin phosphorylation on serine 421 is significantly reduced in the striatum and by polyglutamine expansion in vivo. *Hum Mol Genet* **14**, 1569-77.
- Waters, C.** (1842). *Practice of medicine 1st Edition*.
- Weihofen, A., Lemberg, M. K., Friedmann, E., Rueeger, H., Schmitz, A., Paganetti, P., Rovelli, G. and Martoglio, B.** (2003). Targeting presenilin-type aspartic protease signal peptide peptidase with gamma-secretase inhibitors. *J Biol Chem* **278**, 16528-33.
- Weiss, A., Klein, C., Woodman, B., Sathasivam, K., Bibel, M., Regulier, E., Bates, G. P. and Paganetti, P.** (2008). Sensitive biochemical aggregate detection reveals aggregation onset before symptom development in cellular and murine models of Huntington's disease. *J Neurochem* **104**, 846-58.
- Wellington, C. L., Ellerby, L. M., Gutekunst, C. A., Rogers, D., Warby, S., Graham, R. K., Loubser, O., van Raamsdonk, J., Singaraja, R., Yang, Y. Z. et al.** (2002). Caspase cleavage of mutant huntingtin precedes neurodegeneration in Huntington's disease. *J Neurosci* **22**, 7862-72.
- Wellington, C. L., Ellerby, L. M., Hackam, A. S., Margolis, R. L., Trifiro, M. A., Singaraja, R., McCutcheon, K., Salvesen, G. S., Propp, S. S., Bromm, M. et al.** (1998). Caspase cleavage of gene products associated with triplet expansion disorders generates truncated fragments containing the polyglutamine tract. *J Biol Chem* **273**, 9158-67.

**Wellington, C. L., Leavitt, B. R. and Hayden, M. R.** (2000a). Huntington disease: new insights on the role of huntingtin cleavage. *J Neural Transm Suppl*, 1-17.

**Wellington, C. L., Singaraja, R., Ellerby, L., Savill, J., Roy, S., Leavitt, B., Cattaneo, E., Hackam, A., Sharp, A., Thornberry, N. et al.** (2000b). Inhibiting caspase cleavage of huntingtin reduces toxicity and aggregate formation in neuronal and nonneuronal cells. *J Biol Chem* **275**, 19831-8.

**Wexler, N. S., Lorimer, J., Porter, J., Gomez, F., Moskowitz, C., Shackell, E., Marder, K., Pechaszadeh, G., Roberts, S. A., Gayan, J. et al.** (2004). Venezuelan kindreds reveal that genetic and environmental factors modulate Huntington's disease age of onset. *Proc Natl Acad Sci U S A* **101**, 3498-503.

**Weydt, P., Pineda, V. V., Torrence, A. E., Libby, R. T., Satterfield, T. F., Lazarowski, E. R., Gilbert, M. L., Morton, G. J., Bammler, T. K., Strand, A. D. et al.** (2006). Thermoregulatory and metabolic defects in Huntington's disease transgenic mice implicate PGC-1alpha in Huntington's disease neurodegeneration. *Cell Metab* **4**, 349-62.

**Wheeler, V. C., Auerbach, W., White, J. K., Srinidhi, J., Auerbach, A., Ryan, A., Duyao, M. P., Vrbanac, V., Weaver, M., Gusella, J. F. et al.** (1999). Length-dependent gametic CAG repeat instability in the Huntington's disease knock-in mouse. *Hum Mol Genet* **8**, 115-22.

**Wheeler, V. C., Persichetti, F., McNeil, S. M., Mysore, J. S., Mysore, S. S., MacDonald, M. E., Myers, R. H., Gusella, J. F. and Wexler, N. S.** (2007). Factors associated with HD CAG repeat instability in Huntington disease. *J Med Genet* **44**, 695-701.

**Wheeler, V. C., White, J. K., Gutekunst, C. A., Vrbanac, V., Weaver, M., Li, X. J., Li, S. H., Yi, H., Vonsattel, J. P., Gusella, J. F. et al.** (2000). Long glutamine tracts cause nuclear localization of a novel form of huntingtin in medium spiny striatal neurons in HdhQ92 and HdhQ111 knock-in mice. *Hum Mol Genet* **9**, 503-13.

**White, J. K., Auerbach, W., Duyao, M. P., Vonsattel, J. P., Gusella, J. F., Joyner, A. L. and MacDonald, M. E.** (1997). Huntington is required for neurogenesis and is not impaired by the Huntington's disease CAG expansion. *Nat Genet* **17**, 404-10.

**Wiltfang, J., Arold, N. and Neuhoff, V.** (1991). A new multiphasic buffer system for sodium dodecyl sulfate-polyacrylamide gel electrophoresis of proteins and peptides with molecular masses 100,000-1000, and their detection with picomolar sensitivity. *Electrophoresis* **12**, 352-66.

**Woodman, B., Butler, R., Landles, C., Lupton, M. K., Tse, J., Hockly, E., Moffitt, H., Sathasivam, K. and Bates, G. P.** (2007). The Hdh(Q150/Q150) knock-in mouse model of HD and the R6/2 exon 1 model develop comparable and widespread molecular phenotypes. *Brain Res Bull* **72**, 83-97.

**Wu, P. and Brand, L.** (1994). Resonance energy transfer: methods and applications. *Anal Biochem* **218**, 1-13.

**Wytenbach, A., Swartz, J., Kita, H., Thykjaer, T., Carmichael, J., Bradley, J., Brown, R., Maxwell, M., Schapira, A., Orntoft, T. F. et al.** (2001). Polyglutamine expansions cause decreased CRE-mediated transcription and early gene expression changes prior to cell death in an inducible cell model of Huntington's disease. *Hum Mol Genet* **10**, 1829-45.

**Xia, J., Lee, D. H., Taylor, J., Vandelft, M. and Truant, R.** (2003). Huntington contains a highly conserved nuclear export signal. *Hum Mol Genet* **12**, 1393-403.

**Yamamoto, A., Cremona, M. L. and Rothman, J. E.** (2006). Autophagy-mediated clearance of huntingtin aggregates triggered by the insulin-signaling pathway. *J Cell Biol* **172**, 719-31.

**Yamamoto, A., Lucas, J. J. and Hen, R.** (2000). Reversal of neuropathology and motor dysfunction in a conditional model of Huntington's disease. *Cell* **101**, 57-66.

**Yamamoto, N., Takeshita, K., Shichijo, M., Kokubo, T., Sato, M., Nakashima, K., Ishimori, M., Nagai, H., Li, Y. F., Yura, T. et al.** (2003). The orally available spleen tyrosine kinase inhibitor 2-[7-(3,4-dimethoxyphenyl)-imidazo[1,2-c]pyrimidin-5-

ylamino]nicotinamide dihydrochloride (BAY 61-3606) blocks antigen-induced airway inflammation in rodents. *J Pharmacol Exp Ther* **306**, 1174-81.

**Yan, L. J., Levine, R. L. and Sohal, R. S.** (1997). Oxidative damage during aging targets mitochondrial aconitase. *Proc Natl Acad Sci U S A* **94**, 11168-72.

**Yang, W., Dunlap, J. R., Andrews, R. B. and Wetzel, R.** (2002). Aggregated polyglutamine peptides delivered to nuclei are toxic to mammalian cells. *Hum Mol Genet* **11**, 2905-17.

**Yoshida, M., Horinouchi, S. and Beppu, T.** (1995). Trichostatin A and trapoxin: novel chemical probes for the role of histone acetylation in chromatin structure and function. *Bioessays* **17**, 423-30.

**Young, A. B.** (2003). Huntingtin in health and disease. *J Clin Invest* **111**, 299-302.

**Young, A. B., Shoulson, I., Penney, J. B., Starosta-Rubinstein, S., Gomez, F., Travers, H., Ramos-Arroyo, M. A., Snodgrass, S. R., Bonilla, E., Moreno, H. et al.** (1986). Huntington's disease in Venezuela: neurologic features and functional decline. *Neurology* **36**, 244-9.

**Zafra, F., Hengerer, B., Leibrock, J., Thoenen, H. and Lindholm, D.** (1990). Activity dependent regulation of BDNF and NGF mRNAs in the rat hippocampus is mediated by non-NMDA glutamate receptors. *Embo J* **9**, 3545-50.

**Zala, D., Benchoua, A., Brouillet, E., Perrin, V., Gaillard, M. C., Zurn, A. D., Aebischer, P. and Deglon, N.** (2005). Progressive and selective striatal degeneration in primary neuronal cultures using lentiviral vector coding for a mutant huntingtin fragment. *Neurobiol Dis* **20**, 785-98.

**Zeitlin, S., Liu, J. P., Chapman, D. L., Papaioannou, V. E. and Efstratiadis, A.** (1995). Increased apoptosis and early embryonic lethality in mice nullizygous for the Huntington's disease gene homologue. *Nat Genet* **11**, 155-63.

**Zhang, J. H., Chung, T. D. and Oldenburg, K. R.** (1999). A Simple Statistical Parameter for Use in Evaluation and Validation of High Throughput Screening Assays. *J Biomol Screen* **4**, 67-73.

**Zhang, X., Smith, D. L., Meriin, A. B., Engemann, S., Russel, D. E., Roark, M., Washington, S. L., Maxwell, M. M., Marsh, J. L., Thompson, L. M. et al.** (2005). A potent small molecule inhibits polyglutamine aggregation in Huntington's disease neurons and suppresses neurodegeneration in vivo. *Proc Natl Acad Sci U S A* **102**, 892-7.

**Zourlidou, A., Gidalevitz, T., Kristiansen, M., Landles, C., Woodman, B., Wells, D. J., Latchman, D. S., de Belleruche, J., Tabrizi, S. J., Morimoto, R. I. et al.** (2007). Hsp27 overexpression in the R6/2 mouse model of Huntington's disease: chronic neurodegeneration does not induce Hsp27 activation. *Hum Mol Genet* **16**, 1078-90.

**Zuccato, C., Ciammola, A., Rigamonti, D., Leavitt, B. R., Goffredo, D., Conti, L., MacDonald, M. E., Friedlander, R. M., Silani, V., Hayden, M. R. et al.** (2001). Loss of huntingtin-mediated BDNF gene transcription in Huntington's disease. *Science* **293**, 493-8.

**Zuccato, C., Liber, D., Ramos, C., Tarditi, A., Rigamonti, D., Tartari, M., Valenza, M. and Cattaneo, E.** (2005). Progressive loss of BDNF in a mouse model of Huntington's disease and rescue by BDNF delivery. *Pharmacol Res* **52**, 133-9.

**Zuccato, C., Tartari, M., Crotti, A., Goffredo, D., Valenza, M., Conti, L., Cataudella, T., Leavitt, B. R., Hayden, M. R., Timmusk, T. et al.** (2003). Huntingtin interacts with REST/NRSF to modulate the transcription of NRSE-controlled neuronal genes. *Nat Genet* **35**, 76-83.

## ACKNOWLEDGMENTS

First of all, I would like to thank Dr. Paolo Paganetti for giving me the opportunity to join his lab for doing my thesis, for the many helpful and informative discussions, for his insights into drug discovery research, for his moral support and motivation and for giving me the broadest possible independence in an industrial setting to pursue my scientific interests.

I am very grateful to Prof. Dr. Markus Rüegg who accepted to be my ‘Doctor Father’ and to Prof. Dr. Martin Spiess who accepted to join my thesis committee.

I would especially like to thank Dorothee Bleckman, Muriel Stefani, Dr. Corinna Klein, Dr. Ana Roscic, Dr. Michele Chiesi, Dr. Etienne Régulier, Stefan Grüninger, Dr. Miriam Bibel, Jens Richter, Emmanuel Lacroix and Natacha Stoehr for all the shared experiments, for the many, many interesting scientific and non-scientific discussions, their moral support, the laughter and enjoyable hours and in general for making the last three years a great time! Also special thanks to Dr. Jens Mittag, Dr. Corinna Klein and Dorothee Bleckman for proofreading parts of this thesis.

I would also like to thank Dr. Christian Parker for his support, the interesting and fun discussions and for the insights about high-throughput assay development. Thanks also to Monique Trapp for the fruitful work while developing the compound assay.

I am very grateful to Dr. Rainer Kuhn, Dr. Christoph Wiessner and Dr. Graeme Bilbe for all their encouragements, the helpful discussions, the insights into the pharmaceutical industry and their overall support over the last three years.

I want to thank Prof. Gill Bates, Prof. Steve Hersch, Prof. Marian DiFiglia, Dr. Kimberly Kegel, Prof. Dimitri Krainc, Prof. David Housman, Dr. Ruth Bodner, Dr. Jonathan Fox, Dr. Christian Landles, Dr. Ben Woodman and Dr. Kirupa Sathasivam for the many scientific discussions and fruitful projects we did together.

Last but certainly not least I would like to address my biggest thanks to my parents, my brother and Heidi for their love, patience and support they have given me during my thesis.

## CURRICULUM VITAE

### Address

Alte Strasse 23  
79576 Weil am Rhein, Germany  
Phone: +49 7621 1637193  
E-mail: andreas-1.weiss@novartis.com

### Personal Data

Date of birth: 10. March 1978  
Nationality: German  
Marital status: Single

### Education

- **American High School Diploma (“A“ Honour roll), 1997**
  - Edison High School, Minneapolis, USA
- **German Abitur (in top 5% of graduation class), 1999**
  - Hermann-Billing Gymnasium, Celle, Germany
- **Studies in biochemistry with focus on neuroendocrinology and immunology, Oct 2000 - Sep 2005**
  - University of Bielefeld, Bielefeld, Germany (biochemistry diploma with distinction), Oct 2000 - Sep 2005
  - University of Notre Dame, South Bend, USA (studies on cytoskeleton stability), Feb 2003 - Sep 2003
  - Max-Planck-Institute for Experimental Endocrinology, Hannover, Germany Diploma thesis: “Development of antibodies for immunohistochemical characterization and localization of thyrotropin-releasing-hormone-(TRH)-receptor 1 and TRH-degrading ectoenzyme (TRH-DE)“, (thesis with distinction), Jan 2005 - Sep 2005
- **PhD in neurobiology, Thesis: “Novel methods and therapeutic approaches for diagnosis and treatment of Huntington's Disease“ at Novartis Institutes for BioMedical Research and University of Basel, Basel, Switzerland, Oct 2005 – Sep 2008**
  - PhD studies in the laboratory of Dr. Paolo Paganetti under the supervision of Prof. Dr. Markus Rüegg

### Professional Experience

- **Paritaetischer Wohlfahrtsverband, Aug 1999 - July 2000**
  - Direct care and support for patients affected by various diseases including multiple sclerosis, down syndrome or dementia
- **Own business, July 1997 - July 2000**
  - Registered business at the “Industrie und Handelskammer”, Germany
  - Selling, assembling, configuring and repairing personal computers
  - Profit between 2000 and 3000 Euro/year

### Awards / Scholarships

- “SPOT award“ for above and beyond contributions to the Huntington’s Disease Project awarded by Novartis Neuroscience Research, Switzerland
- “Th!nk Ahead award“ by Novartis Pharma Affairs, Switzerland
- “DAAD scholarship“ by University of Bielefeld, Germany
- “Business student of the year award“ awarded by Edison High School, USA

### Patents

- Bioassay for detection of mutant huntingtin in human samples (patent in progress)

## Publications

- **Andreas Weiss**, Corinna Klein, Ben Woodman, Kirupa Sathasivam, Miriam Bibel, Etienne Régulier, Gillian P. Bates and Paolo Paganetti "*Sensitive Biochemical Aggregate detection reveals aggregation onset before Symptom development in Cellular and Murine Models of Huntington's Disease*", Journal of Neurochemistry, 2008
- **Andreas Weiss**, Steven Hersch, Corinna Klein, Kimberly Kegel, Ruth Bodner, David Housman, Marian DiFiglia, Jonathan Fox, Etienne Regulier, Graeme Bilbe and Paolo Paganetti "*Single-Step Detection of Soluble Poly-Huntingtin in Cellular, Animal and Human Tissue Samples: a BioAssay for Huntington's Disease*", manuscript submitted
- **Andreas Weiss** & Paolo Paganetti, Monique Trapp, Dorothee Bleckmann, Ruth Bodner, David Housman, Ina Hammerl and Christian N. Parker „*Development of a Method for the High-Throughput-Quantification of Cellular Protein Levels*“, manuscript submission after patent in August 2008
- **Andreas Weiss**, Stephan Grueninger, Emmanuel Lacroix, Dorothee Bleckmann, Muriel Stefani, Miriam Bibel, Etienne Régulier and Paolo Paganetti „*Inducible mutant huntingtin expression in a neuronal cell model leads to transcriptional dysregulation and cell death*“, manuscript submitted
- Corinna Klein, Natacha Stoehr, **Andreas Weiss**, Jens Richter, Emmanuel Lacroix, Paolo Paganetti, Etienne Regulier and Miriam Bibel "*Modeling Huntington's Disease in primary cortical neurons and neurons derived from mouse embryonic stem cells*", manuscript submitted

## Conferences and Workshops

- Hereditary Disease Foundation, 6th Meeting, Cambridge 2008 (invited speaker)
- Molecular Mechanisms of Neurodegeneration, 3rd Meeting, Mailand 2007 (poster presentation)
- D0 Target Discovery Expo, Basel 2007 (poster presentation)
- McKinsey DIVE workshop, Pontresina 2006 (invited participant)
- Hereditary Disease Foundation conference, Cambridge 2006 (poster presentation)
- Neuroscience Novartis Retreat, Thun 2006 (poster presentation)
- American Society for Cell Biology Annual Meeting, San Francisco 2005 (poster presentation)

## Other Activities and Interests

- Creative Writing (novel published, next novel in preparation)
- Andreas Weiss: "Eine Person namens Balthasar", belletristic novel, ISBN 3865826288, Publisher: Mosenstein & Vannerdat
- Translator German <> English for Plan International's correspondence between foster parents and foster children
- Philosophy (empiricism, epistemology and skepticism)
- Sports (basketball, soccer)
- Finance (stock market, investment decisions)